amU
Aix Marseille Université

NNT : 2025AIXM0013

THÈSE DE DOCTORAT

Soutenue à AMU — Aix-Marseille Université
le 17 janvier 2025 par

Kenza AMROUNE

Connectivité Fonctionnelle des Projections Corticostriatales Somatosensorielles et Plasticité Induite par l'Apprentissage

Discipline
Biologie-Santé

Spécialité
Neurosciences

École doctorale
ED 62
Sciences de la Vie et de la Santé

Laboratoire
Institut de Neurobiologie de la Méditerranée (INMED)
INSERM U1249

Composition du jury

Valérie Ego-Stengel Directrice de recherche CNRS	Rapporteur NeuroPSI – Paris Saclay
Nicolas Mallet Chargé de recherche CNRS	Rapporteur Université de Bordeaux
Corrine Beurrier Chargée de recherche CNRS	Examinateur INT – Marseille
Stéphane Charpier Professeur des Universités	Examinateur, Président du jury ICM – Paris
David ROBBE Directeur de recherche INSERM	Co-Encadrant de thèse INMED – Marseille
Ingrid BUREAU Chargée de recherche INSERM	Directrice de thèse INMED – Marseille

Inmed
Institut de neurobiologie de la méditerranée

Inserm

NeuroSchool
Aix*Marseille Université

AFFIDAVIT

I, undersigned, Kenza Amroune, hereby declare that the work presented in this manuscript is my own work, carried out under the scientific supervision of Ingrid Bureau, and David Robbe in accordance with the principles of honesty, integrity and responsibility inherent to the research mission. The research work and the writing of this manuscript have been carried out in compliance with both the french national charter for Research Integrity and AMU charter on the fight against plagiarism.

This work has not been submitted previously either in this country or in another country in the same or in a similar version to any other examination body.

Marseille, 29/10/2024.



This work is licensed under Creative Commons Attribution-NonCommercial-NoDerivatives 4.0 International Public License

LIST OF PUBLICATIONS AND CONFERENCES ATTENDED

List of publications:

1. Kenza Amroune, Lorenzo Fontolan, David Robbe, Ingrid Bureau. Sparse and specific somatosensory functional innervation of dorsolateral striatal neurons. 2024. ⟨hal-04567026v2⟩.

2. Kenza Amroune, Maud Schaffhauser, Thomas Morvan, Ingrid Bureau*, David Robbe*. Lateralized foraging induces unexpected asymmetric corticostriatal plasticity. *In prep.*

Conferences attended:

Talks:

1. French Basal Ganglia Club 2023. Marseille, France.

Posters:

1. FENS 2024. Vienna, Austria.
2. SFN 2023. Washington, USA.
3. Neuralnet 2023. Marseille, France.
4. Neurofrance 2023. Lyon, France.
5. NeuroDays 2022. Marseille, France.
6. SWEBAGS 2022. online.
7. FENS 2022. Paris, France.
8. NeuroDays 2021. Marseille, France.

ABSTRACT

Animals rely on sensory input from their environment to guide their behavior and make adaptive decisions. In rodents, the whisker system provides tactile information crucial for navigation. These sensory signals are processed in the barrel cortex (S1), part of the primary somatosensory cortex, and relayed to decision-making centers like the basal ganglia (BG). The dorsolateral striatum (DLS) is a key region within the BG that receives dense glutamatergic inputs from the cortex via corticostriatal (CS) projections and plays a critical role in motor control and action selection. The DLS is mainly composed of two populations of striatal projection neurons (SPNs), forming the direct (D1 SPNs) and indirect (D2 SPNs) BG pathways. Activation of these pathways has opponent effects on movement, with D1 SPNs facilitating behavior and D2 SPNs suppressing it. Thus, the sensory CS projection onto D1/D2 SPNs is one important determinant of striatal activity. The much larger number of cortical neurons compared to their fewer striatal targets suggests highly convergent processing of cortically-derived information within sensory modalities. However, DLS neuronal responses to sensory stimuli exhibit unexpected selectivity, raising questions about the functional convergence of CS inputs.

This thesis explores the functional organization of sensory CS projections onto individual D1/D2 SPNs and how this organization is shaped by behavior. We used *ex vivo* patch-clamp recordings in the DLS, combined with glutamate uncaging for focal stimulation in the barrel cortex, to assess the synaptic strength of CS inputs and to investigate the exact location of presynaptic neurons connected to individual SPNs in both naïve animals and animals trained in a whisker-guided foraging task.

1) In naive animals, we found low convergence of CS inputs: SPNs received projections from either a single or a small number of whisker cortical columns scattered across the barrel field, and neighboring SPNs shared few inputs. Despite this sparse and unique innervation of individual SPNs, the overall projection was topographically organized. D1 and D2-type SPNs did not segregate in different connectivity patterns. Our results are consistent with low connectivity and weak convergence between the sensory cortex and individual projection neurons of the DLS, that might allow fine-tuning of corticostriatal functional connectivity according to sensorimotor behaviors.

2) Because the activation of D1 and D2 SPNs bidirectionally modulates movement, it is expected that faster and more stereotyped rewarded action arise from a strengthened (weakened) connectivity on movement-facilitating (inhibiting) D1-SPNs (D2-SPNs). To test this hypothesis, we designed a lateralized whisker guided foraging task that required mice to make unidirectional 90 degree turns to obtain rewards, based on the well-established observation that activation of D1-SPNs and D2-SPNs have opposing effects on rotational behavior (respectively contralateral and ipsilateral to the stimulated hemisphere), and designed a whisker guided foraging task that required mice to make unidirectional 90 degree turns to obtain rewards. Surprisingly, comparing naïve and trained animals, we found no significant changes in CS connections to D1 or D2 SPNs. However, we observed plastic changes in the ipsilateral hemisphere, unengaged in task execution. The number of cortical columns innervating SPNs in this hemisphere increased, along with the sum of synaptic inputs. In contrast, S1 pyramidal neurons in the contralateral hemisphere had an increased excitability compared to naïve animals and the ipsilateral side. These findings suggest an asymmetric reorganization of CS circuits following lateralized learning. We hypothesize that the imbalance in cortical excitation induced by the task leads to a rearrangement of corticostriatal projections to maintain balanced excitation level to SPNs in the two hemispheres.

Keywords: Electrophysiology, Cortico-Striatal projection, Synaptic plasticity, Behavior, Learning

RÉSUMÉ

Les animaux utilisent les informations sensorielles de leur environnement pour guider leur comportement et prendre des décisions adaptatives. Chez les rongeurs, le système vibrissal fournit des informations tactiles essentielles pour la navigation. Ces signaux sont traités dans le cortex des vibrisses, au sein du cortex somatosensoriel primaire, puis transmis aux centres de décision comme les ganglions de la base (GB). Le striatum dorsolatéral (DLS), une région clé des GB, reçoit des afférences glutamatergiques denses du cortex via les projections corticostriatales (CS) et joue un rôle crucial dans le contrôle moteur et la sélection des actions. Le DLS est principalement composé de deux populations de neurones de projection striataux (SPNs), formant les voies directe (D1 SPNs) et indirecte (D2 SPNs). L'activation de ces voies a des effets opposés sur le mouvement : les D1 SPNs facilitent le comportement tandis que les D2 SPNs le suppriment. Ainsi, les projections sensorielles CS sur les D1/D2 SPNs déterminent les sorties des GB. Le grand nombre de neurones corticaux par rapport à leurs cibles striatales suggère un traitement convergent des informations corticales. Cependant, les réponses des neurones du DLS aux stimuli sensoriels montrent une sélectivité inattendue, soulevant des questions sur la convergence fonctionnelle des entrées CS.

Cette thèse explore l'organisation des projections CS sensorielles vers les D1/D2 SPNs et comment cette organisation est modulée par le comportement. Nous avons utilisé des enregistrements ex vivo en patch-clamp dans le DLS et le dégagement de glutamate avec photostimulation laser dans le cortex des vibrisses pour cartographier les connexions aux SPNs chez des animaux naïfs et ceux entraînés à une tâche de recherche guidée par les vibrisses.

1) Chez les animaux naïfs, nous avons observé une faible convergence des entrées CS : les SPNs recevaient des projections d'un petit nombre de colonnes corticales du cortex à barils, et les SPNs voisins partageaient peu d'entrées communes. Malgré cette innervation clairsemée, la projection restait topographiquement organisée. Les D1 et D2 SPNs ne montraient pas de différences de schémas de connectivité. Nos résultats suggèrent une faible connectivité entre le cortex sensoriel et les neurones du DLS, permettant peut-être un ajustement fin de la connectivité selon les comportements sensorimoteurs.

2) Comme l'activation des D1 et D2 SPNs module le mouvement dans des directions opposées, il est supposé que des actions plus rapides et stéréotypées résulteraient d'une connectivité renforcée des D1 SPNs et diminués des D2 SPNs. Pour tester cela, nous avons entraîné des souris à courir le long des murs de tours carrées dans l'obscurité et à effectuer des virages de 90° pour obtenir des récompenses, tirant profit de l'observation que l'activation unilatérale des D1 et D2 SPNs induit des rotations opposées (respectivement controlatéraux et ipsilatéraux). À notre surprise, la comparaison entre animaux naïfs et entraînés n'a montré aucun changement significatif du nombre ou de la force des connexions vers les D1 ou D2 SPNs. Cependant, des changements plastiques ont été observés dans l'hémisphère ipsilatéral, non sollicité pendant la tâche. Le nombre de colonnes corticales innervant les SPNs ipsilatéraux a augmenté, ainsi que la force synaptique globale. En outre, l'excitabilité des neurones pyramidaux du S1 controlatéral a augmenté par rapport aux animaux naïfs et à l'hémisphère ipsilatéral. Ces résultats montrent une asymétrie dans la réorganisation des circuits CS après l'apprentissage d'une tâche latéralisée. Nous supposons que le déséquilibre de l'excitation corticale provoque une réorganisation des projections CS pour maintenir des niveaux d'entrée similaires vers les SPNs dans les deux hémisphères.

Mots-clés : Electrophysiologie, Projection cortico-striatale, Plasticité synaptique, Comportement, Apprentissage

ACKNOWLEDGMENTS

Je tiens tout d'abord à remercier les membres de mon jury de thèse pour avoir pris le temps d'évaluer mon travail : à Valérie Ego-Stengel et Nicolas Mallet pour avoir rapporté mon travail, à Corinne Beurrier pour son rôle d'examinatrice. Un merci particulier à Stéphane Charpier, qui, en plus de sa fonction d'examinateur et de président de mon jury, a suivi de près ma thèse lors des comités de suivi individuel. Merci pour ces discussions enrichissantes.

Merci à Ingrid Bureau et David Robbe pour leur encadrement durant ce projet, la confiance et l'autonomie qu'ils m'ont accordées, tout en restant disponibles en cas de besoin. J'ai énormément appris à vos côtés, tant sur le plan scientifique que personnel, et je vous en suis très reconnaissante.
Ingrid, merci pour votre encadrement, votre expertise scientifique, votre disponibilité (même en vacances!) et vos précieux conseils, qui m'ont permis de m'épanouir tout au long de cette thèse. Merci également de m'avoir permis de réaliser un rêve d'étudiante : participer à la SFN !
David, merci pour ta contribution scientifique réfléchie, le challenge intellectuel que tu as apporté, tes recommandations pour l'après-thèse, et les nombreux livres prêtés (j'ai maintenant le temps de les lire !).

Je souhaite remercier chaleureusement tous les membres, passés et présents, du CBGCB lab : Anass, Élodie, Hoda, Juliette, Maewenn, Maud, Mostafa, Nihaad, Sanziana, Simona, Stefania, Thomas, Tom et Zelda. Merci à chacun pour les discussions (plus ou moins scientifiques !) qui ont, j'espère, enrichi autant votre travail que le mien. Un merci spécial à Élodie, marraine officieuse de thèse : merci pour ton écoute, tes conseils scientifiques et personnels, et la machine à café, si précieuse ces derniers mois!
Merci à Thomas d'avoir été un incroyable labmate, pour m'avoir appris (ou forcé) à utiliser Overleaf, pour l'aide avec mes codes Python, et pour ton soutien moral (gerber). J'ai hâte de découvrir la suite de ton arc naratif.

Merci à l'ensemble de l'INMED et aux différentes plateformes, sans qui cette thèse n'aurait pas été possible. Un merci particulier à Rosa et Fanny pour votre disponibilité, votre écoute et votre accompagnement. Merci à l'administration, notamment Gwendoline et Christine, pour votre aide et réactivité. Merci également à Francesca et Aurélie pour les génotypages de dernière minute, et à Victor pour tes enquêtes sur les mystérieuses disparitions de souris. Merci à Pascale pour ta présence lors de mes comités de thèse, tes conseils ont été précieux. Agnès, Céline, Emmanuelle, Françoise, Julie, Nadine, Olivier (x2), Robert: merci pour nos discussions de couloir, de patio, de labo, de machine a café...
Au copain du labo sans qui les pauses dans le patio n'en seraient pas vraiment : Alba, Alex, Alla, Aurélien, Célanie, Cloé, Daniela, Felix, Louison, M-So, Masha, Melanie, Mira, Sarah, Ugo, Vinca... Vous avez été un rayon de soleil à l'INMED, merci d'avoir été bien plus que des collègues.

Léa, quelle chance nous avons eue de faire notre thèse ensemble, et dans le même institut ! Merci d'être une amie exceptionnelle, avec qui j'ai partagé tant de repas et de souvenirs, que ce soit au labo, en congrès, en voyage. Depuis le master jusqu'à la soutenance, ces six années ont une place chère dans mon cœur !
Un remerciement particulier à mes amis : merci d'avoir été présents, pendant cette thèse et bien au-delà. Merci pour les bons repas (et les bonnes bouteilles !), pour les super soirées et pour les moments de rires inoubliables. À Ana, Antho, Bastien, Cem, Chloé, Estelle, Flo, Gael, Geoffrey, Géromine, Hector, Louis (x2), Martin, Marilyn, Mégane, Myriam, Romi, Shana et Simon : votre amitié a rendu cette période beaucoup plus joyeuse. Merci pour tous ces moments précieux, et pour être toujours prêts à nous retrouver, peu importe la distance. P.S. : Les noms sont listés par ordre alphabétique.

Merci à ma famille, pour votre amour et votre soutien, non seulement pendant ces années de thèse, mais depuis toujours. Merci d'avoir encouragé ma soif de curiosité et d'avoir fait semblant de comprendre mon sujet de thèse. Merci pour tous les merveilleux moments en famille, passés et à venir.
Merci Charles pour tout. Merci d'avoir été présent et de m'avoir soutenue/supportée tout au long de ces années universitaires, depuis l'apprentissage du chant des oiseaux jusqu'à ma thèse sur les moustaches des souris !

Finalemment, merci au Ministère de l'Education National et de la Recherche, à la Neuroschool, et à l'Agence National de la Recherche d'avoir financé ce projet.

CONTENTS

Affidavit **2**

List of publications **3**

Abstract **4**

Résumé **6**

Acknowledgments **8**

Contents **10**

List of Figures **13**

List of Tables **15**

Acronyms **16**

I INTRODUCTION **18**

1 Sensorimotor processing: from S1 to the DLS **19**

1.1 The Rodent Whisker-Barrel System 21

1.1.1 Somatotopy 21

1.1.2 Laminar organization 23

1.1.3 Somatosensory micro circuits . . . 25
1.1.4 S1 outputs . . . 27
1.2 The Basal Ganglia . . . 28
1.2.1 Striatum history . . . 29
1.2.2 Basal Ganglia anatomy . . . 29
1.2.3 Striatal cell types . . . 31
1.3 Corticostriatal projections . . . 38
1.3.1 Parallel cortico-basal ganglia loops . . . 38
1.3.2 Overlapping corticostriatal projections . . . 40
1.3.3 Types of Corticostriatal Projection Neurons . . . 41
1.3.4 Corticostriatal innervation of D1-D2 SPNs . . . 43
1.3.5 Convergence of Corticostriatal Projections . . . 45
1.3.6 Focus on S1 to DLS projections . . . 46
1.4 Summary . . . 49

2 Role of Corticostriatal Projections in sensorimotor learning 50
2.1 Plastic Changes in S1 During Tactile Sensorimotor Learning . . . 52
2.2 Role of the Dorsal Striatum in the Expression of Learned Behavior 54
2.2.1 Striatal Activity Changes Through Motor Learning . . . 55
2.2.2 Behavioral Modulation by D1 and D2 SPNs . . . 59
2.3 Corticostriatal Plasticity in Learning . . . 63
2.4 Summary . . . 68

Gap of knowledge and projects 69

II RESULTS 72

3 Study 1: Organization of Functional Corticostriatal Projections 73
3.0.1 Supplementary: IT and PT innervation of SPNs . . . 100

4 Study 2: Changes in Corticostriatal Circuits Following Learning 102

III DISCUSSION 134

5 Discussion 135
5.1 Organization of Corticostriatal Inputs to SPNs . . . 137
5.1.1 Topography of Cortical Inputs . . . 137

5.1.2 Layer-Specific Patterns of Innervation to SPNs 138
5.1.3 Cortical Sensory Projections to SPNs 139
5.2 Cortical and Thalamic Contributions to Striatal Sensory Processing 141
5.3 Development of a Lateralized Whisker-Guided Foraging Task . . 142
5.4 Plasticity in the Cortex Following Learning 144
5.5 Corticostriatal Projections After Learning 145
5.5.1 Asymmetry in the CS connectivity 145
5.5.2 Beyond the D1/D2 Dichotomy in Learning 146
5.5.3 Task-Specific Neuronal Ensembles and Inhibitory Reorganization 147
5.5.4 Interplay of Cortical and Thalamic Inputs in Learning . . . 148
5.5.5 Modulation of Striatal Responses: Role of the Dopamine . 149
5.6 Conclusion 151

Bibliography **152**

List of Figures

1.1 Organization of the whisker to barrels pathways. 22
1.2 Columnar Organization of the Somatosensory cortex. 24
1.3 Somatosensory circuits. 26
1.4 Cortical outputs to subcortical areas. 28
1.5 Diagram of Basal Ganglia circuit. 30
1.6 Disinhibitory circuits from the direct pathway. 32
1.7 Dichotomous anatomy and physiology of direct- and indirect-pathway SPNs. 34
1.8 Convergent inputs onto single SPN. 36
1.9 Organization of the striatal microcircuit. 37
1.10 Striatal somatotopic map in the DLS. 39
1.11 Multisensory integration in the dorsal striatum. 41
1.12 Subtypes of corticostriatal neurons. 42
1.13 Differences in input to D1 and D2 SPNs. 45
1.14 Anatomical organization of Corticostriatal projection from the barrel cortex. 47

2.1 Barrel cortex function during a task requiring detection of a passive whisker deflection. 53
2.2 The striatum is involved in habit learning in a place response task. 55
2.3 Activity in the DLS reflects behavioral chunking. 56
2.4 DLS activity during a sensorimotor task. 58

2.5 In vivo activation of direct or indirect pathways reveals pathway specific regulation of motor function. 60
2.6 D1 and D2 SPNs activity during a whisker detection task. 61
2.7 Motor learning selectively strengthens striatal synapses of motor engram neurons. 66
2.8 Corticostriatal projections drive decision-making and undergo plasticity during auditory discrimination learning. 67

3.1 Different implication of IT and PT neurons in SPNs innervation. . 101

5.1 Schematic representation of the lateralized movement pattern in the whisker-guided foraging task. 143

List of Tables

1.1 **Comparison of the Morphological and Physiological Traits Distinguishing IT-Type and PT-Type Corticostriatal Neurons** *Adapted from Steiner & Tseng 2017* 25

ACRONYMS

BG basal ganglia. 19, 28, 29, 31, 38, 49, 50, 54, 59, 145

ChINs cholinergic interneurons. 37

CS corticostriatal. 19, 41, 44, 45, 48, 49, 63–68, 70, 100, 135, 138, 139, 141, 145

DLS dorsolateral striatum. 19, 29, 38, 40, 47, 49, 50, 53, 55–57, 62–64, 68, 69, 135, 137–141, 145, 146

DMS dorsomedial striatum. 29, 38, 40

EPSC excitatory postsynaptic currents. 44

GPe external globus pallidus. 29–31, 38, 40

GPi internal globus pallidus. 29–31, 38, 39

IB intrinsic bursting. 24, 43, 100

IT intra-telencephalic. 24, 27, 41–44, 100, 138, 139

LFP local field potential. 66

LSPS Laser Scanning Photostimulation. 70

LTD long-term depression. 63

LTP long-term potentiation. 63, 64

POm posterior medial nucleus of the thalamus. 24, 26, 27, 141, 148

PT pyramidal tract. 24, 27, 41–44, 100, 138

PV Parvalbumin. 35, 147

RS Regular Spiking. 24, 42, 100

S1 primary somatosensory cortex. 19, 21, 46, 48–50, 52, 68, 141

SNc substantia nigra pars compacta. 29, 34, 35, 37

SNr substantia nigra pars reticulata. 29–31, 40

SPNs spiny projection neurons. 30, 31, 33, 35, 38, 40, 43–49, 55, 57, 59, 60, 62, 63, 65, 68–70, 100, 135, 137, 139, 141, 142, 148

SST Somatostatin. 35, 148

STN subthalamic nucleus. 29, 30, 38

TANs tonically active neurons. 37

VPM ventral posterior medial nucleus of the thalamus. 23–27, 142

Introduction

CHAPTER 1

Sensorimotor processing: from S1 to the DLS

Sensorimotor processing involves the integration of sensory inputs to guide motor actions, which is fundamental for animals to interact effectively with their environment. In rodents, the whisker system serves as an ideal model to study sensory integration, given its precise anatomical organization and well-defined pathways. In the primary somatosensory cortex (S1), the barrel cortex receives and integrates tactile information from the whisker pad and sends projections to the dorsolateral striatum (DLS), part of the basal ganglia (BG), which plays a role in motor control and action selection. Thus, corticostriatal (CS) projections are a key link between sensory perception and motor output. The first goal of this thesis was to study the organisation - and thus have a glance at the integration- of sensory (tactile) inputs at the cellular level within the BG. To do so, we focused on the barrel cortex projections to the DLS. In the following chapter, we will discuss the sensorimotor pathway linking the S1 (dedicated to tactile representation) to the DLS in rodents.

Contents

1.1 The Rodent Whisker-Barrel System 21
1.1.1 Somatotopy 21
1.1.2 Laminar organization 23
1.1.3 Somatosensory micro circuits 25
1.1.4 S1 outputs 27
1.2 The Basal Ganglia 28
1.2.1 Striatum history 29
1.2.2 Basal Ganglia anatomy 29
1.2.3 Striatal cell types 31
1.2.3.1 Striatal Projection Neurons 33
1.2.3.2 Striatal Interneurons 35
1.3 Corticostriatal projections 38
1.3.1 Parallel cortico-basal ganglia loops 38
1.3.2 Overlapping corticostriatal projections 40
1.3.3 Types of Corticostriatal Projection Neurons 41
1.3.4 Corticostriatal innervation of D1-D2 SPNs 43
1.3.5 Convergence of Corticostriatal Projections 45
1.3.6 Focus on S1 to DLS projections 46
1.4 Summary 49

1.1 The Rodent Whisker-Barrel System

Rodents are nocturnal animals that live in dark tunnels and rely heavily on their whiskers for navigation. These tactile organs enable rodents to gather information through a behavior called whisking, where they actively and rhythmically sweep their whiskers back and forth. This mechanism is akin to human palpation with fingertips and allows rodents to detect, recognize, and locate objects, as well as discriminate textures and engage in social interactions. Whisking helps rodents effectively explore their surroundings, avoid obstacles, and forage for food, making it an essential adaptation for their survival.

The absence of whiskers in humans might lead us to classify them as a highly specialised sensory organ and dismiss their study. However, studying the integration of whiskers inputs provide a unique opportunity to study the fundamental functional unit of the cerebral cortex: the cortical column, as theorized by Mountcastle (1957). Therefore, this system happens to be an ideal model to study and understand cortical circuitry.

1.1.1 Somatotopy

Whiskers are organized in arcs (1-8) and rows (A-E) on the snout, and this spatial pattern is stereotyped from animal to animal. When a whisker is deflected, the tactile information is relayed to the barrel cortex through a well-defined pathway involving the trigeminal nerve and the thalamus (section 1.1). In contrast to the continuous distribution of thalamic afferents in layer 4 observed in other areas of S1, the whisker-related region is characterized by thalamic afferents that form discrete clusters (Figure 1.1). These clusters are separated by gaps with sparse thalamocortical branches (septa). Those cylindrical structures ($\sim$ 200-300 µm) were first described and named *barrels* by Woolsey & Van der Loos (1970).

Neurons in each barrel respond more strongly - and in some cases exclusively - to a specific whisker (Simons 1978), and a single barrel receives rapid inputs from one specific whisker (Armstrong-James & Fox 1987). The evidence was strong enough to propose the name *barrel column*, referring to the cortical column hypothesis (Mountcastle 1957), including the radial column of cells located above

and below the layer 4, containing the barrels.

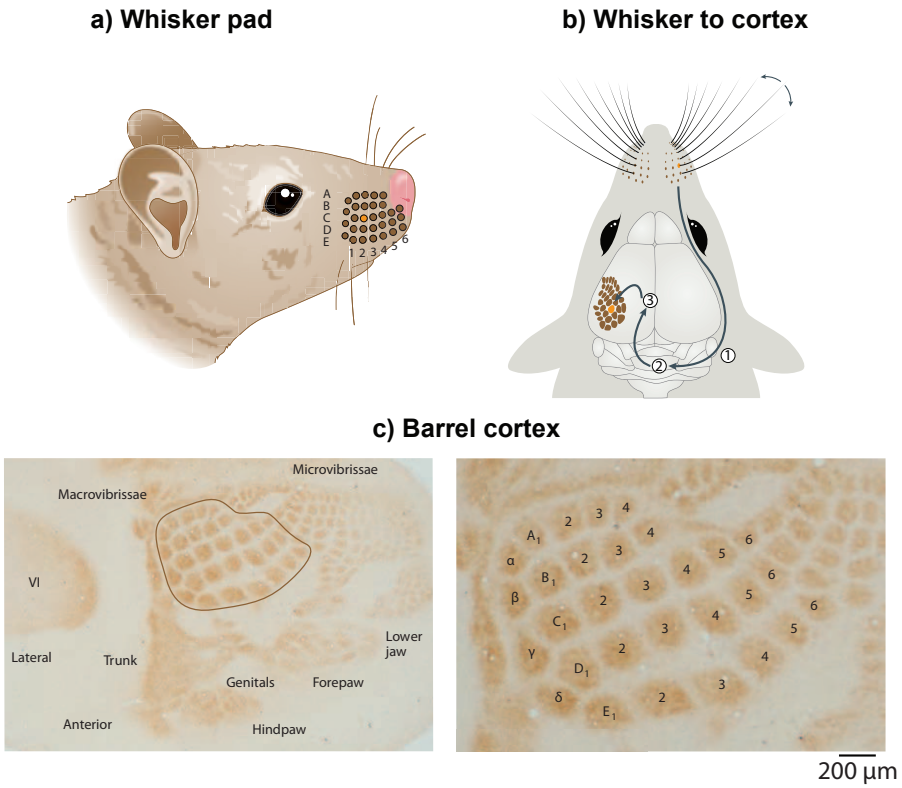

Figure 1.1: Organization of the whisker to barrels pathways.
a,b) Deflection of a whisker evokes a sequence of activity in trigeminal ganglion primary sensory neurons **(1)**, brainstem neurons **(2)** and thalamic neurons **(3)** before reaching S1. **c**) The whisker-related primary somatosensory cortex (wS1) of rodents contains obvious anatomical units called *barrels*, each of which represents an individual mystacial whisker and is somatotopically organized. *Addapted from* Petersen 2019; Kandel *et al.* 2021

.

The barrel cortex, like other neocortical areas, is predominantly composed of excitatory pyramidal neurons (80%), who make recurrent horizontal connections within the column (see subsection 1.1.2), supporting the theory of functional unit. The position of individual barrels is not random; rather, it corresponds precisely to the position of the corresponding whisker on the snout. Thus, the barrel cortex exhibits somatotopic organization: whiskers that are spatially close on the pad have adjacent representations in the barrel field (S1) (Figure 1.1). This

precise mapping enables the investigation of the relationship between specific sensory inputs and corresponding cortical responses.

1.1.2 Laminar organization

In addition to its horizontal and topographical organization, each column in the barrel cortex comprises six distinct horizontal layers: L6, L5B, L5A, L4, L2/3, and L1, spanning from the white matter to the pia surface. This layered arrangement, originally described by Santiago Ramón y Cajal in the late 19th century, separates these layers by their specific input sources, output destinations, and the types of neurons they contain. (Figure 1.2)

Layer 1: The molecular layer, also known as the plexiform layer, contains few neuronal cell bodies but is rich in horizontally oriented dendrites and axons. It contains a dense network of tangentially running axons from other cortical columns that synapses onto the apical dendrites of pyramidal neurons, whose somas are located in other layers within the column. This arrangement allows the molecular layer to modulate input from various cortical and subcortical regions.

Layers 2/3: contain medium-sized pyramidal neurons and are essential in the cortical relay and processing of information within the cortex. These layers primarily receive inputs from other cortical areas (corticocortical connections) and are heavily involved in corticocortical communication, sending and receiving inputs within the same hemisphere (association fibers) and across the opposite hemisphere (commissural fibers), thereby facilitating the processing and relay of information within the cortex.

Layer 4: is the primary recipient of thalamocortical inputs (from the ventral posterior medial nucleus of the thalamus (VPM)), making it the main input layer for sensory information. It contains densely packed excitatory stellate cells, which relay sensory input from the thalamus to the pyramidal cells in layers 2/3 and 5.

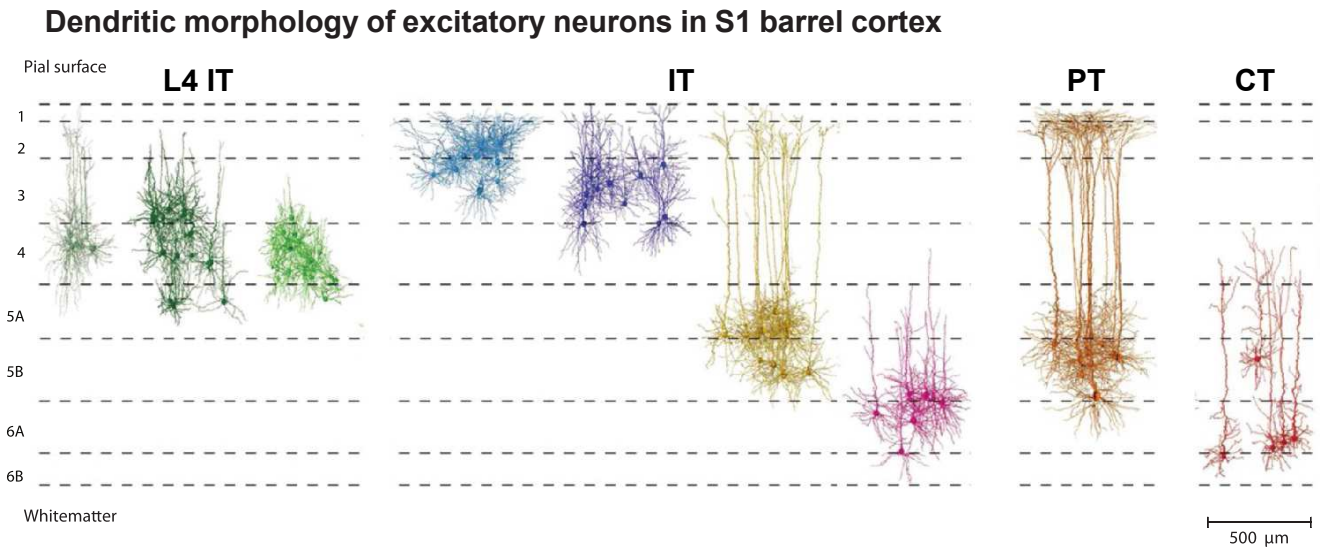

Figure 1.2: Columnar Organization of the Somatosensory cortex.
Cortical excitatory neurons in the six layers of a barrel column. L4 IT shows the three morphological classes of L4 IT neurons: pyramidal, star pyramidal and spiny stellate cells. Under IT are other intratelencephalic neurons of L2, L3, 5A/B and 6. PT shows pyramidal tract neurons of L5B. CT shows corticothalamic neurons of L6. *Adapted from* Harris & Shepherd 2015

Layer 5: contains large pyramidal neurons that integrate columnar information and project to cortical and subcortical structures. It is divided into two sublaminae, **5a** and **5b**, which differ in cell density, cell type, connectivity, and their specific inputs and outputs (Mercier *et al.* 1990; Schubert *et al.* 2001). While the pyramidal neurons in L5a are only intra-telencephalic (IT) (or Regular Spiking (RS)), L5b contains both pyramidal tract (PT) (intrinsic bursting (IB)) and IT neurons (Harris & Shepherd 2015; Petersen 2019) (Figure 1.2 ; Table 1.1, for further details, please refer to section 1.3).

Layer 6: consists of a diverse population of neurons, including fusiform cells and smaller pyramidal cells. The axons of these neurons project to the VPM and posterior medial nucleus of the thalamus (POm), forming part of the corticothalamic feedback loop (Figure 1.4).

Table 1.1: Comparison of the Morphological and Physiological Traits Distinguishing IT-Type and PT-Type Corticostriatal Neurons
Adapted from Steiner & Tseng 2017

Traits	IT-Type Neurons	PT-Type Neurons
Morphological	Medium-sized cell body	Large cell body
	Located in layer 3 and upper layer 5	Located in lower layer 5
	No layer 1 apical dendrites	Prominent layer 1 apical dendrites
	Output only within telencephalon	Striatal projection is a collateral of axon to brainstem and spinal cord
	Striatal projection is bilateral	Striatal projection is ipsilateral
Physiological	Slow conduction velocity	Rapid conduction velocity
	Low spontaneous activity (1.4 spikes/s)	Moderate spontaneous activity (14.8 spikes/s)
	Show spike adaptation	Do not show spike adaptation
	Not routinely activated by sensory input	Routinely activated by sensory input

1.1.3 Somatosensory micro circuits

To process tactile information, two primary pathways exist — lemniscal and paralemniscal —, each processing different levels of sensory information. The lemniscal pathway conveys precise tactile signals from the whiskers, such as fine texture and object location, while the paralemniscal pathway processes sensory information from whisking, which include motion information.

The **lemniscal pathway** relays sensory information from whiskers to the VPM nucleus of the thalamus, where thalamocortical axons project topographically

and massively to L4 of the cortex and to some extent to layers 2/3 and L5b (Petersen 2019; Bureau *et al.* 2006). The excitatory input from the VPM recruits layer 4 spiny stellate cells, which are part of highly interconnected, bidirectional intralaminar connections (Petersen & Sakmann 2000). These connections amplify the excitatory signals arriving in layer 4 (Pinto 2003) and facilitate recurrent connectivity within their own columns, connecting principally with neurons in layer 2/3 (Silver *et al.* 2003; Shepherd & Svoboda 2005). Pyramidal cells in layer 2/3 also target pyramidal cells in layer 5B (Thomson & Bannister 1998). Thus, the excitatory input that reaches layer 4 is integrated and subsequently distributed across layers 2/3 and 5 within a barrel column (Figure 1.3).

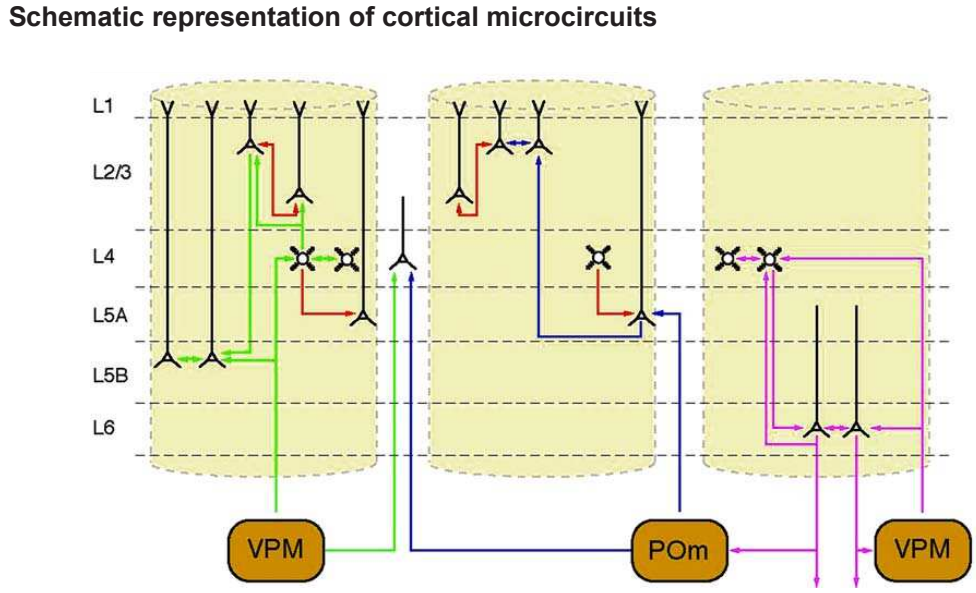

Figure 1.3: Somatosensory circuits.
Left: The 'canonical' microcircuits receiving lemniscal thalamic input from the VPM predominantly in layer 4 (and to lesser degree in layer 5B). Middle: Intracortical microcircuits involved in the processing from signals arriving from the paralemniscal pathway (input from the POm to L5A pyramidal neurons). Right: Synaptic connections involved in the thalamo-cortical-corticothalamic feedback circuit between layer L4 spiny neurons, L6 pyramidal cells and the VPM. *Adapted from* Lübke & Feldmeyer 2007

The barrel column also receives excitatory inputs from another thalamic nucleus: the POm, which forms the **paralemniscal pathway**. This pathway makes highly specific innervations onto L5a neurons (Manns *et al.* 2004; Bureau *et al.* 2006), contributing to the integration of higher-order sensory information across

larger cortical networks (Figure 1.3). It has been shown that the paralemniscal pathway can transform temporally encoded whisking information into a rate code, meaning that changes in whisker movement frequency are translated into varying neuronal firing rates. This mechanism plays a crucial role in integrating higher-order sensory information across broader cortical networks, contributing to more sophisticated tactile processing. For instance, the paralemniscal pathway is particularly active during changes in behavioral state, especially in relation to sensory and nociceptive processing (Chiaia *et al.* 1991a; Diamond *et al.* 1992; Petty *et al.* 2021; Osaki *et al.* 2022). These studies suggest that the POm is essential for modulating sensory responses in different arousal states and in the perception of pain.
Additionally, the paralemniscal pathway is implicated in driving learning-related plasticity at its cortical synapses, involving mechanisms such as sensory-evoked long-term potentiation (LTP) and rapid synaptic plasticity (Gambino *et al.* 2014; Audette *et al.* 2019; Zhang & Bruno 2019). These processes enable the cortex to adapt and refine its sensory representations through experience and learning.
In summary, the POm serves a dual role in both dynamic sensory processing and learning-related synaptic modifications, underscoring its importance in complex sensory integration and behavioral adaptation.

1.1.4 S1 outputs

The barrel cortex makes cortical and subcortical connections, mainly throughout L5 axons (intra-telencephalic (IT) and pyramidal tract (PT), Figure 1.4). These neurons serve as major output pathways, with PT neurons projecting within the ipsilateral hemisphere and IT neurons having bilateral projections (Harris & Shepherd 2015). The barrel cortex projects back to the somatosensory thalamic nuclei (VPM and POm) via cells in layers 5 and 6 (Wright *et al.* 2000; Cruz *et al.* 2023; Fox 2008). Layer 5 pyramidal neurons form extensive corticocortical and corticosubcortical connections, reaching the basal ganglia, brainstem, and spinal cord (Cowan & Wilson 1994; Petersen 2019). Additionally, neurons in layer 2/3 also project outside the cortical column, although to a lesser extent, reaching some subcortical regions (Fox 2008).

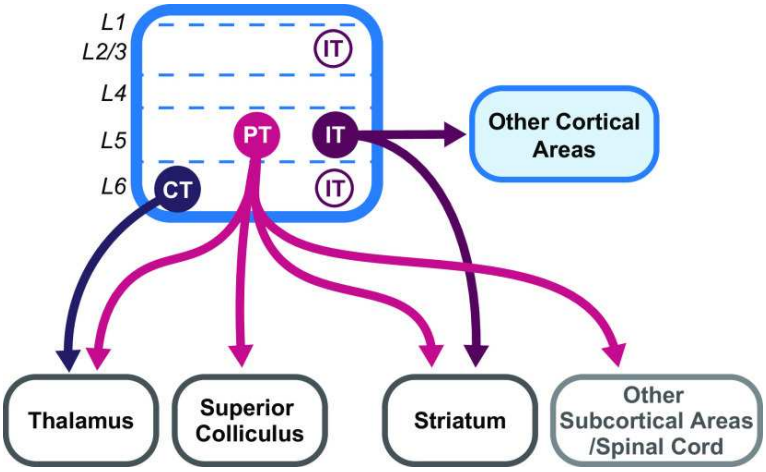

Figure 1.4: Cortical outputs to subcortical areas.
The thalamus is the exclusive noncortical target of corticothalamic (CT) neurons found in layer 6. Pyramidal tract (PT) neurons in layer 5 have subcortical projections (thalamus, superior colliculus, striatum, and spinal cord). Intratelencephalic (IT) neurons are found throughout cortical layers and make cortico-cortical, corticostriatal and subcortical connections. *Adapted from* Cruz *et al.* 2023

S1 sends dense projections to the dorsal striatum, the main input structure of the basal ganglia. The basal ganglia are involved in the expression of sensorimotor behavior, as it plays crucial roles in motor control and decision making. In the next section, we will focus on the description of this structure, as it is thought to play pivotal roles in sensorimotor processing.

1.2 The Basal Ganglia

The basal ganglia (BG) are a set of forebrain nuclei that receive inputs from sensory, associative, and motor cortices, playing a key role in motor control. The striatum is the largest nucleus of the BG and also its main input nucleus. Integrating diverse cortical and thalamic signals, the striatum targets other BG nuclei and plays a crucial role in modulating motor regulation and decision-making. However, the fine organization of cortical inputs to the striatum, which continuously provide sensory and motor information from the entire body to the BG, is still under debate.

1.2.1 Striatum history

First described by Thomas Willis in 1664 as the *corpus striatum* in his book *Cerebri Anatome*, the striatum was hypothesized to be a key structure related to sensory and motor functions due to its anatomical proximity to the ascending and descending fiber bundles from these regions. In 1876, neurologist David Ferrier proposed a link between the striatum and movement control: he found that unilateral electrical stimulation of the striatum in dogs resulted in contraversive movements (Ferrier 1876). Despite this early hypothesis, its precise role remained largely unknown for a century. At the beginning of the 20th century, studies began to shed light on its function: brain lesions in the striatum were observed to result in movement disorders (Wilson 1914; Wilson 1912). This discovery marked the beginning of a deeper understanding of the striatum's crucial role in motor control and coordination.

1.2.2 Basal Ganglia anatomy

The BG are a group of interconnected subcortical nuclei: the striatum (see subsection 1.3.1 for anatomical details), the subthalamic nucleus (STN), the globus pallidus (external and internal, GPe and GPi, respectively), and the substantia nigra (pars reticulata and pars compacta, SNr and SNc) (Figure 1.5). The two primary outputs nuclei of the BG are the GPi and the SNr, both composed exclusively of inhibitory projection neurons that exert tonic inhibition on premotor centers in the brainstem and thalamus (Mink 1996). In the following section, we will briefly describe the different BG nuclei and their connections.

Striatum: The main input nucleus of the BG and the largest subcortical structure in the mammalian brain: approximately 10 cm^3 in humans (Schröder *et al.* 1975; Yin *et al.* 2009a), 2 cm^3 in non-human primates (Yin *et al.* 2009a), and between 20 and 37 mm^3 in mice (Rosen & Williams 2001). The striatum receives cortical, thalamic, and dopaminergic inputs, and it is organized into dorsal and ventral regions based on the origins of these inputs and their efferent targets (see subsection 1.3.1). The dorsal striatum consists of the caudate nucleus and putamen in humans, or the dorsomedial striatum (DMS) and dorsolateral striatum (DLS) in rodents (Voorn *et al.* 2004). It contains two populations of

GABAergic projection neurons (spiny projection neurons (SPNs)) that project either monosynaptically, or through relay nuclei (STN/GPe), to the SNr/GPi (direct and indirect pathways, respectively; see subsubsection 1.2.3.1, Figure 1.5).

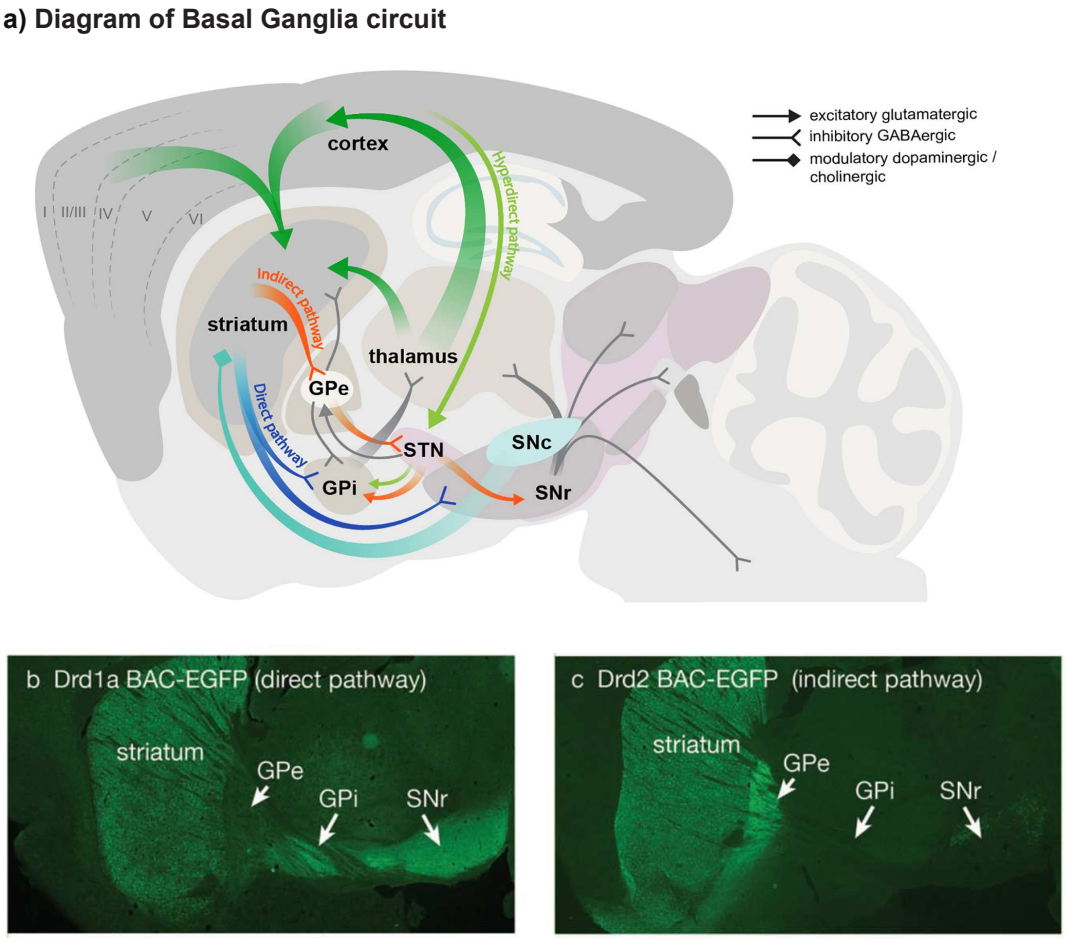

Figure 1.5: Diagram of Basal Ganglia circuit.
a) Schematic sagittal view of BG pathway. The striatum receives excitatory corticostriatal and thalamic inputs. Outputs of the basal ganglia arise from the internal segment of the GPi and SNr, which are directed to the thalamus, superior colliculus and pendunculopontine nucleus (PPN). The direct (blue) and indirect pathway (orange) pathway originates in the striatum. **b,c**) Fluorescent image of a sagittal brain section from a mouse expressing eGFP under regulation of the Drd1a or Drd2 promoter, revealing the 2 pathways targeting different nuclei. *Adapted from* Gerfen & Surmeier 2011; Blumenstock & Dudanova 2020

STN: Part of the indirect pathway of the basal ganglia circuitry, the STN receives inhibitory input from the GPe and provides excitatory glutamatergic input to the GPi and SNr.

Globus Pallidus: Divided into the external globus pallidus (GPe) and internal globus pallidus (GPi), these segments have distinct anatomical connections and functional roles. The GPe receives inhibitory input from the striatum and sends inhibitory projections to the STN, GPi, and SNr, acting as a relay and modulator within the BG circuitry. In contrast, the GPi, which receives inhibitory inputs from the striatum and excitatory inputs from the STN, projects inhibitory signals to the thalamus and brainstem. This projection regulates thalamocortical and brainstem motor circuits, making the GPi a major output nucleus of the BG with a critical role in movement regulation.

SNc: Provides dopaminergic inputs to the striatum, where it modulates the activity of SPNs. It exerts excitatory effects on the direct pathway and inhibitory effects on the indirect pathway, thereby influencing the overall balance and function of the basal ganglia circuitry.

SNr: Receives input from the striatum, GPe, and STN, and sends inhibitory projections to the thalamus and brainstem, serving as a major output nucleus of the BG.

As we can see from the description of the different interconnections within the BG, the striatum gives rise to two distinct pathways within the basal ganglia, each leading to opposite effects on behavior. The direct pathway inhibits the SNr and GPi, thereby releasing tonic inhibition on the thalamus and facilitating movement (Figure 1.6). In contrast, the indirect pathway maintains this inhibition.

1.2.3 Striatal cell types

In rodents, 95% of striatal cells are GABAergic SPNs (Figure 1.9). All SPNs synthesize GABA via Glutamic Acid Decarboxylase (GAD) and thus provide inhibitory inputs to target cells (Oertel & Mugnaini 1984). These neurons can be classified into two equally distributed populations, differentiated by their projection targets, dopamine receptor expression, and neurochemical markers. SPNs expressing the D1 receptor project directly to the GPi and SNr, forming the direct pathway. In contrast, SPNs expressing the D2 receptor project to the GPe, which then projects to the GPi, constituting the indirect pathway (Figure 1.5).

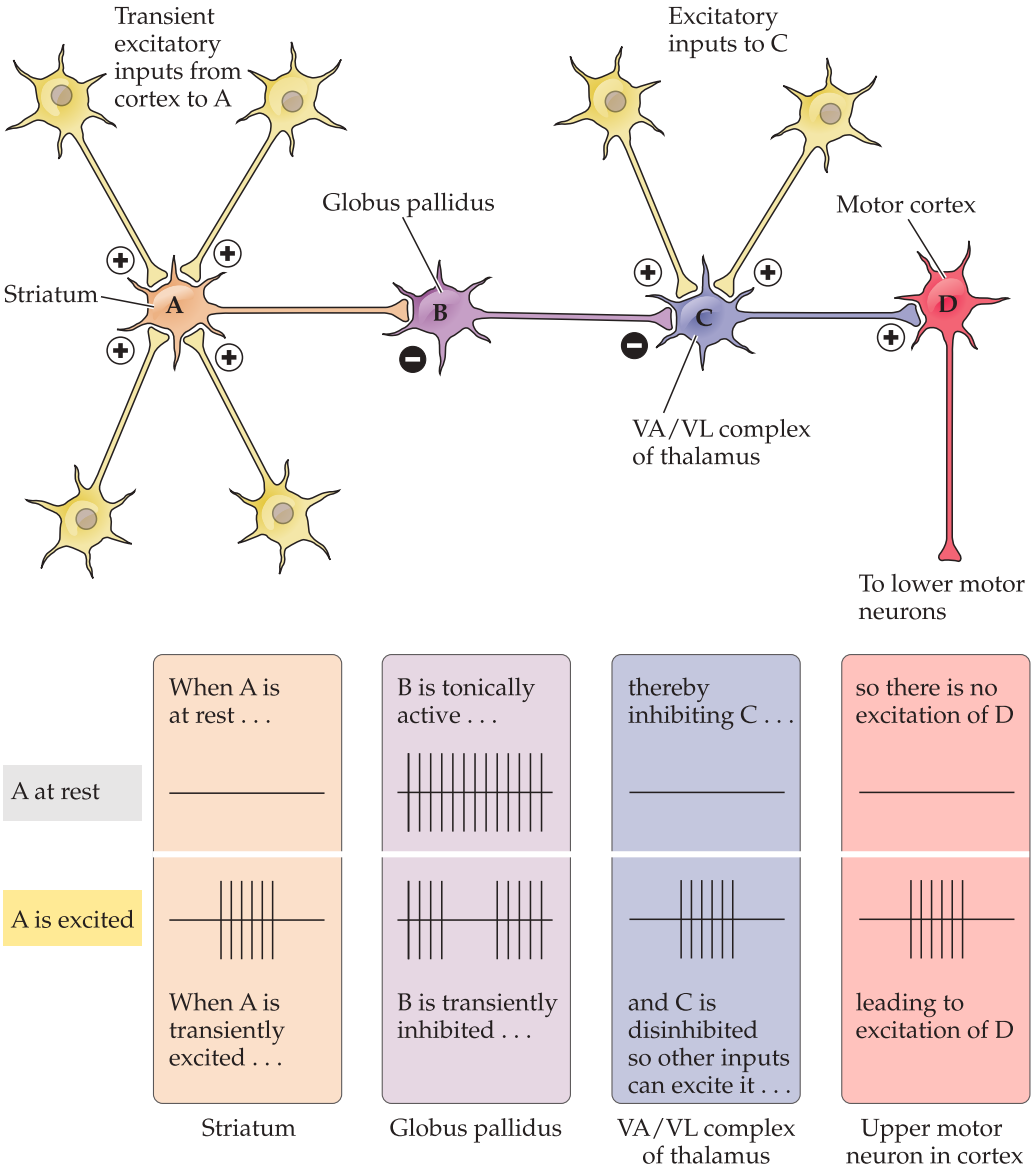

Figure 1.6: Disinhibitory circuits from the direct pathway.
Because the medium spiny neurons of the striatum are GABAergic (inhibitory), the net effect of the phasic excitatory inputs that reach the striatum from the cortex is to open a physiological gate by inhibiting the tonically active inhibitory cells of the globus pallidus and substantia nigra pars reticulata. When the pallidal cells are inhibited by activation of the medium spiny neurons, the thalamic neurons are disinhibited and can trigger the activation of upper motor neurons in the cortex. This disinhibition allows the upper motor neurons to send commands to local circuit neurons and lower motor neurons that in turn initiate movement. *Adapted from* Purves *et al.* 2018

Dopamine affects these two types of SPNs differently. When dopamine binds

D1 receptors, it stimulates adenylyl cyclase to produce cAMP, increasing intracellular calcium and neuron excitability. Conversely, D2 dopamine receptors inhibit adenylyl cyclase activity, which decreases neuron excitability (Figure 1.7). Activation of the direct pathway reduces inhibitory activity in the output nuclei, thereby disinhibiting downstream targets, while the indirect pathway increases downstream inhibition (Figure 1.6). Consequently, activation of the direct and indirect pathways is thought to have opposite effects on the basal ganglia output nuclei.

The remaining 5% are interneurons, which do not project out of the striatum. Their axons remain within the striatum and modulate the activity of the SPNs (Figure 1.9).

1.2.3.1 Striatal Projection Neurons

SPNs are characterized by medium-sized soma and extensive dendritic arborizations (Figure 1.7). In rodents, their cell bodies are approximately 12 to 20 µm in diameter with 4 to 5 primary dendrites exhibiting high spine density. These dendrites can extend up to 300 µm, forming a complex arborization which is crucial for synaptic integration (Wilson & Groves 1980). SPNs axons arise from the soma or a large dendritic trunk, projecting both locally and distally within and outside the striatum. The spiny dendrites and local axon collaterals facilitate both local and long-range inhibitory innervation, which is essential for proper basal ganglia function (Kawaguchi *et al.* 1990) (Figure 1.7).
SPNs exhibit a highly hyperpolarized resting membrane potential, typically lower than -75 mV, and a low input resistance (15-30 MΩ, Wilson & Groves 1981). They display inward rectification of the I/V curve, and a long delay to initial spike (Charpier & Deniau 1997; Nisenbaum & Wilson 1995). These intrinsic properties, mainly governed by inwardly rectifying potassium channels (Kirs), lead to quiescent cells that require significant excitatory input to generate action potentials (Wilson 1993; Mahon *et al.* 2000; Mermelstein *et al.* 1998).
D1R- and D2R-SPNs, while having similar electrophysiological profiles, differ in their intrinsic excitability and morphological features. D2R-SPNs are generally more excitable with a lower rheobase, whereas D1R-SPNs possess more extensive dendritic arbors with numerous primary dendrites, branch points, and tips (Cepeda *et al.* 2008; Gertler *et al.* 2008; Planert *et al.* 2013) (Figure 1.7).

SPNs receive various excitatory and inhibitory inputs that regulate their activity. Major excitatory inputs come from the cortex and thalamus, while dopaminergic inputs from the SNc (Dorsal striatum) or VTA (Ventral Striatum: Nucleus Accumbens) play crucial modulatory roles (McGeorge & Faull 1989; Berendse & Groenewegen 1990; Bentivoglio *et al.* 1979). Inhibitory inputs are provided by local axon collaterals from other SPNs and by striatal interneurons (Figure 1.9).

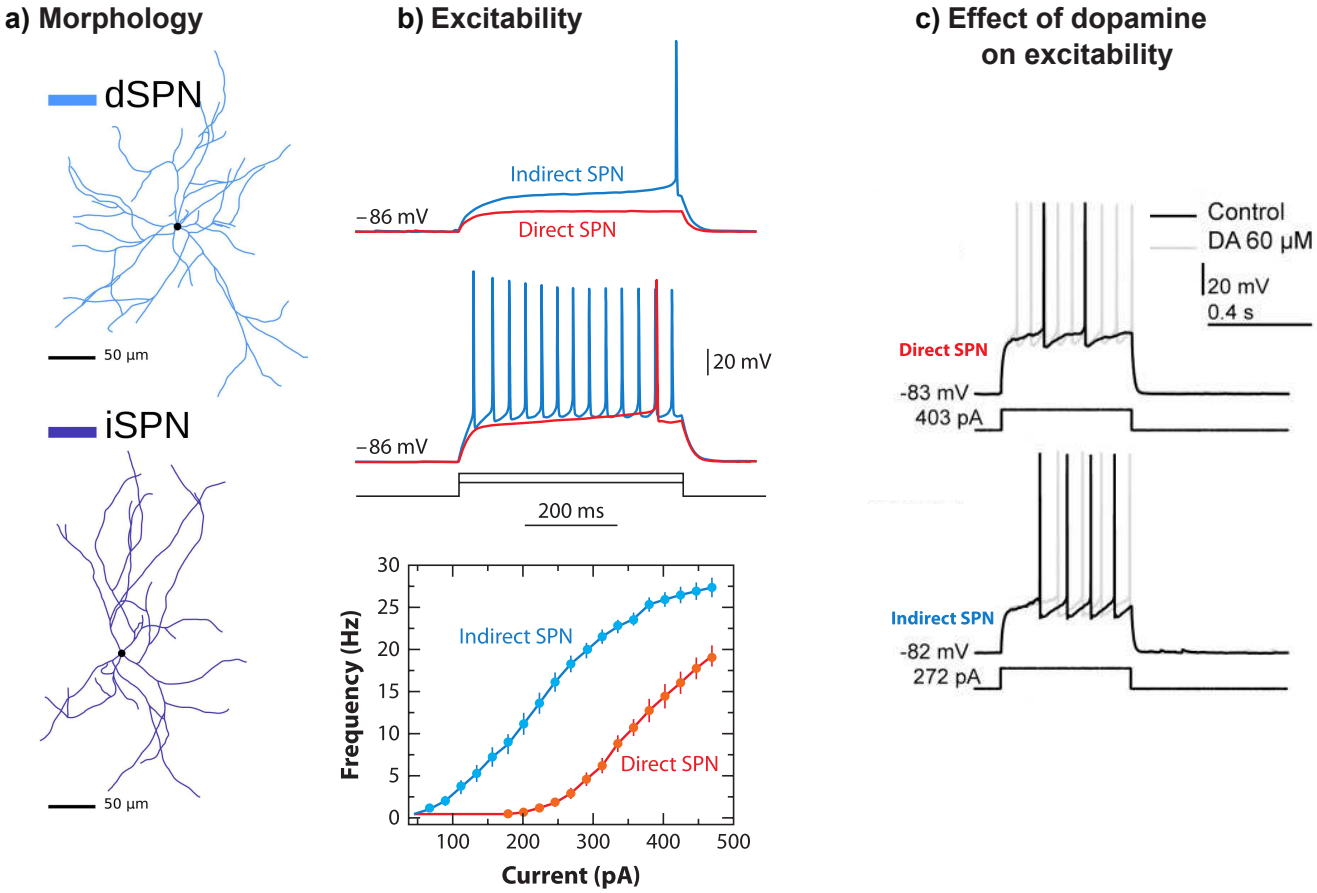

Figure 1.7: Dichotomous anatomy and physiology of direct- and indirect-pathway SPNs.
a) Reconstruction of a single dSPN (D1) and iSPN (D2) with dendrites (blue) and black dot for the soma. **b**) Summary of the responses of direct- and indirect-pathway SPNs to a range of intrasomatic current steps; indirect-pathway SPNs were more excitable over a broad range of injected currents. **c**) The effect of dopamine (DA) was tested near -80 mV, direct-pathway SPNs increased spiking in response to the same step current. *Adapted from* Carannante *et al.* 2024; Gerfen & Surmeier 2011; Planert *et al.* 2013

In contrast to cortical afferents, which synapse on the dendritic spines of SPNs (section 1.3), local circuit neurons form synapses on the dendritic shafts and near the cell soma (Figure 1.8), thereby modulating the effectiveness of cortical activation of more distal dendrites. In addition, the dorsal striatum also receives dense dopaminergic innervation from the SNc. Dopamine influences SPNs activity as well as the activity of different striatal interneurons and corticostriatal afferents, further impacting the overall activity within the striatum (Bamford *et al.* 2004; Gerfen & Surmeier 2011; Tritsch & Sabatini 2012). Dopaminergic synapses are positioned at the base of SPN dendritic spines, close to cortical synapses, allowing for selective modulation of cortical input (Figure 1.8).

1.2.3.2 Striatal Interneurons

Striatal interneurons, though less numerous than SPNs (5%, see Figure 1.9), are crucial for modulating striatum's activity. These interneurons are categorized into GABAergic and cholinergic types (Figure 1.9).

GABAergic Interneurons

Parvalbumin (PV)-Expressing Interneurons: Constituting about 1-2% of striatal neurons, these interneurons have spherical cell bodies ($\simeq$ 16 µm) and short, densely arborized axons. They are characterized by a hyperpolarized resting membrane potential ($\simeq$ -70 to -75 mV) and the ability to fire at high frequencies (Tepper *et al.* 2010; Kawaguchi *et al.* 1995).

Somatostatin (SST)/NPY/NOS-Expressing Interneurons: These interneurons have small cell bodies ($\simeq$ 15 µm) with 3-4 aspiny dendrites and sparse axonal arborization. Known as persistent and low-threshold spiking interneurons, they have a depolarized resting membrane potential ($\simeq$ -60 to -55 mV) and high input resistance (>500 MΩ), allowing them to fire persistently at low thresholds (Tepper *et al.* 2010; Kawaguchi 1993).

Calretinin-Expressing Interneurons: Medium-sized ($\simeq$ 12-20 µm), these interneurons have less dense dendritic arborizations (Tepper *et al.* 2010; Bennett & Bolam 1993). Their exact functional roles are less understood, but they contribute to inhibitory control within the striatum.

All of these GABAergic interneurons are innervated by thalamic and cortical neurons and provide strong feedforward inhibition on SPNs. Parvalbumin interneurons offer robust inhibition, while somatostatin interneurons provide weaker but essential synaptic inhibition. The specific roles of these interneurons are believed to be region-specific within the striatum, differing between the DMS and the DLS (Gittis *et al.* 2010; Fino *et al.* 2018).

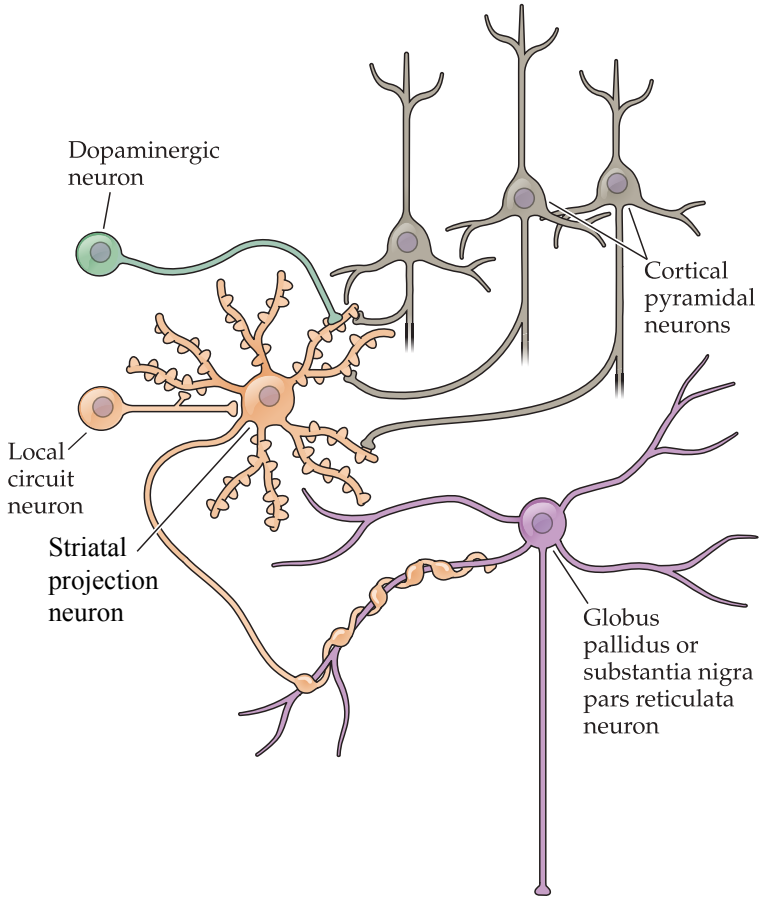

Figure 1.8: Convergent inputs onto single SPN.
Diagram showing convergent inputs onto a SPN from cortical neurons, dopaminergic cells of the SNc, and local circuit neurons within the striatum. The arrangement of these synapses indicates that the response of the medium spiny neurons to their principal input, derived from the cerebral cortex, can be modulated by dopamine and the inputs of local circuit neurons. The primary output of the medium spiny cells is to neurons in the globus pallidus and substantia nigra pars reticulata. *Adapted from* Purves *et al.* 2018

Cholinergic Interneurons

These giant aspiny interneurons, called cholinergic interneurons (ChINs) or tonically active neurons (TANs), represent about 1% of striatal neurons. They are characterized by large cell bodies ($\simeq$ 50 µm) and extensive axonal fields ($\simeq$ 2 mm) (Tepper *et al.* 2010). They express choline acetyltransferase (Bolam *et al.* 1984; Difiglia 1987) and fire tonically at 2-10 Hz (Schulz & Reynolds 2013). Their tonic activities are interspersed with phasic responses, including short pauses in their firing in response to salient or reward-predictive stimuli (Apicella 2007; Apicella *et al.* 2011). These pauses occur after conditioning and are associated with bursts in dopaminergic neuron firing, thereby highlighting their role in learning. It is therefore thought that TANs play a role in regulating striatal activity in response to salient environmental stimuli and interact closely with dopaminergic inputs from the SNc (Tritsch & Sabatini 2012; Tepper & Bolam 2004; Schulz & Reynolds 2013).

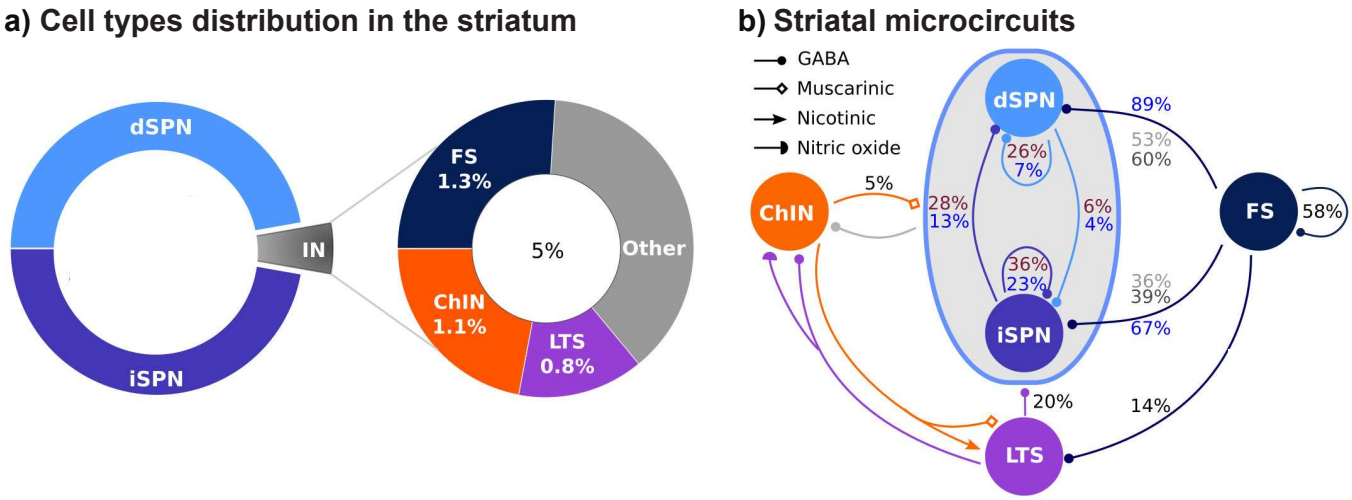

Figure 1.9: Organization of the striatal microcircuit.
a) The main cells in the striatum are the striatal projection neurons (SPN), they constitute around 95% of the neurons and they are divided into two subpopulations (D1-dSPNs and D2-iSPNs). The remaining 5% of the neurons are interneurons, among which are the cholinergic, fast-spiking, and low threshold-spiking subtypes. **b**) Schematic connectivity within dSTR involving dSPN, iSPN, FS, LTS, and ChIN. Connection probabilities within and between neuronal subtypes are shown by respective arrows; numbers in red correspond to connection probabilities for a somatic pair at a distance of 50 µm, while numbers in blue correspond to 100 µm. *Adapted from* Carannante *et al.* 2024

1.3 Corticostriatal projections

The activity of striatal cells is directly influenced by excitatory inputs from the neocortex and thalamus. Therefore, the information relayed by SPNs within the basal ganglia circuits is shaped by the activity of corticostriatal and thalamostriatal afferents. Cortical inputs to the striatum originate from pyramidal neurons in layer 5 and, to a lesser extent, from cells in other layers of various cortical regions. These inputs are bilateral, with a predominance on the ipsilateral cortex, and are believed to convey sensory and motor planning information to the striatum, thus enabling motor control (Reig & Silberberg 2014; de la Torre-Martinez *et al.* 2023). These neurons use glutamate as their neurotransmitter. However, it has been recently demonstrated by Rock *et al.* 2016, using optogenetic tool, that sparse direct GABAergic projections from the auditory and motor cortices also reach SPNs.

1.3.1 Parallel cortico-basal ganglia loops

Cortico-striatal afferents are organized topographically, maintaining spatial relationships between cortical areas within the striatum (Selemon & Goldman-Rakic 1985; Alexander & Crutcher 1990; Lee *et al.* 2020). This topographic organization is also preserved across other BG nuclei (Parent 1990; Parent & Hazrati 1995), which has led to the hypothesis of three parallel loops within the BG: the sensorimotor, associative, and limbic loops. (Figure 1.10).

The **sensorimotor loop** originates in the sensorimotor cortex, including the motor, premotor, supplementary, and somatosensory cortices. It projects to the dorsolateral striatum (DLS) in rodents (putamen in primates), and extends to the dorsolateral regions of other BG nuclei. It loops back to the cortex via the ventrolateral thalamus.
The **associative loop** begins in the dorsolateral prefrontal and lateral orbitofrontal cortices, projects to the dorsomedial striatum (DMS) (caudate nucleus in primates), proceeds through the dorsomedial GPi, and returns to the cortex via the ventral anterior thalamus.
The **limbic loop** involves projections from limbic areas to the ventral striatum. This loop connects through the limbic portions of the GPe, medioventral STN,

and ventral GPi, and it loops back to the cortex via the medio-dorsal thalamus. These loops delineate three functional regions within the striatum: dorsolateral (sensorimotor), dorsomedial (associative), and ventral striatum or nucleus accumbens (limbic) (Figure 1.10).

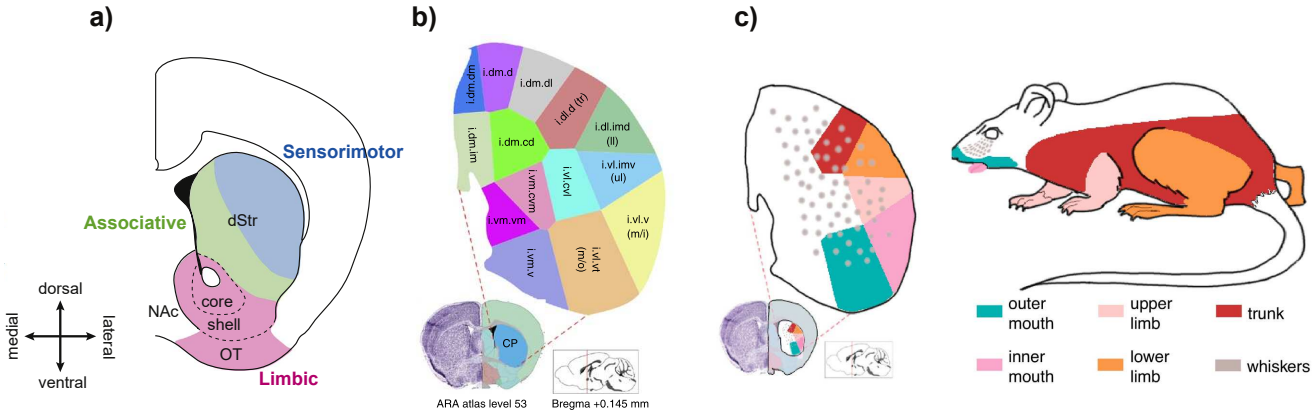

Figure 1.10: Striatal somatotopic map in the DLS.
a) Segregation of the striatum into associative, sensorimotor and limbic parts. **b**) overview of striatum domains based on their connectivity. The DMS is divided into intermedial, dorsomedial, dorsal, centromedial and dorsolateral domains. The DLS is divided into dorsal and intermedial dorsal, and the ventrolateral striatum into intermedial ventral, ventral and ventrolateral. The dorsolateral and ventrolateral parts both received inputs from sensorimotor cortical areas. **c**) Somatotopic organization of the DLS. DLS divided into five domains. Mouse body parts color-coded based on the striatal body map. *Adapted from* Chuhma *et al.* 2017; Hintiryan *et al.* 2016; Robbe 2018

Within each loop, corticostriatal inputs maintain the somatotopic organization seen in the cortex (Figure 1.10). For example, the spatial organization of cortical hindlimb and forelimb areas is preserved in the dorsolateral striatum (Takada *et al.* 2013). This supports the notion that each cortical region drives a specific loop, facilitating parallel processing of cortical information via segregated circuits. Moreover, functional studies have demonstrated that activity in striatal subregions is closely aligned with activity in their corresponding cortical areas, further validating the presence of multiple parallel cortico-basal ganglia loops (Choi *et al.* 2012; Peters *et al.* 2021).

Recent studies have however challenged this traditional view of well segregated projections within the dorsal striatum. Hunnicutt *et al.* 2016 and Hintiryan

et al. 2016 used connectomics to map corticostriatal projections in the dorsal striatum, identifying 29 distinct domains based on these projections. They further subdivided the DLS into five subregions associated to different body parts: trunk, lower limbs, upper limbs, inner mouth, and outer mouth (Hintiryan *et al.* 2016, Figure 1.10). Additionally, sensory and motor corticostriatal projections were not limited to the classically defined DLS but cover most of the dorsal striatum, including the DMS. Notably, projections from the whisker-related barrel cortex extended into five DLS subregions and beyond.
In 2021, the same group mapped the output pathways of the basal ganglia (SNr, GPe) from the striatum, identifying six parallel cortico-basal ganglia-thalamic subnetworks. These subnetworks sequentially transmit specific subsets of cortical information through every element of the cortico-basal ganglia-thalamic loop (Foster *et al.* 2021).

1.3.2 Overlapping corticostriatal projections

Although the corticostriatal projections are highly topographically organized, they exhibit partial overlap and interdigitation (Flaherty & Graybiel 1991; Flaherty & Graybiel 1995; Hoffer & Alloway 2001; Brown *et al.* 1998; Takada *et al.* 1998). Any given region of the striatum receives convergent inputs from multiple, often functionally related or anatomically interconnected, cortical areas (Brown *et al.* 1998; Hooks *et al.* 2018; Hoffer & Alloway 2001; Wall *et al.* 2013; Hintiryan *et al.* 2016). For instance, cortical areas involved in triggering arm movements or representing sensory stimuli from the arm project to a specific striatal region, while cortical regions related to sensory and motor representation of the face project to a more ventral region of the striatum (Flaherty & Graybiel 1991; Flaherty & Graybiel 1994; Flaherty & Graybiel 1995; Hoover *et al.* 2003).

As described in subsection 1.3.1, Hintiryan *et al.* 2016 found that sensory and motor corticostriatal projections are not restricted to the DLS and cover most of the dorsal striatum, including the DMS. Functional studies in these striatal regions have shown that SPNs can respond to various modalities, including motor, tactile, auditory, and visual, highlighting the convergence and overlap of multiple channels within specific striatal subregions (Nagy *et al.* 2005; Reig & Silberberg 2014; Charpier *et al.* 2020; Chudler *et al.* 1995) (Figure 1.11).

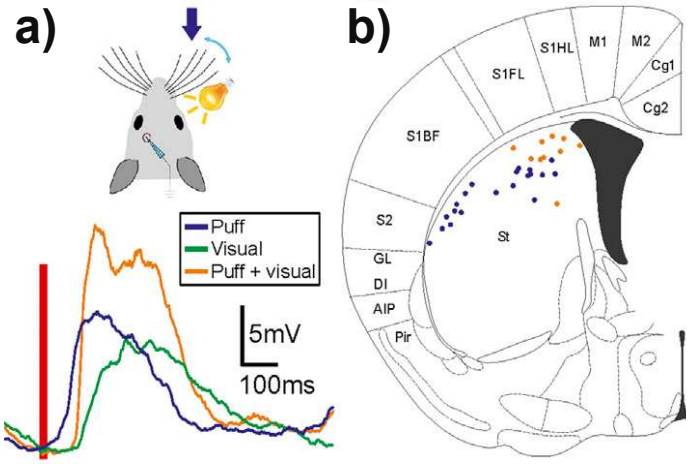

Figure 1.11: Multisensory integration in the dorsal striatum.
a) Schematic of the stimulation procedure (top) and waveform average of the visual, tactile, and simultaneous visual and tactile responses in the same MSN (bottom). **b**) Topographic distribution of multisensory striatal neurons. Circles represent the somatic locations of all neurons tested for both visual and whisker stimulation. All neurons (colored blue and orange) responded to whisker stimulation, and only dorsomedial neurons (marked in orange) responded to both sensory modalities. *Adapted from* Reig & Silberberg 2014

1.3.3 Types of Corticostriatal Projection Neurons

The striatum is the only subcortical area receiving inputs from both intra-telencephalic (IT) and pyramidal tract (PT) neurons (Shepherd 2013). Early descriptions by Ramón y Cajal (1911) suggested that the corticostriatal (CS) projection arises as a collateral projection of corticofugal fibers from pyramidal neurons in deep layer 5, descending through the striatum via the internal capsule.

The two subtypes of CS neurons have been identified through studies using either anterograde or retrograde tracers (Wright *et al.* 1999; Wright *et al.* 2001). Wright *et al.* 1999 used two anterograde pathway tracers, PHA-L and BDA, and showed that two distinct types of CS pathways arise from the barrel cortex. One system, termed the "diffuse" system, gives rise to a grossely topographic projection to the striatum, characterized by a broad intrastriatal arborization. These neurons resemble IT-type neurons in their size, shape, and localization in upper layer 5 based on Wilson and al. previous work (Cowan & Wilson 1994; Wilson 1987). The second CS projection, termed the "discrete pathway," gives

rise to a topographically ordered projection with dense focal innervation patches, originating from corticofugal axons, suggesting it originates from PT-type corticostriatal neurons (Cowan & Wilson 1994; Wilson 1987) (Figure 1.12).

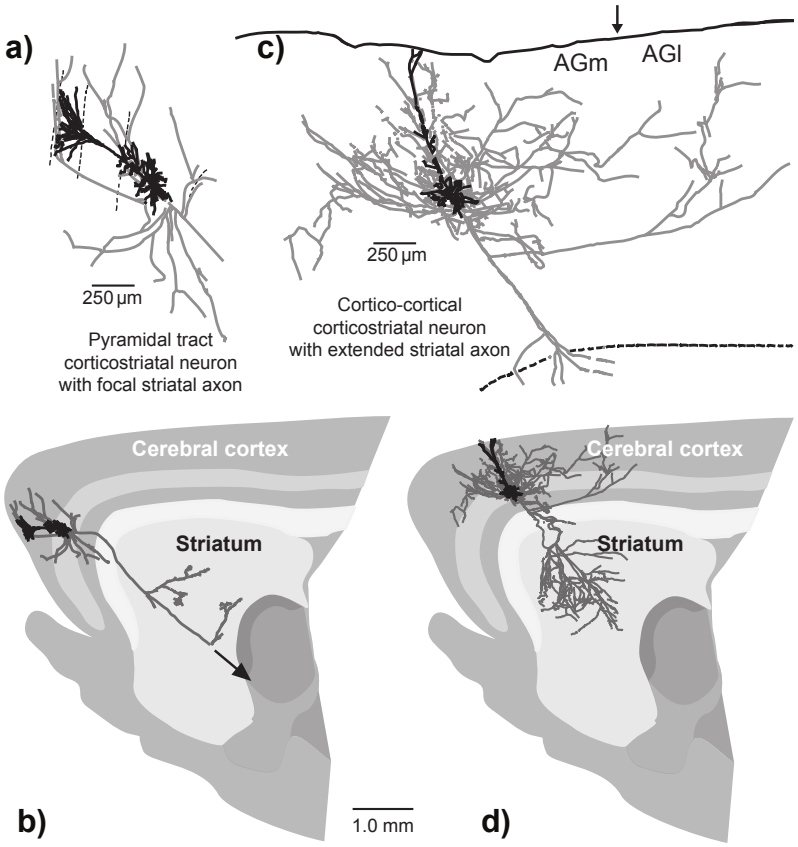

Figure 1.12: Subtypes of corticostriatal neurons.
Tracings of dendrites (black) and cortical (a and c) and striatal axons (b and d) (gray) show the two subtypes of corticostriatal neurons, which had been intracellularly labeled. **a**) The corticostriatal neuron depicted provides an axonal projection to the PT-type neuron. **b**) The PT axon (arrow) of this neuron gives off collaterals in the striatum, which display focal terminal arborizations. **c**) The corticostriatal neuron shown, located in the medial agranular cortex (AGm), is a bilaterally projecting cortico-cortical neuron that also extends axon collaterals bilaterally into the striatum (intra-telencephalic (IT)). **d**) This neuron has an axon that provides an extensive arborization pattern within the striatum but does not extend collaterals beyond the striatum. *Adapted from* Steiner & Tseng 2017; Cowan & Wilson 1994

The IT-type corticostriatal neurons have axon collaterals confined to the striatum and cerebral cortex (Cowan & Wilson 1994; Wilson 1987; Wise & Jones 1977; Zheng & Wilson 2002). These cells are found in the superficial half of layer 5 (L5a), with some also present in layers 2/3. They exhibit a Regular Spiking (RS)

pattern, firing at regularly spaced intervals when depolarized (Kim *et al.* 2015; De Kock *et al.* 2021). Their intrastriatal axon arborizes extensively and uniformly, covering a wide expanse of the striatum (about 1.5 mm in diameter) with sparse en passant terminals (Cowan & Wilson 1994; Kincaid & Wilson 1996).
In contrast, PT-type corticostriatal neurons project mainly to the brainstem or spinal cord, with collateral branches extending into the striatum (Cowan & Wilson 1994; Donoghue & Kitai 1981; Landry *et al.* 1984). These neurons are predominantly located in the deeper parts of layer 5 (L5b) and occasionally in layer 6. PT-type neurons, also known as intrinsic bursting (IB) neurons (Kim *et al.* 2015; De Kock *et al.* 2021), exhibit a high-frequency burst of spikes upon depolarization. Their striatal projections consist of fine collateral branches that scatter small, dense focal clusters of terminals (about 250 µm in diameter) across a 1- to 2-mm region of the striatum (Cowan & Wilson 1994). Additionally, their axon collaterals extend to multiple components of the basal ganglia circuits, such as the thalamus, STN, zona incerta, GPi, SNr, superior colliculus, and pontine nuclei (Gerfen *et al.* 2013; Gong *et al.* 2007). Thus, while the striatum is a target of PT corticostriatal projections, the same information is also sent to multiple components of the basal ganglia circuits.

1.3.4 Corticostriatal innervation of D1-D2 SPNs

While both types of corticostriatal neurons project to the striatum, anatomical studies have suggested some bias in the innervation of both types of SPNs (D1 and D2), with D1 SPNs being preferentially targeted by IT neurons and D2 SPNs by PT neurons. This prevailing view is supported by detailed analyses of the size of rat cortical axon terminals synapsing on SPNs (Lei *et al.* 2004; Reiner *et al.* 2003; Reiner 2010; Deng *et al.* 2015). These studies found that cortical terminals on D1 SPNs tend to be smaller than those on D2 SPNs. These observations have led to the conclusion that IT neurons project to D1 SPNs, whereas PT neurons project to D2 SPNs (Lei *et al.* 2004).

Despite these anatomical findings, electrophysiological studies have shown more nuanced results. For instance, Ballion *et al.* 2008 did not find robust differences in cortical responsiveness between SPNs identified by antidromic methods. Further studies by Ding *et al.*(2008) and Kreitzer & Malenka (2007) revealed

that cortical EPSCs evoked in D2 SPNs exhibit a lower paired-pulse ratio compared to D1 SPNs. This suggests that excitatory synapses on D2 SPNs have a higher probability of transmitter release. Since large terminals and perforated postsynaptic densities are characteristics of more efficacious synaptic contacts (Geinisman 1993; Sulzer & Pothos 2000), PT-type terminals are likely to have a higher probability of transmitter release and may more effectively activate their target neurons than IT-type terminals. Thus, those results could suggest stronger PT-type inputs to D2 SPNs. Additional research supports this notion: Takada *et al.* (2013) demonstrated that immunotoxin-mediated depletion of PT-type neurons in monkeys reduced cortical activation of D2 SPNs but not D1 SPNs. Surprisingly, Kress *et al.* (2013) reported that both types of cortical neurons (IT and PT) synapse onto both D1/D2 SPNs, however with stronger EPSC from PT for D1 SPNs compare to D2 SPNs.

Other studies have shown that the inputs to direct and indirect striatal neurons are differently organized based on cortical area. Anatomically, Wall *et al.* (2013) found that somatosensory and limbic areas preferentially provide inputs to D1 SPNs, whereas motor cortical areas target D2 neurons. They observed a 5:1 ratio of virus-labeled neurons in upper versus lower layer 5, rather than the expected 2:1 ratio based on the work of Reiner's group (Deng *et al.* 2015). This anatomical study (Wall *et al.* 2013), along with some electrophysiological studies, suggests that cortical area influence the relative strengths of CS inputs to D1 and D2 SPNs (Filipović *et al.* 2019; Lee *et al.* 2019; Johansson & Silberberg 2020) (Figure 1.13).

Thus, previous anatomical and functional studies have produced ambiguous results regarding the specific CS projections to D1 and D2 SPNs: does this organization vary based on the types of corticostriatal neurons that project, or the specific presynaptic cortical areas involved? Understanding how cortical inputs are organized in the direct and indirect pathways is crucial for developing models of how activity in these pathways can influences behavior (Morita *et al.* 2012; Carannante *et al.* 2024).

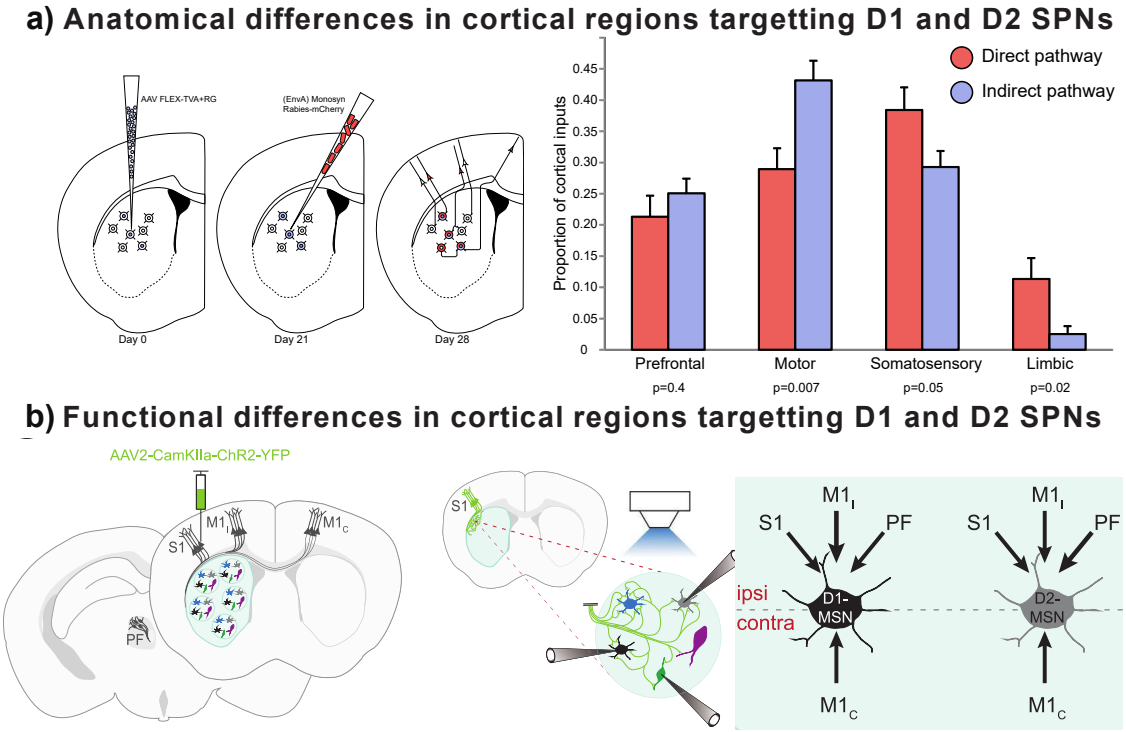

Figure 1.13: Differences in input to D1 and D2 SPNs.
a) Left: Monosynaptic rabies virus system to generate brain-wide maps of neurons that form synapses with direct- or indirect-pathway striatal projection neurons. Right: sensory cortical and limbic structures preferentially innervated the direct pathway, whereas motor cortex preferentially targeted the indirect pathway. **b**) Optogenetics activation of terminals from ipsi- or contralateral primary somatosensory cortex (S1) or primary motor cortex (M1), while obtaining simultaneous whole-cell recordings from pairs or triplets of SPNs. M1 and S1 differentially innervate D1 and D2 SPNs *Adapted from* Wall *et al.* 2013; Johansson & Silberberg 2020

1.3.5 Convergence of Corticostriatal Projections

Regarding the degree of convergence of CS inputs onto individual SPNs, quantitative studies have highlighted several key points. There would be an estimated 6:1 ratio between corticostriatal neurons (17 million) and SPNs (2.8 million) (Oorschot 1996). The dendritic field of each SPNs (400 µm in diameter) would cover a volume with around 2,850 other striatal neurons. Within this volume, projections from roughly 380,000 CS neurons could potentially reach the dendritic field of a single SPN (Steiner & Tseng 2017). However, each SPN receives approximately 5,360 corticostriatal synapses, indicating a maximum of 5,360

presynaptic partners per SPN (Kincaid *et al.* 1998).
As each individual corticostriatal axon typically makes about 40 synaptic boutons, it would imply that any given axon would establish only a few contacts with an individual SPN in its target area (Kincaid *et al.* 1998). This would result in each CS axon making contact with roughly 1% of the striatal neurons within its range. Given these observations, each SPN receives around 5,360 CS synapses and each CS neuron forms approximately 40 boutons, Kincaid *et al.* 1998 predicted that several thousand cortical neurons could connect to a single SPN. However, if each CS axon were to establish all of its synaptic contacts on a single postsynaptic neuron, this number would decrease to hundreds.

It seems that individual cortical neurons have CS axons organized to maximize their reach across numerous target neurons while minimizing the number of contacts with each specific postsynaptic neuron (Zheng & Wilson 2002).

Overall, cortical inputs to SPNs would be unique, and postsynaptic excitatory activation of individual SPN would be dependent on the convergence of inputs from multiple corticostriatal neurons (as there would be only few contacts from the same cell on a single SPN).

1.3.6 Focus on S1 to DLS projections

As discussed in section 1.1, the barrel cortex can be used to study if neurons located in a same barrel project to same region, and if neurons located in different barrels have some convergence in their targets. In other words, the presence of visible barrels in layer 4 allows the study of the topographic organization of projections from S1.

Projections from S1 (barrel field) are found throughout the dorsal striatum, with a higher concentration in the dorsolateral striatum (Hintiryan *et al.* 2016) (Figure 1.10). These projections are predominantly from cells in layer 5a, with some contribution from other layers (Mercier *et al.* 1990; Alloway *et al.* 1999; Wright *et al.* 1999; Wall *et al.* 2013). Anatomically, axons from different whisker cortical columns overlap in the dorsal striatum, suggesting broad vibrissal input to SPNs (Wright *et al.* 2000; Alloway *et al.* 2000). Yet, the topographic organization

of these projections is such that barrels located in the same row (e.g., A1, A2, A3, A4) project to a continuous stripe in the striatum (Figure 1.14). In contrast, barrels from different rows (e.g., A2, E2) project to distinct stripes arranged parallel to one another in the striatum, with the A-stripe lying laterally and the E-stripe lying medially (Alloway *et al.* 1999; Wright *et al.* 1999; Wright *et al.* 2000; Leergaard *et al.* 2000) (Figure 1.14).

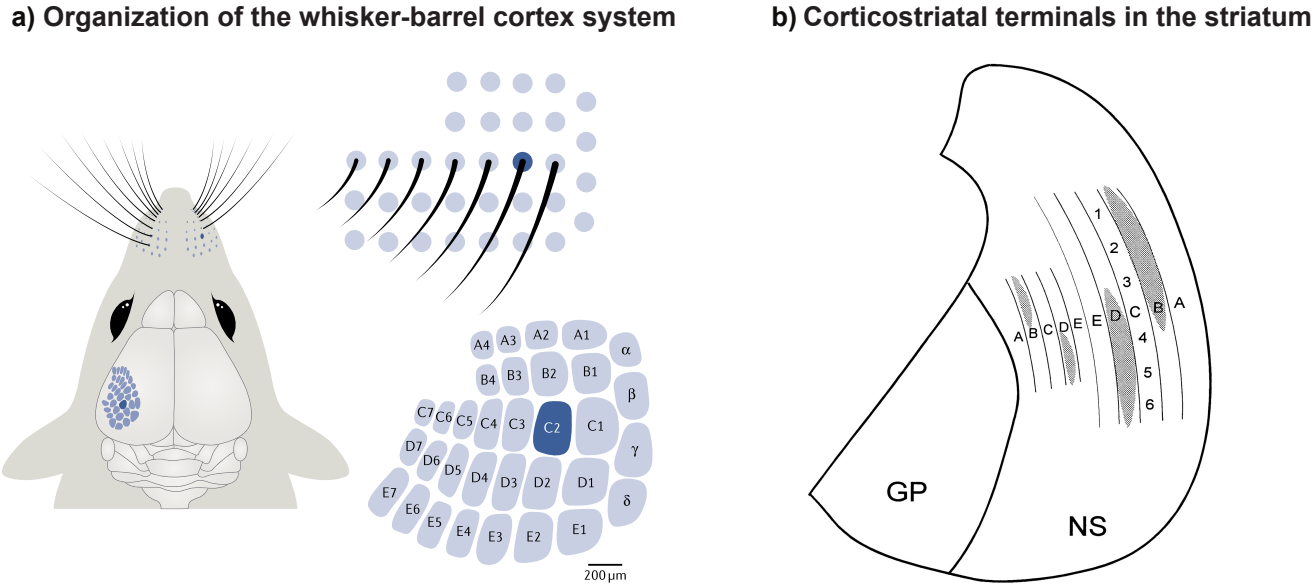

Figure 1.14: Anatomical organization of Corticostriatal projection from the barrel cortex.
a) Organization of the whisker-barrel cortex circuit, as seen in section 1.1. **b**) Diagram of a coronal section through the neostriatum illustrating the topography of projections from the SI whisker barrel cortex. The lateral neostriatum contains a prominent representation of rows A–E; the medial neostriatum contains a smaller, mirror-image representation of rows E–A. The relative location of whiskers within each row is represented by numbers 1 (posterior whisker) through 6 (anterior) in row C. GP, Globus pallidus; NS, neostriatum. *Adapted from* Petersen 2019; Alloway *et al.* 1999

The overabundance of cortical neurons compared to their SPNs target (Oorschot 1996) has led to the hypothesis that individual SPNs could receive extensive cortical inputs. Predictions suggest that if synapses were made indiscriminately, several thousand cortical neurons could connect to a single SPN (Kincaid *et al.* 1998). However, the response of SPNs in the DLS to whisker deflection is highly variable: some SPNs are broadly tuned, some respond selectively to a single

whisker, and others are unresponsive (Carelli & West 1991; Pidoux *et al.* 2011). This variability deviates from Peters' rule, which states that connectivity should match the overlap of axons and dendrites (Peters 1979; Braitenberg & Schüz 1998). This rule would predict more uniform responses among SPNs based on the extensive overlap of corticostriatal axons and SPN dendrites. Another possible explanation for this discrepancy between the anatomical and functional data is that feedforward inhibition mediated by local interneurons (Mallet *et al.* 2005; Pidoux *et al.* 2011) obscures the true extent of cortical input convergence by shunting some of the inputs, thereby accounting for the observed variability in SPN responses.

Both type of SPNs (D1 and D2) respond to whisker deflections (Reig & Silberberg 2014; Sippy *et al.* 2015; Charpier *et al.* 2020). Yet, D1 and D2 SPNs seem to have different wiring from S1 (Wall *et al.* 2013), and different synaptic responses either to whisker deflection (Reig & Silberberg 2014; Filipović *et al.* 2019), or optogenetic activation of S1 CS projections in slices (Johansson & Silberberg 2020). This differential wiring and response pattern may be due to several factors, including the type of cortical neurons projecting to these SPNs, the specific cortical areas involved, and the presence of local inhibitory circuits within the striatum.

1.4 Summary

In this first chapter, we have described the sensorimotor pathway involving the tactile sensory system in rodents, specifically focusing on the barrel cortex, and motor control through the basal ganglia (BG). The barrel cortex projects densely to the dorsolateral striatum (DLS). Spiny projection neurons (SPNs) are the main type of striatal neurons (95%) and can be divided in two populations (D1 or D2 SPNs), leading to two different basal ganglia pathways, which upon activation lead to different behavioral responses (promoting or inhibiting motor responses). The degree of CS input convergence onto SPNs is one major determinant of their activity, and thus regulate BG ouptuts, and motor production.
Anatomical and electrophysiological studies have so far produced an ambiguous model regarding the degree of tactile input convergence onto individual D1 and D2 SPN in the DLS. The barrel cortex has been used to study the somatotopic organization of sensory system, as functional cortical unit (i.e cortical column) can be visually distinguished. This system can also be used to study the degree of convergence/divergence in sensory CS projections in the striatum.
Anatomically, corticostriatal projections from the barrel cortex are diffuse and overlapping, while still respecting a topographic organization that is not as precise as in the thalamocortical system. The ratio of presynaptic cortical neurons to striatal targets is approximately 6:1, which suggests a high convergence of inputs onto individual SPNs. However, electrophysiological study in the DLS have found that SPNs show heterogeneity in their responses to whiskers stimulation (no response, response to one whisker, or multiple whisker). This heterogeneity could indicate lower input convergence than expected based on anatomy. Alternatively, it could also be due to feedforward inhibition by nearby striatal interneurons. Thus, the functional degree of input convergence from S1 to individual SPNs remains unclear.

CHAPTER 2

Role of Corticostriatal Projections in sensorimotor learning

An animal's survival depends on its ability to learn which actions are associated with positive outcomes (e.g finding food) and which are linked to negative events (e.g. danger). This learning process relies heavily on sensory inputs and sensory feedback from the environment. Initially, animals refine their actions through trial and error, with dopaminergic neuron activity increasing in response to unexpected rewards and decreasing when anticipated rewards are absent (Schultz *et al.* 1993; Waelti *et al.* 2001; Eshel *et al.* 2015). This feedback gradually strengthens successful neural pathways.

The primary somatosensory cortex (S1) cortex and dorsolateral striatum (DLS) in the basal ganglia (BG) are thought to participate in the learning of rewarding behavior to specific environmental stimuli, as the former integrates salient cues and the latter integrates sensory and motor information (rewarded cue and action) while also receiving motivational signals through dopaminergic inputs. Both structures undergo plastic changes during learning and participate in the refinement of rewarded sensorimotor behaviors. The second goal of my thesis was to study the plasticity of CS projections to individual SPNs after sensorimotor learning.

Contents

2.1 Plastic Changes in S1 During Tactile Sensorimotor Learning . . . 52
2.2 Role of the Dorsal Striatum in the Expression of Learned Behavior 54
2.2.1 Striatal Activity Changes Through Motor Learning 55
2.2.2 Behavioral Modulation by D1 and D2 SPNs 59
2.3 Corticostriatal Plasticity in Learning 63
2.4 Summary 68

2.1 Plastic Changes in S1 During Tactile Sensorimotor Learning

In addition to its role in sensory perception, S1 also plays a key role in learning and executing sensorimotor tasks.
Pioneering research by Recanzone and colleagues demonstrated that sensory cortical representations are plastic and could change with learning. For instance, when monkeys were trained in a tactile discrimination task, the cortical representation of the trained digit expanded and became more complex compared to the same digit on the non-trained hand (Recanzone *et al.* 1992). The extent of this expansion also correlated with behavioral performance.

To investigate the role of the barrel cortex in sensorimotor learning, whisker detection tasks have been used, where animals learn to associate whisker stimulation with a rewarded motor response, such as licking a reward spout (Figure 2.1). In these tasks, typically involving a brief ($\sim$ 1 ms) deflection of a single whisker (e.g. C2), neuronal recordings in the barrel cortex show trial-by-trial correlations with task performance (Sachidhanandam *et al.* 2013; Yang *et al.* 2016; Mehta *et al.* 2007; Knutsen *et al.* 2006; O'Connor *et al.* 2010; Yamashita & Petersen 2016). For example, Sachidhanandam *et al.* (2013) performed whole cell recording in the barrel cortex of trained mice to study how membrane potential relates to sensory perception. They found that whisker stimulation triggers an early and reliable sensory response within less than 50 ms, that is followed by a late depolarization (observed at 50 to 400 ms after the stimulus onset), which is stronger on hit trials compared to misses ones (Figure 2.1).

Moreover, the role of S1 in those tasks was confirmed by optogenetic and pharmacological experiments, were inactivation of the barrel cortex reduced hit rates, suggesting that the barrel cortex activity is critical for task execution (Figure 2.1)(Sachidhanandam *et al.* 2013; Mayrhofer *et al.* 2019; Yang *et al.* 2016; Guo *et al.* 2014; Le Merre *et al.* 2018; Kwon *et al.* 2016; Hong *et al.* 2018). Conversely, stimulation of the barrel cortex can substitute for whisker stimulation, leading to licking responses in trained animals (Sachidhanandam *et al.* 2013; Houweling & Brecht 2008; Tanke *et al.* 2018). Therefore, neuronal activity in S1 participates in the conversion of whisker sensory inputs into licking motor output during the

execution of whisker detection tasks, likely through the downstream targets of S1, like the DLS (Figure 1.4).

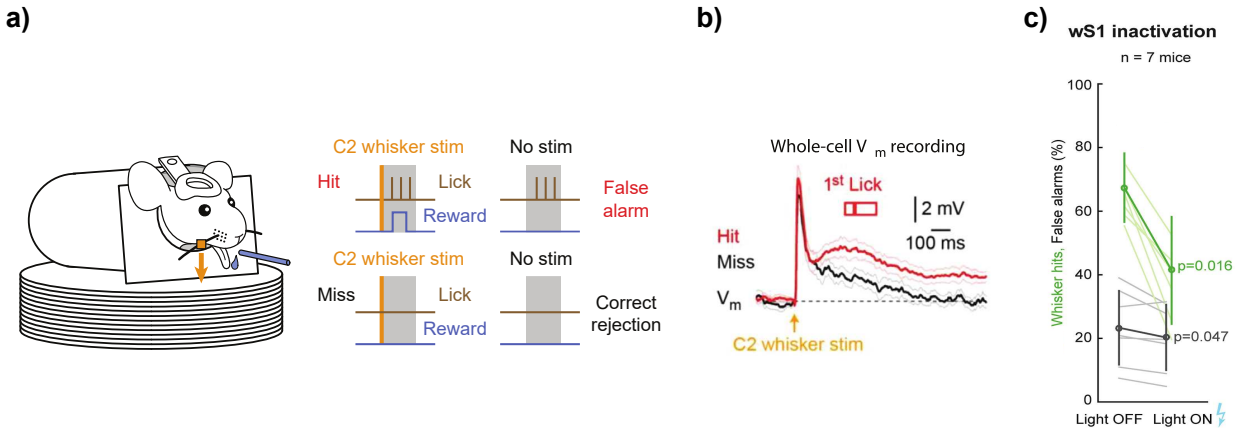

Figure 2.1: Barrel cortex function during a task requiring detection of a passive whisker deflection.
a) Head-restrained thirsty mice can be trained to lick a water reward spout after deflection of the C2 whisker. If the whisker deflection is perceived and the mouse licks during a brief reward window after the whisker stimulus, then the mouse is given a drop of water, and the trial is considered a 'Hit'. If the mouse fails to lick in response to whisker deflection, the trial is considered a 'Miss'. If the mouse licks in a catch trial, i.e., a trial without a whisker deflection, the trial is considered a 'False alarm'. If the mouse does not lick in the absence of a whisker stimulus, then the trial is considered a 'Correct rejection'. *Adapted from* Sachidhanandam *et al.* 2013 **b**) A 1-ms impulse delivered to the C2 whisker evokes a biphasic response upon neurons in wS1, with a stronger modulation of the late secondary depolarization in hit trials in which the mouse licks and receives reward, compared to miss trials in which the mouse fails to lick in response to the same whisker stimulation *Adapted from* Esmaeili *et al.* 2020. **c**) Lick probability for the whisker (green), and Correct rejection (gray) trials during optogenetic inactivation of wS1 (n = 7 mice) *Adapted from* Mayrhofer *et al.* 2019

In our group, Camon *et al.* (2019) developed a task where mice had to associate a single whisker stimulation with behavioral response to get a reward. This study revealed that the timing of neuronal activity in the untrained cortical columns - adjacent to the cortical column of the trained whisker - correlated with behavioral responses. Therefore, the changes in S1 activity following sensorimotor learning extend beyond the trained whisker cortical columns, involving a broader reorganization within the barrel cortex.

In summary, S1 plays a pivotal role in sensorimotor learning by linking sensory inputs (e.g. whisker stimulation) to motor outputs (e.g. licking response). One of our goals was to study the projections from S1 to one of the structures likely involved in associating sensory stimuli with appropriate actions: the DLS.

2.2 Role of the Dorsal Striatum in the Expression of Learned Behavior

Historically, the role of the BG) in motor learning was proposed in the mid-1980s by Mishkin and colleagues (Mishkin *et al.* 1984; Mishkin & Petri 1984), partly based on previous behavioral study that described the persistance of stimulus-response (S-R) or habit learning memory after hippocampal damage (Hirsh 1974). Subsequent research provided direct support for this, showing that lesions or inactivation of the dorsal striatum disrupt procedural memory (habits/S-R) in tasks such as maze navigation (Packard & McGaugh 1992; Packard & McGaugh 1996; Packard 1999; Featherstone & McDonald 2005).

Packard and colleagues developed a plus-maze test where rats are trained to find a food reward in one arm of a T-shaped maze. Initially, rats rely on place learning (environmental cues, hippocampus-dependant) but shift to response learning after repeated trials, adopting habitual strategies like consistently turning left or right to find a reward, regardless of the environmental cues (Figure 2.2, Packard & McGaugh 1996). However, if the dorsal striatum is temporarily inactivated (via lidocaine injection), this shift from place to response strategy is reversed, highlighting the dorsal striatum's critical role in habit formation (Figure 2.2 Packard & McGaugh 1996). Irreversible lesion studies further confirmed the selective role of the dorsal striatum in this form of procedural learning (Compton 2004).

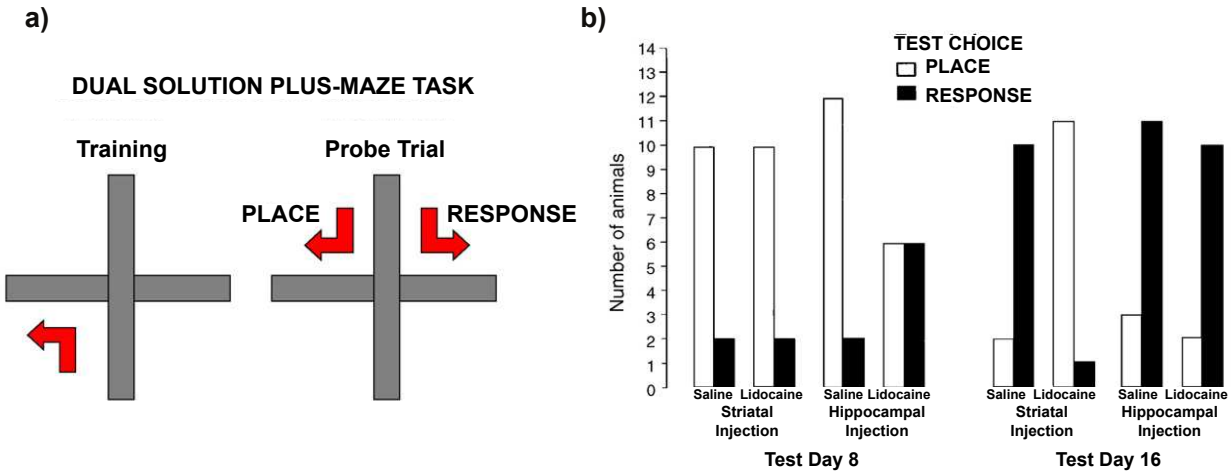

Figure 2.2: The striatum is involved in habit learning in a place response task. **a**) Left: training of animals to go to the left on a plus-maze. Right: the starting point of the animal is changed to the top arm of the maze. Its chosen direction indicates the nature of the strategy : a right turn towards the reward indicates a use of the place strategy, a lack of adaptation with a left turn indicates a response strategy. *Adapted from*Packard 2009. **b**) After a lidocaine lesion of the striatum, animals do not follow a response strategy. When the hippocampus is injected with lidocaine, place strategy is avoided. *Adapted from* Packard & McGaugh 1996

2.2.1 Striatal Activity Changes Through Motor Learning

Even if the dorsal striatum appears to be involved in learning and expression of appropriate motor responses, its exact role has been a subject of debate. Its role in motor learning has mainly been viewed through two main hypotheses that will be presented in the following section.

One hypothesis is that the DLS will segment motor actions into distinc chunks and would act as a controller for initiating and terminating sequences of actions. This hypothesis is based on the observation that striatal neurons, in a wide variety of tasks, have preferential firing around the boundaries of a learned motor sequence (Barnes *et al.* 2005; Jin & Costa 2010; Martiros *et al.* 2018). Jin & Costa (2010) proposed that distinct populations of SPNs encode start and stop signals during task execution, with one population showing increased firing before the initiation of the first action and another at the termination of a motor sequence (Figure 2.3). Martiros *et al.* (2018) extended these findings by showing

that sequence-bracketing activity in the DLS occurs only for reinforced motor sequences and conclude that the DLS is involved in action selection and the chunking of learned behaviors.

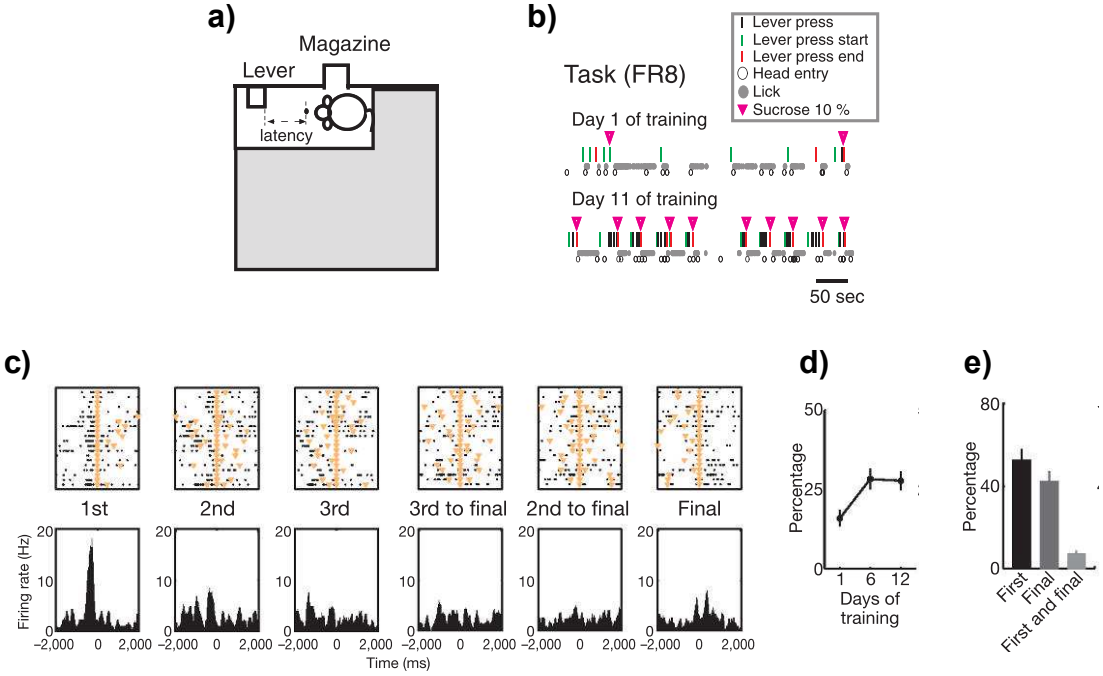

Figure 2.3: Activity in the DLS reflects behavioral chunking.
a) Experimental setup showing the operant box and the position of an infrared beam in the path from the reward magazine to the lever. **b**) Representative example of the behavioral time stamps from one C57BL/6J mouse during two stages of training. Vertical lines represent the time stamps of lever presses; they are color-coded to highlight the first and last press in a sequence. a) and b) *Adapted from* Tecuapetla *et al.* 2016 **c**) Example of a striatal MSN showing significantly higher phasic firing selectively before the first press of a sequence. Top, raster plot where each black dot indicates a spike and each orange triangle represents a lever press; bottom, PETH for the same neuron. From left to right, each column shows the PETH of the same neuron related to the first, second, third, third to final, second to final and final press of each sequence. **d**) Proportion of striatal MSNs showing sequence start/stop-related activity (including only initiation, only termination or both) throughout training. **e**) Proportion of striatal MSNs showing activity signalling sequence initiation, termination, or both initiation and termination (day 12). Error bars denote s.e.m. c), d) and e) *Adapted from* Jin & Costa 2010

An alternative hypothesis is that the DLS does not merely chunk actions but

instead continuously monitors and adjusts movement throughout task execution. Studies by Markowitz *et al.* (2018) and Sales-Carbonell *et al.* (2018) showed that SPNs in the DLS exhibit continuous and dynamic firing during movement, suggesting that the DLS integrates sensory feedback in real-time to adjust motor control. For example, these neurons modulate their activity during changes in speed or coordination (e.g. licking), indicating that the DLS's role extends beyond action segmentation to the fine-tuning of motor behavior in real-time. This ongoing adjustment function contrasts with the chunking hypothesis by emphasizing that the contribution of the DLS to movement is not limited to initiating and terminating actions, but rather involves continuous monitoring of movement dynamics (Dhawale *et al.* 2021).

Further evidence of the DLS's role in movement kinematics comes from Rueda-Orozco & Robbe (2015), who demonstrated that the firing rates of DLS neurons correlate with running speed and spatial information during motor learning. As learning progresses, these neurons become more strongly tuned to these variables. Disrupting DLS function with muscimol injections increased variability in task execution, reinforcing its role in optimizing learned movements.

Concordant results were found by Barbera *et al.* (2016), who used calcium imaging techniques to record striatal activity during motor learning (rotarod task). They demonstrated that SPNs in the DLS encoded key motor parameters such as speed, limb placement, and coordination. As learning progressed, these neurons became increasingly specialized, suggesting that the DLS plays a critical role in fine-tuning motor skills during movement refinement.

Directly relevant for this thesis project, Zareian *et al.* (2023) investigated the role of the DLS in sensorimotor learning. In a whisker detection task, where mice were trained to associate brief whisker deflections with a licking response, Zareian *et al.* demonstrated that neuronal activity in the DLS was link withe task performance, and that inactivation of the DLS, but not the motor cortex, impaired the performances in the task (Figure 2.4). They concluded that the DLS is essential for translation of sensory signal to motor actions.

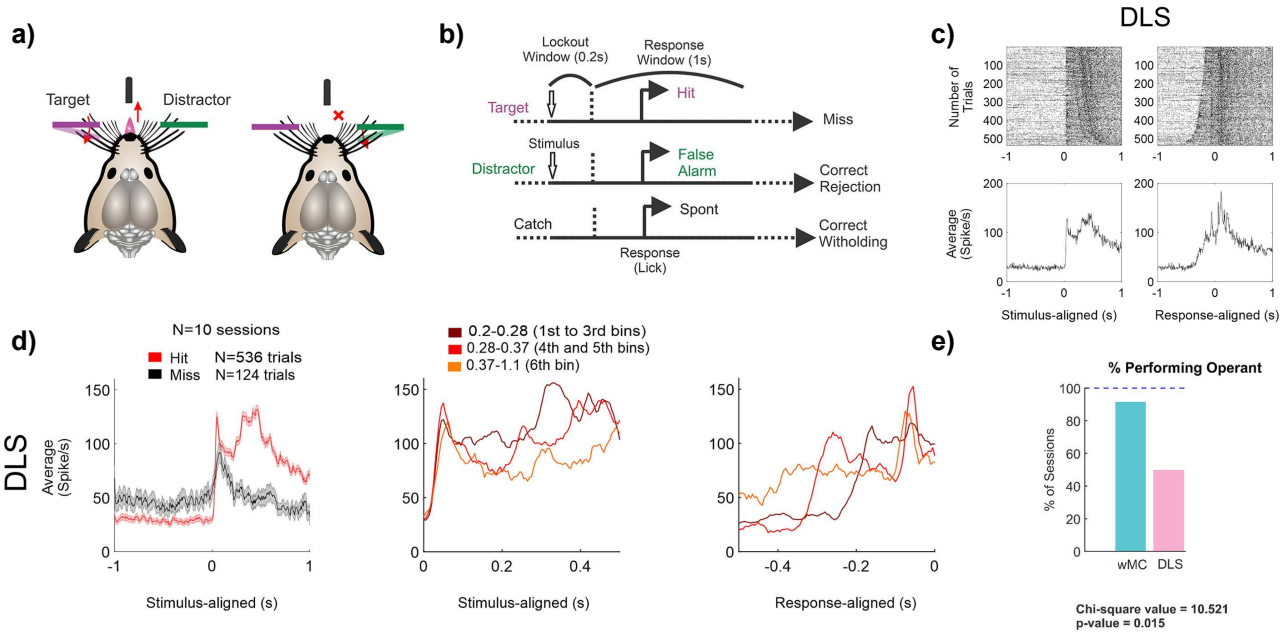

Figure 2.4: DLS activity during a sensorimotor task.
a) Illustration of the behavioral task. Mice learn to respond (lick) to small, transient whisker deflections in one of their whisker fields (purple, target) and to withhold licking to identical deflections in their opposite whisker field (green, distractor). **b**) Diagram of task structure for the operant, selective detection task. Following a variable (5–9 s) intertrial interval, mice receive either a target stimulus, distractor stimulus, or catch trial. After stimulus onset, a lockout window of 0.2 s is implemented in which responding is punished. Responses during the response window of target trials are considered hits and responses during the response window of distractor trials are considered false alarms. **c**) Multiunit activity (MUA) recorded from the DLS for all hit trials, pooled across sessions. The left column depicts MUA aligned to the target stimulus onset and the right column depicts MUA aligned to the reaction time. Top panels show raster plots sorted based on reaction times from fast (top) to slow (bottom) hits trials. Bottom panels show average of all trials shown in the top panels. **d**) Left: Average of all hit trials (red) and miss trials (black), recorded from the DLS. Middle: Hit trials, pooled across sessions from the DLS, grouped based on reaction time and aligned to the stimulus onset. Darker colors depict faster reaction time trials. Right: Hit trials, pooled across sessions from the DLS, grouped based on reaction time and aligned to the reaction time. **e**) Muscimol inactivation impacts on task performance. Percentage of sessions meeting threshold performance for the operant, selective detection task. *Adapted from* Zareian *et al.* 2023

The change in striatal activity observed during learning involves plastic striatal mechanisms, as c-fos expression increases in SPNs in the DLS during motor learning, and blocking NMDA receptors, with the antagonist AP5, severly im-

pact motor learning (Nakamura *et al.* 2017). Interestingly, similar results were previously described by Palencia & Ragozzino (2005). Moreover, Packard (1999) found that post-training intra-DLS glutamate injections accelerate this switch to response strategy. Thus, the change in DLS activity during learning could imply NMDA dependant plasticity at corticostriatal or thalamostriatal synapses.

2.2.2 Behavioral Modulation by D1 and D2 SPNs

The classical model of basal ganglia function, as proposed by Mink (1996), is based on a dichotomy between the direct and indirect pathways in the basal ganglia, each exerting opposing effects on movement via their respective targets within the BG (subsection 1.2.3). In this model, the direct "Go" pathway, involving D1 receptor-expressing striatal projection neurons (D1 SPNs), facilitates movement by disinhibiting the thalamus and reactivating the cortex, thus promoting the selection of appropriate actions. In contrast, the indirect "No-Go" pathway, mediated by D2 receptor-expressing neurons (D2 SPNs), suppresses competing actions by maintaining thalamic inhibition. Using optogenetics, Kravitz *et al.* 2010 provided one of the first direct evidence for the Go/No-Go hypothesis by selectively stimulating D1 or D2 SPNs in the basal ganglia. Stimulation of D1 SPNs led to movement initiation, whereas D2 SPNs stimulation suppressed movement, supporting the idea that the striatum plays a role in action selection and initiation through balanced activation of the direct and indirect pathways (Figure 2.5).

However, the role of D1 and D2 SPNs seems to extend beyond simple action initiation or suppression. Yttri & Dudman (2016) performed closed-loop photostimulation of dorsomedial striatal D1 and D2 SPNs in head-fixed mice trained to perform bimanual forelimb movements for a delayed water reward. Movement velocity was monotonically tuned to single-neuron activity, with faster movements triggering photostimulation of either D1 or D2 neurons. Stimulation of D1 SPNs increased movement velocity, while D2 SPN stimulation reduced it. Interestingly, stimulating the slowest third of movements had the opposite effect: D1 activation reduced velocity, and D2 activation increased it. Movement parameters like amplitude and duration remained unchanged, suggesting that SPN activation specifically controlled movement vigor. Additionally, the effects

on velocity persisted across multiple trials, indicating that actions associated with D1 stimulation became preferred, while those linked to D2 activation were less likely to be repeated (Yttri & Dudman 2016).

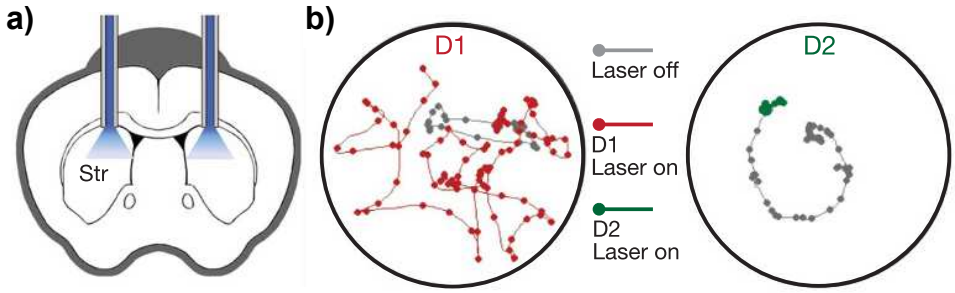

Figure 2.5: In vivo activation of direct or indirect pathways reveals pathway specific regulation of motor function.
a) Coronal schematic of cannula placement and bilateral fibre-optic stimulation. **b**) Example of altered open-field motor activity during bilateral striatal illumination in D1-ChR2 (left) and D2-ChR2 (right) mice. Lines represent the mouse's path; dots represent the mouse's location every 300 ms. Grey paths represent 20 s of activity before illumination; colored paths represent 20 s of activity during subsequent illumination. *Adapted from* Kravitz *et al.* 2010

The opposite role of the two pathways was further explored in sensorimotor learning by Sippy *et al.* (2015; 2021), who performed *in-vivo* patch-clamp recordings of D1 and D2 SPNs in the striatum while mice performed a whisker detection task.

In the 2015 study, head-restrained mice were trained to lick a reward spout in response to single whisker deflections (similar as in section 2.1). Sippy *et al.* found that early lick-related responses were amplified during rewarded licks compared to spontaneous ones. Specifically, the rapid depolarization phase (<50 ms after whisker stimulus) was larger and faster in D1 SPNs than in D2 SPNs and occurred more quickly during rewarded behaviors than during spontaneous ones (Figure 2.6). Since changes in membrane potential (Vm) started several hundred milliseconds before licking, they concluded that D1 SPNs activity might contribute to the initiation of the licking motor response. Optogenetic stimulation of D1 SPNs (but not D2 SPNs) could also substitute for the whisker stimulus to evoke a lick, suggesting a causal role for D1 SPNs in goal-directed sensorimotor transformation, consistent with other studies on D1 vs. D2 SPNs in movement and vigor (Kravitz *et al.* 2010; Freeze *et al.* 2013; Yttri & Dudman 2016).

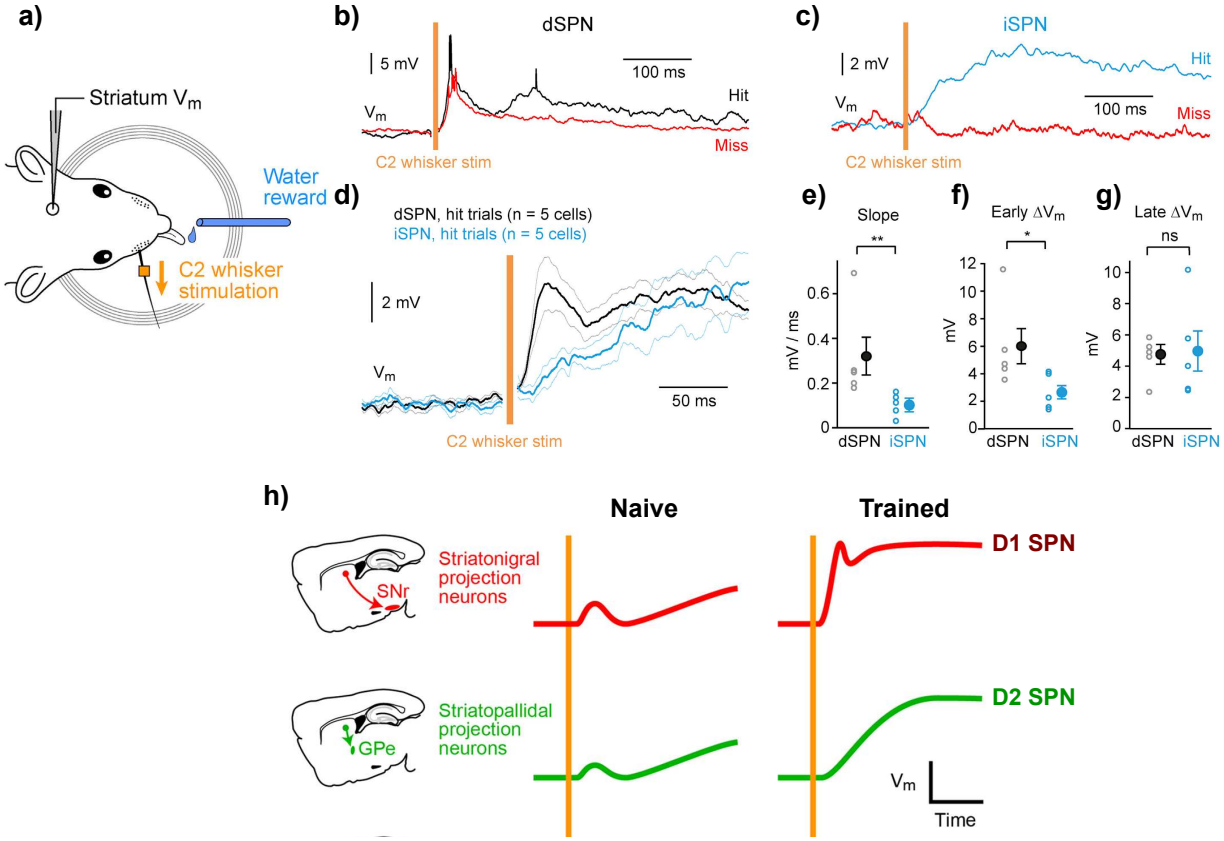

Figure 2.6: D1 and D2 SPNs activity during a whisker detection task.
a) Mice were head-restrained above an electromagnetic coil. Metal particles were placed on the right C2 whisker, which was deflected with a 1ms current pulse delivered to the electromagnetic coil at random time intervals (6–10 s) without any preceding cue. Mice learned to lick the spout within 1 s of the whisker stimulus in order to receive a water reward. To control for random licking, stimulation trials were interleaved with catch trials in which no stimulation was given. **b**) Average hit and miss traces from an example positively identified dSPN (D1 SPNs). **c**) Average hit and miss traces from an example positively identified iSPN (D2 SPNs). **d**) Grand average Vm of hit trials across all positively identified dSPNs (black, n = 5 cells) and iSPNs (blue, n = 5 cells), showing an early sensory response specifically in dSPNs. Lighter shaded lines represent SEM. **e**) The slope of the early response was significantly larger in dSPNs versus iSPNs (n = 5 of each cell type, Wilcoxon Mann-Whitney two-sample rank test, p = 0.008). **f** The amplitude of the early response (Early DVm), was significantly larger for dSPNs versus iSPNs (n = 5 of each cell type, Wilcoxon Mann-Whitney two-sample rank test, p = 0.03). **g**) The late response (Late DVm) was not significantly different in dSPNs versus iSPNs (n = 5 of each cell type, Wilcoxon Mann-Whitney two-sample rank test, p = 1). **a) - g):** *Adapted from* Sippy *et al.* 2015. **h**) Learning induces cell type-specific changes in striatal membrane potential dynamics across the learning of a simple goal-directed sensorimotor transformation. *Adapted from* Sippy *et al.* 2021

In a following study, Sippy *et al.* (2021) expanded thei investigation by comparing the membrane responses of both D1 and D2 SPNs in naive (untrained) and trained animals. This approach revealed that learning induced plasticity in the membrane responses of both D1 and D2 SPNs (Figure 2.6). However, the early component of the whisker sensory response was specifically enhanced after learning in D1 SPNs, but not in D2 SPNs. They hypothesized that this could reflect differences in cortical innervation between the two types of SPNs.

While the Go/No-Go model proposes an opponent relationship between D1 and D2 SPNs during movement control, recent studies have nuanced this view. Studies using calcium imaging (Tecuapetla *et al.* 2014; Cui *et al.* 2013; Barbera *et al.* 2016) or optogenetics (Jin *et al.* 2014) tools in the DLS have shown that both types of SPNs are more active when an animal is engaged in a task or spontaneously moving and less active when the animal is at rest. These neurons display distinct activity patterns, but interestingly, both are simultaneously activated during spontaneous contralateral movements (Tecuapetla *et al.* 2014) and during the initiation of movement in tasks such as lever press (Cui *et al.* 2013; Jin *et al.* 2014). These findings challenge the classical action selection model of SPNs function:

- during the execution of a specific action, D1 SPNs should exhibit localized activation to promote that action, while surrounding D2 SPNs should be active to suppress competing actions

- during periods of immobility, D2 SPNs should be active across the striatum to maintain the suppression of movement.

Interestingly, the studies from Tecuapetla *et al.* highlighted that, although both types of SPNs where active during spontaneous rotational movements, optogenetic activation of D1-SPNs was associated with an increased in contralateral movements, whereas activation of D2-SPNs induces ipsilateral movements. Conversaly inhibition of D1 SPNs resulted in an increase in ipsiversive movement, whereas inhibition of D2 SPNs results in contraversive turns (Tecuapetla *et al.* 2014). However, if both pathways are simultaneously activated, similar as during spontaneous contralateral turns, animals perform contralateral movements. Altogether, those studies suggest that a balanced activity between the two pathways exist during normal locomotion, and both neuronal types may be involved in fine-tuning movement vigor and coordination, rather than simply promoting or inhibiting movement.

In summary, while the classical Go/No-Go model presents a dichotomy between D1 and D2 SPNs in the control of movement, recent findings suggest a more integrative role for these pathways during actions, with an involvement in fine-tuning movement vigor and coordination.

2.3 Corticostriatal Plasticity in Learning

As discussed in section 2.1 and subsection 2.2.1, changes in neuronal activity have been observed in both the cortex and the DLS during sensory and motor learning. These changes likely involve the reorganization of the corticostriatal projections, which link the cortex and striatum (refer to section 1.3 for anatomical details). The striatum receives dopaminergic inputs, and dopamine plays a key role in modulating plasticity at CS synapses by reinforcing task-relevant connections while suppressing those that are irrelevant (Miller 1981; Reynolds & Wickens 2002). The CS synapses onto SPNs are located in close proximity to dopaminergic afferents (see subsubsection 1.2.3.1), which suggests that the anatomical arrangement may facilitate interactions between glutamatergic and dopaminergic signaling. The release of dopamine, often triggered by positive outcomes (Schulz & Reynolds 2013; Mirenowicz & Schultz 1996), could thus selectively strengthen synapses involved in successful task performance.

There are several forms of synaptic plasticity, including long-term potentiation (LTP) and long-term depression (LTD), which respectively enhance or weaken synaptic strength. On a molecular level, plasticity can involve changes in synaptic connectivity, such as dendritic spine dynamics (e.g, increase or decrease in synaptic connections, Yu & Zuo 2011), or alterations in receptor dynamics, such as AMPA-type glutamate receptors (Roth *et al.* 2017) and receptor signaling (Diering & Huganir 2018). These forms of plasticity are believed to contribute to sensorimotor learning, leading to circuit adaptations.

In two papers, Calabresi *et al.* (1992; 1992) described both LTP and LTD at corticostriatal synapses in slices. However, they found that LTP induction required specific conditions, such as the absence of magnesium in the extracellular medium, blocking of metabotropic glutamate receptors, or dopaminergic den-

ervation (Calabresi *et al.* 1992b). These findings led to the hypothesis that LTP may represent a pathological form of plasticity at CS synapses. Additionally, dopamine was shown to be essential for LTD induction, as blocking D1 and D2 dopamine receptors inhibited LTD, which was also absent in animals with lesioned nigrostriatal dopamine pathways (Calabresi *et al.* 1992a). Similar to LTD, the induction of LTP at corticostriatal synapses was inhibited by unilateral dopamine denervation or selective D1 receptor antagonism (Centonze *et al.;* Kerr & Wickens). Thus, the induction of synaptic plasticity in the striatum depends on the interplay between dopamine and other neurotransmitters, such as glutamate receptors and acetylcholine. These findings have been corroborated by numerous studies (Lovinger *et al.* 1993; Pawlak & Kerr 2008; Surmeier *et al.* 2009; Shen *et al.* 2008; Calabresi *et al.* 2007). To conclude,the expression of CS plasticity as either LTD or LTP is influenced by the timing of inputs and cortical activity levels (Fino *et al.* 2005). This bidirectional plasticity at striatal synapses may provide an efficient homeostatic mechanism, helping to reset CS synapses and prevent synaptic saturation (Fino *et al.* 2005).

In 1997, Charpier & Deniau 1997 provided the first *in vivo* evidence for synaptic plasticity in the striatum, demonstrating LTP in anesthetized animals. These findings have since been confirmed in other studies (Charpier *et al.* 1999; Reynolds & Wickens 2000).

Corticostriatal plasticity is crucial for learning and refining various behavioral and motor skills. It is particularly important for mice in learning specific behavioral patterns that lead to rewards (Santos *et al.* 2015). This plasticity supports both simple and complex forms of learning, including procedural learning, motor skill acquisition, and habit formation (Di Filippo *et al.* 2009; Koralek *et al.* 2012; Lerner & Kreitzer 2011; Yin *et al.* 2009b).
Various parameters can be used as proxies for synaptic plasticity, such as the firing rate and coherence of neuronal activity between the cortical and the striatal regions. For example, over time, the ability to consistently perform a skilled action becomes associated with coordinated neural activity across the motor cortex and the striatum during task execution (Lemke *et al.* 2019; Koralek *et al.* 2013; Santos *et al.* 2015). For instance, Koralek and colleagues (2012; 2013) demonstrated that during the late phases of learning, there is an increase in the coherence of firing rate between the DLS and the motor cortex. This increase was

accompanied by *ex-vivo* changes in the NMDAR/AMPA receptor ratio, changes that were absent in NMDAR-knockout mice, highlighting the role of NMDA dependent plasticity in CS circuits (Koralek *et al.* 2012). This NMDA dependant plasticity has been described in other studies (Dang *et al.* 2006; Jin & Costa 2010; Santos *et al.* 2015), suggesting that the activity-dependent potentiation of cortical inputs to the striatum may be required (Calabresi *et al.* 1992b; Charpier & Deniau 1997).
A recent study combined genetic tools to selectively label task-relevant neurons with slice electrophysiology, and revealed that synaptic connections between task-relevant cortical neurons and striatal targets are strengthened following motor learning (Hwang *et al.* 2022, Figure 2.7). Moreover, these projections converge onto spatially clustered spines in SPNs. This synaptic clustering as already been described in cortical neurons, where it permits supralinear effects on neuronal activity through local dendritic computations (Stuart & Spruston 2015). Thus, clustering might play a role in enhancing the process of task-related information.

The role of sensory corticostriatal projections in sensorimotor task has also been demonstrated by some studies. Znamenskiy & Zador (2013) showed that optogenetic stimulation of CS axons from the auditory cortex, which are tuned to specific frequencies, can significantly bias behavioral decisions in an auditory discrimination task. In this task, rats learned to associate high and low tones with two different actions, and they were required to report whether a mix of overlapping tones contained more high or low frequencies (Figure 2.8). The researchers then stimulated CS auditory axons that were selectively tuned to a particular auditory frequency (their preferred frequency). This stimulation biased the animals' choices toward the action associated with that frequency, even when the sensory evidence was ambiguous (Figure 2.8). Conversely, inactivation of these CS axons resulted in the opposite effect, biasing choices away from the action linked to the inactivated frequency band. This finding highlights the role of corticostriatal projections in decision-making after sensorimotor learning, as both activation and inactivation of these axons influenced behavioral choices in an opposite manner.

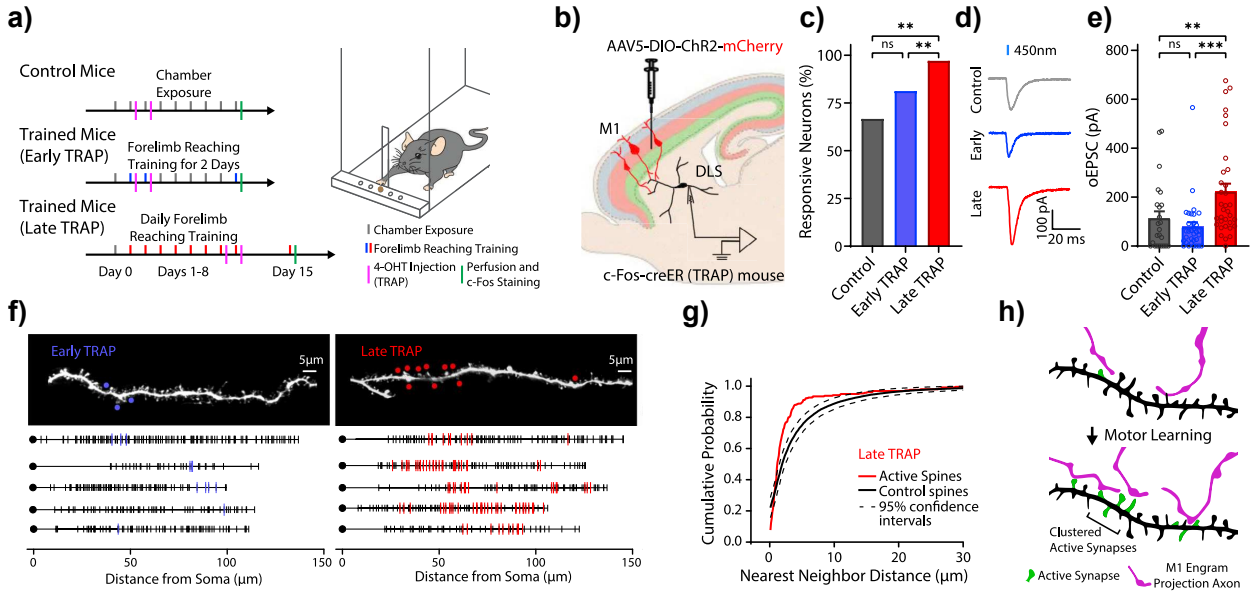

Figure 2.7: Motor learning selectively strengthens striatal synapses of motor engram neurons.
a) Experimental timeline and schematic drawing of the reaching task. **b**) Schematic drawing of M1 TRAP neurons and their projection to striatal SPNs. **c**) Fraction of SPNs receiving direct projection from TRAPed M1 neurons. Higher proportion of cells received projections from M1 engram neurons in late TRAP mice compared with early TRAP and control mice. **d**) Representative traces of oEPSCs in striatal SPNs. **e**) oEPSC amplitude in SPNs in late TRAP mice is higher than in either control or early TRAP mice. **f**) Left: Spatial distribution of active spines along SPN dendrites in early TRAP mice. Upper: representative dendrite image with active spines labeled (circles). Lower: 5 representative dendrospinograms, identifying the spatial location of somas (black circles), active spines (colored vertical lines), and non-active spines (black vertical lines). Right: Spatial distribution of active spines along SPN dendrites in late TRAP mice. **g**) Cumulative distribution of nearest neighbor distance (NND) for late TRAP (left) and Thy1-ChR2 mice (right). Red and green lines denote the NND distribution of active spines and black lines denote the distribution from Monte Carlo simulated "control spines" with 95% confidence interval (dashed). **h**) Schematic model showing increased numbers of active spines (green) that receive input from M1 engram neurons (magenta) and formation of clusters of active spines on striatal SPN dendrites after motor learning. *Adapted from* Hwang *et al.* 2022

In a following study, Xiong *et al.* (2015) provided additional insights into the plasticity of these projections. They used an elegant optogenetic approach combined with local field potential (LFP) recordings to show that synaptic potentiation occurred at auditory CS synapses during learning of an auditory

discrimination task (Figure 2.8). This potentiation was further studied in *ex vivo* slices with LFP, where they found that the late component of the response was mediated mainly by AMPA-type glutamate receptors, as pharmacological blockage with CNQX abolished the response (Figure 2.8). As the task is lateralized, they were also able to study the effect of contralateral hemisphere: they found that learning selectively potentiates CS synapses that are tuned to frequencies associated with contralateral responses. For example, in animals trained to associate low-frequency sounds with a rightward choice, they observed stronger activation when low-frequency tones were presented in the left auditory striatum (which is contralateral to the rightward response) .

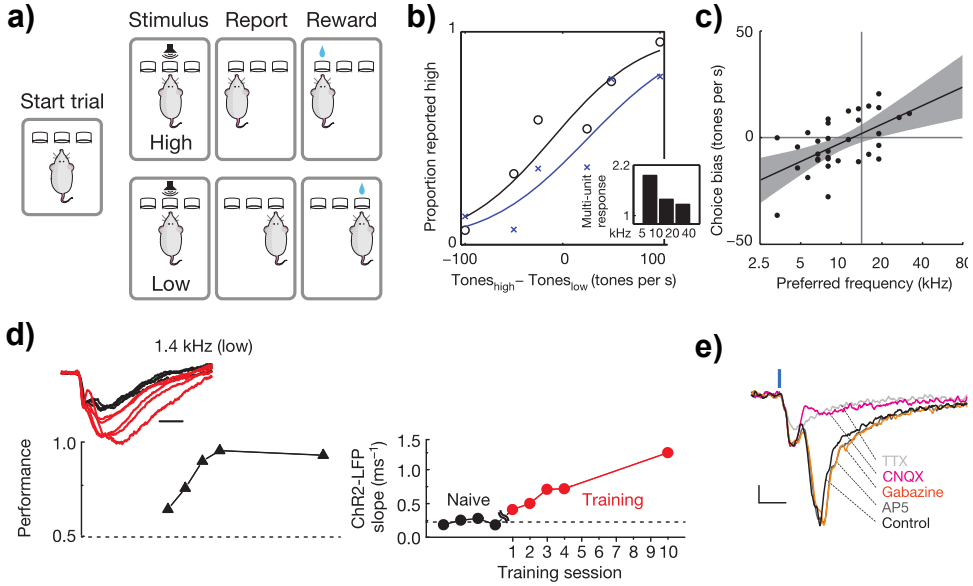

Figure 2.8: Corticostriatal projections drive decision-making and undergo plasticity during auditory discrimination learning.
a) Format of the behavioural cloud-of-tones task. **b**) Psychometric performance during a behavioural session in control trials (black) and during stimulation of corticostriatal neurons (blue). Stimulation evoked choice bias. Inset shows frequency tuning of multi-unit responses normalized to baseline, binned by octave. **c**) Across the population, the direction and magnitude of choice biases evoked by stimulation depend on the frequency preference of the stimulation site. Grey shading, 95% confidence interval for regression line. **d**) ChR2-LFP before (black) and during (red) training at example sites tuned to low frequency. Session 1 is defined as the first session in which the animal performed the full task. Scale bars, 2 ms. **e**) Pharmacological dissection of ChR2-LFP in a striatal slice. Scale bars, 50 mV and 5 ms. *Adapted from* Znamenskiy & Zador 2013; Xiong *et al.* 2015

2.4 Summary

In this chapter, we examined the role of corticostriatal (CS) projections in sensorimotor learning. Learning-dependent changes in neuronal activity have been observed in both S1 and the DLS, as well as in CS projections, reflecting key adaptations in these circuits. This plasticity is NMDA and glutamate dependant, indicating that some synaptic modifications occur and are critical for learning.
Based on their different targets within basal ganglia, D1 and D2 SPNs are thought to have opponent roles in behavior modulation. Some studies have found that activation of D1 or D2 SPNs produces opposing behavioral effects (facilitating vs inhibiting movement) (Kravitz *et al.* 2010; Tecuapetla *et al.* 2014), while others have found co-activation of the two pathways during spontaneous behaviors (Cui *et al.* 2013; Barbera *et al.* 2016). Following sensorimotor learning, both types show an increase in their response to sensory stimulus (Sippy *et al.* 2021), though with some critical differences in the early phase of their responses (Sippy *et al.* 2015; Sippy *et al.* 2021). This difference may arise from difference in the cortical innervation to each types of SPNs.
Sensory CS projections contribute to sensorimotor transformation during learning (Xiong *et al.* 2015), and optogenetic manipulation of CS axons bias behavioral responses based on learned associations (Znamenskiy & Zador 2013). Training selectively enhanced the synaptic strength of relevant CS projections (Xiong *et al.* 2015). However, the precise nature of the modifications in CS inputs to individual SPNs following sensorimotor learning remains unclear. Several mechanism could be implied, including increased synaptic strength, an increase in the number of cortical neurons innervating single SPNs, or a combination of both. Additionally, the plasticity in CS projections may differ between D1 and D2 SPNs.

GAP OF KNOWLEDGE AND PROJECT

This project aims to bridge the gap between anatomical and functional understanding of the role of sensory cortiostriatal projections in the dorsolateral striatum in sensorimotor processes (in naive and trained animals).

The first goal of this thesis was to investigate the organization of functional projections from the barrel cortex to the dorsolateral striatum (DLS).
Anatomical studies show a loose somatotopic organization, where functionally related cortical areas project to overlapping striatal regions (Alloway *et al.* 1999; Hintiryan *et al.* 2016). Given the abundance of cortical axons in the striatum, it has been hypothesized that each SPN might be innervated by a large number of cortical cells, potentially up to several thousand if synapses were formed promiscuously (Kincaid *et al.* 1998).
However, these anatomical studies do not fully capture the functional properties of corticostriatal projections, that could be more selective than expected solely based on anatomy (Shepherd & Svoboda 2005). In fact, in vivo electrophysiological studies have shown that the responses of SPNs are heterogenous, being either broadly tuned, selective to a single whisker, or unresponsive (Carelli & West 1991; Pidoux *et al.* 2011).
Moreover, weather D1 and D2 SPNs exhibit differences in their cortical innervation is still debated. Anatomical studies have found differences in the laminar localization of presynaptic soma (Reiner *et al.* 2003), or based on the cortical area (Wall *et al.* 2013). Silberberg's group found similar results using electrophysiological approach (Johansson & Silberberg 2020; Filipović *et al.* 2019; Gómez-Ocádiz & Silberberg 2023).

The pattern of corticostriatal input convergence plays a crucial role in activating (or not) SPNs, and thus is one determinant of the BG output activity. However its precise organization remains unclear. To address this we combined glutamate uncaging with Laser Scanning Photostimulation (LSPS) and patch-clamp recording of individual SPNs in brain slices to study the topographic organization and synaptic strength of sensory projections onto individual D1 or D2 SPNs. We took advantage of the barrel cortex system that allowed us to study how the cortical functional unit (i.e single cortical column) innervates single SPNs.

The second goal of this thesis was to better understand the role of CS projection in sensorimotor behavior, and will be further introduced after this first publication.

During reward-oriented behavior, animals refine their movements to maximize successful outcomes, transitioning from variable actions to more automated, stereotyped behaviors. As movements become more consistent, their execution speed increases. This refinement is tightly linked to striatal activity, as disrupting the striatum—through inactivation or lesions—impairs movement kinematics. Moreover, striatal neuron spiking activity correlates with both movement speed and task performance (Yttri & Dudman 2016; Rueda-Orozco & Robbe 2015; Zareian *et al.* 2023). Spiny projection neurons (SPNs) are divided into two main types: D1 SPNs, which express dopamine D1 receptors, and D2 SPNs, which express dopamine D2 receptors. These neurons form distinct pathways within the basal ganglia: the direct pathway (D1 SPNs) facilitates movement, while the indirect pathway (D2 SPNs) suppresses it (Mink 1996; Kravitz *et al.* 2010).

Both SPN types have distinct roles in rotational behaviors. For instance, unilateral activation of D1 SPNs induces contraversive (opposite side) turns, while D2 SPN activation leads to ipsiversive (same side) turns. Conversely, inhibiting D1 SPNs causes ipsiversive turns, and inhibiting D2 SPNs results in contraversive turns (Tecuapetla *et al.* 2014; Kravitz *et al.* 2010). We designed a highly lateralized foraging task, where mice were required to make either contraversive or ipsiversive turns around towers to obtain water rewards, in order to study the change in CS projections to SPNs. The task was conducted in darkness, requiring mice to rely heavily on tactile whisker input for navigation. Our aim was to investigate how sensory cortical inputs to D1 and D2 SPNs

— drivers of their activity — relate to voluntary, stereotyped turning behavior. We hypothesized that, in the striatum contralateral to the rewarded direction, corticostriatal input strength would differ between D1 and D2 SPNs. Specifically, we anticipated an increase in cortical inputs to D1 SPNs and/or a reduction in inputs to D2 SPNs.

RESULTS

CHAPTER 3

Study 1: Organization of Functional Corticostriatal Projections

Sparse innervations and local heterogeneity in the vibrissal corticostriatal projection

Abbreviated title : Sparse somatosensory corticostriatal connectivity

Authors and affiliations:

Kenza Amroune[1], Lorenzo Fontolan[2], David Robbe[2] and Ingrid Bureau[1]*

[1] Aix-Marseille Université, INSERM, INMED, Marseille, 13009, France

[2] Aix-Marseille Université, INSERM, INMED, Turing Centre for Living Systems, Marseille, 13009, France

corresponding author email address: ingrid.bureau@inserm.fr

Number of pages:

Number of figures: 5 + 1 extended data

Number of words for abstract, introduction, and discussion:

Conflict of interest. The authors declare no competing financial interests

Acknowledgments:

This work was supported by funding from the Institut National de la Santé et de la Recherche Médicale and a grant from the Agence Nationale de la Recherche (Corticostriatal, ANR-20-CE16-0002). K. Amroune is supported by fellowships from the Ministère de l'Enseignement Supérieur et de la Recherche and from the French government under the "France 2030" program via A*Midex (Initiative d'Excellence d'Aix-Marseille Université, AMX-19-IET-004) and ANR funding (ANR-17-EURE-0029). L. Fontolan is supported by funding from Excellence Initiative of Aix Marseille Université - A*MIDEX (Turing Centre for Living Systems). We thank the staff at the animal and genotyping facilities of INMED, Marie Giorgi-Kurz and Agnès Baude for their technical assistance in histology, the members of the CBGB group for their help and support and Elodie Fino, Rosa Cossart, Ede Rancz, Roustem Khazipov, Thomas Morvan, Corinne Beurrier and Lydia Kerkerian Le Goff for their critical reading of the manuscript.

Abstract

The density and overlap of cortical axons in the dorsolateral striatum (DLS) have suggested that striatal neurons integrate widespread information from cortical regions that are functionally-related. However, DLS neuronal responses to sensory stimuli have shown unexpectedly high selectivity, raising questions about the actual degree of input convergence of functional corticostriatal projection. Here, we investigated this question by focusing on the projections from different whisker cortical columns, as they overlap in the striatum and are co-active during behavior. Using *ex vivo* patch-clamp recordings in the DLS and glutamate uncaging for focal stimulations in the barrel cortex, we were able to map the precise location of presynaptic neurons to individual striatal projection neurons (SPNs). We found that input convergence was limited because each SPNs was innervated by either a single or a small number of whisker cortical columns scattered across the barrel region in the slice. In addition, the inputs converging onto each SPN were specific, with neighboring SPNs sharing few common inputs. Despite this sparse and distinct innervation of individual SPNs, the overall projection remained topographically organized at the population level. Finally, we found no significant differences in the innervation patterns of D1 and D2-type SPNs. Our results are consistent with sparse and non redundant connectivity between the sensory cortex and the projection neurons of the DLS.

Significance statement

The striatum is the subject of intense research due to its role in motor control, but the generation of its activity is unclear. Cortical innervation is dense in the dorsolateral striatum, but in vivo striatal neurons often respond to a single sensory organ. Here, we investigated this paradox using a method that localizes neurons in the somatosensory cortex that synapse with a striatal cell. We found that these connections are surprisingly scarce and thinly scattered within this cortex. Our results suggest that sensory corticostriatal connections, sparse and unique, are formed selectively. The overabundance of sensory axons might provide functional flexibility to neurons, allowing their input to be tuned to behavior.

Introduction

The dorsolateral striatum receives dense glutamatergic innervation from all sensory cortical areas. Their presumed function is to monitor the animal's ongoing sensory information, contributing to the modulation of sensory-guided behaviors and the learning of voluntary tasks (Pennartz et al., 2009; Znamenskiy and Zador, 2013; Sippy et al., 2015; Robbe, 2018). The observations that cortical neurons

are overabundant compared to striatal projection neurons (SPN) (Oorschot 1996), that projections originating from functionally linked regions overlap in the striatum (Flaherty and Graybiel, 1991; Alloway et al., 1999; Wright et al., 1999; Hooks et al., 2018) and that synaptic glutamatergic inputs must overcome strong feedforward inhibition (Mallet et al., 2005; Pidoux et al., 2011), have led to the idea that striatal neurons need to integrate multiple cortical inputs in order to be activated. In fact, studies examining the overlap of axons with single cell dendritic spines have predicted that several thousand cortical neurons could connect a single SPN if synapses were formed promiscuously (Kincaid et al., 1998). However, this prediction has not yet been functionally verified.

Here, we investigated the functional whisker-related inputs received by individual SPNs from the barrel cortex of mice. . Whiskers are organized in arcs and rows on the snout, and as they are co-stimulated during locomotion or whisking, tactile information is transmitted to the primary somatosensory cortex (S1) through parallel sensory channels, with each channel corresponding to an individual whisker (Adibi 2019). In S1, layer 4 contains optically dense barrel-shaped structures that reflect the spatial arrangement of whiskers on the snout. This unique feature has made the so-called barrel cortex a widely used model for studying neuronal connectivity and the organization of projections in cortical slices, particularly in relation to the whisker cortical columns. Despite this, the barrel cortex model has not yet been used to examine convergence within the functional somatosensory corticostriatal projection, leaving the underlying principles of connectivity in this pathway unclear. Axons of neurons located in different whisker cortical columns overlap in the dorsal striatum, suggesting that SPNs could receive broad vibrissal input (Wright et al., 1999; Alloway et al., 2000). However, responses of SPNs in the DLS to whisker deflection showed notable heterogeneity: they were either tuned to multiple whiskers, selective to a single whisker, or yet absent (Carelli and West, 1991; Pidoux et al., 2011). These observations suggested that the vibrissal innervation of SPNs violated Peters'rule, which states that connectivity is proportional to the overlap of axons and dendrites (Peters, 1979; Braitenberg and Schüz, 1998).

Two distinct populations of SPNs can be differentiated based on their projection targets and the expression of different dopamine receptors: D1 receptors for the direct pathway and D2 receptors for the indirect pathway (Alexander and Crutcher, 1990; Smith et al., 1998; Kravitz et al., 2010) (neurons are hereafter referred to as D1 and D2 SPNs). Studies have found that inputs received by D1 SPNs are stronger than those received by D2 SPNs (Kress et al., 2013; Reig and Silberberg, 2014; Parker et al.,

2016; Filipović et al., 2019). These observations may indicate that inputs converge to different degrees to D1 and to D2 SPNs.

To investigate the connectivity and input convergence on SPNs, we used a functional mapping technique that combines patch-clamp recordings and laser scanning photostimulation (LSPS) with glutamate uncaging on a novel slice preparation, that preserves the vibrissal corticostriatal projection, from the cell body of neurons in the barrel cortex to the DLS. The sites in the barrel cortex where LSPS evoked synaptic currents indicated the location of neuronal somas that were presynaptic to the recorded SPN. We found overall discrete innervations, as presynaptic neurons were either located in a single cortical column or thinly scattered across the barrel field. Each SPN had a distinct pattern of innervation, albeit with occasional overlap of presynaptic cells in the barrel cortex for SPNs closely positioned in the DLS. No difference was found between the D1 or D2 population of SPNs.

Materials and Methods

Animals and ethics

Hemizygous male and female B6.Cg-Tg(Drd1a-tdTomato)6Calak/J mice (JAX stock #016204; (Ade et al., 2011)(postnatal day [PND] 22–43) were used in accordance with institutional guidelines and the French Ministry of Research (APAFIS#27242). Mice were ear punched for identification. Mice were housed at constant room temperature (21° C) and humidity (60 %) and exposed to a reverse light cycle of 12 h light/dark with food and water available ad libitum.

Brain slices preparation and electrophysiology.

Mice were deeply anesthetized with isoflurane (4 %) prior to cervical dislocation and decapitation. We prepared corticostriatal slices (350 µm thick) from the brain left hemisphere, based on stereotaxic coordinates placing the striatal cells 1-2 mm anteriorly to the projection neurons in the barrel cortex (Aronoff et al., 2010; de la Torre-Martinez et al., 2023). Parasagittal slices were cut with a 60° angle from the midline and a 10° angle in the dorso-ventral axis (Fig. 1A, Extended data Fig. 1-1A) in a chilled cutting solution containing (in mM): 110 choline chloride, 25 $NaHCO_3$, 25 D-glucose, 11.6 sodium ascorbate, 7 $MgCl_2$, 3.1 sodium pyruvate, 2.5 KCl, 1.25 NaH_2PO_4, and 0.5 $CaCl_2$ (Sigma Aldrich). Slices were then transferred to artificial cerebrospinal fluid (ACSF) containing (in mM): 127 NaCl, 25 $NaHCO_3$, 25 D-glucose, 2.5 KCl, 1 $MgCl_2$, 2 $CaCl_2$, and 1.25 NaH_2PO_4, aerated with 95% O_2/5% CO_2. Slices were first incubated at 34 °C for 30 min and then maintained at room temperature for 20 min prior to use. Slices used for LSPS contained barrels in the L4 of cortex, the globus pallidus, its external segment (GPe), the

internal capsule, the ventral posteromedial nucleus of thalamus and the anterior hippocampus. ~ 8 barrels (5-13) were visible in the slice. 2 rows of barrels may be superimposed. At the end of each experiment, a picture of the slice was saved in order to superimpose it digitally to other slices, according to visual landmarks (Adobe Photoshop; Adobe Inc.). SPNs 50–150 µm deep in the slice were visualized under infrared and fluorescent lights in a BX61WI microscope (Olympus) and patched with borosilicate electrodes (3–6 MΩ) and recorded in the voltage-clamp whole-cell configuration using a Multiclamp 700A amplifier (Axon Instrument, Molecular Devices). The holding membrane potential was – 80 mV. The intracellular solution contained (in mM) 128 Cs-methylsulfate, 4 MgCl2, 10 HEPES, 1 EGTA, 4 Na2ATP, 0.4 Na2GTP, 10 Na-phosphocreatine, 3 ascorbic acid; pH 7.25; 290-300 mOsm. Cells in L5 and L2/3 of the barrel cortex were recorded in the current-clamp mode, with an intracellular solution in which Cs-methylsulfate was replaced by K-methylsulfate (Fig. 1E and Extended Data Fig.1-1C,D). All experiments were performed at room temperature (21°C).

LSPS with glutamate uncaging

LSPS was performed as described previously (Bureau, von Saint Paul, and Svoboda 2006). Recirculating (2 mL/min) ACSF solution contained (in mM): 0.2 MNI-caged glutamate (Tocris), 0.005 CPP [()-3-(2-carboxypiperazin-4-yl) propyl-1-phosphonic acid], 4 $CaCl_2$, and 4 $MgCl_2$. Focal photolysis of caged glutamate was accomplished with a 2 ms 20 mW pulse of a pulsed UV (355 nm) laser (DPSS Lasers Inc.) through a 0.16 NA 4 × objective (Olympus). 25 mW laser pulses were used for stimulating cortical neurons in mice older than P30 to maintain their excitation at a similar level than in younger mice (Extended Data Fig. 1-1D). The stimulus pattern for mapping the corticostriatal projections was 464 positions spaced by 75 µm on a 29 × 16 grid (2.1 × 1.1 mm) over barrel cortex. The corticostriatal slice and the LSPS grid were oriented in such a way that layer 5a was laid out horizontally. UV stimuli were applied every 700 ms and their successive positions on the LSPS grid were such as to maximize the time between stimulations of neighboring sites. Electrophysiological traces consisted of 100 ms baseline, a 450 ms window followed by a -5 mV 100 ms test pulse. A minimum of 2 and up to 4 stimulations were performed at each site at several minutes intervals. Custom software for instrument control and acquisition (Suter et al. 2010) was written in Matlab (Mathworks). Excitation profiles of pyramidal neurons were generated under similar conditions except that cells were recorded in current-clamp mode and glutamate was uncaged on a smaller 8 × 8 grid covering their soma and dendrites (50 µm spacing; 350 × 350 µm). In a subset of L5a cell recordings, a 8 × 24 grid was used to stimulate up in L1 (50 µm spacing).

Analysis of LSPS data

Synaptic input maps of neurons were constructed by taking the peak amplitude of EPSCs detected in a 50 ms time window starting at stimulation onset for each position in the LSPS grid. Measures were averaged across repetitions of stimulations (2-4). The threshold for EPSC detection was 3 standard deviations from baseline, or 9.2 ± 0.4 pA. To disambiguate evoked responses from spontaneous activity, synaptic responses occurring less than 2 times across repetitions of maps were set to zero. Averaged maps were superposed taking L5a as reference in the vertical axis and the junction of the GPe, dorsal striatum and internal capsule as reference in the horizontal axis (Ref_{hor}). In order to detect clusters and the center of mass of inputs in the LSPS map, we used the binary version of the map reporting the location of connected and non-connected sites (i.e., yielding EPSCs or none in the recorded SPN) and collapsed it along its vertical axis. A cluster of inputs comprised 1 or more consecutive connected sites in the collapsed map that was framed by 1 or more non-connected sites. Thus, a cluster here may include connected sites that were not adjacent on the vertical axis in the original map, and may combine synaptic inputs from different layers. The number of cortical columns was estimated based on the number of consecutive connected sites (ConsSites) in the collapsed map and the mean width of a barrel in the slice, 150 µm, which is equal to 2 connected sites in the map. Hence, the number of cortical columns = Σ (ceiling(ConsSites / 2)). The input center of mass in the horizontal axis was computed as : Σ (connected sites × lateral distances from Ref_{hor}) /Σ (connected sites). Traces from current clamp recordings were analyzed in a 50 ms time window at stimulus onset to count the number of action potentials (APs) elicited upon glutamate uncaging at every site and in the entire stimulation grid. Non parametric statistical tests were used. Everywhere n is the number of cells and N the number of mice.

Labeling of cortical cells and histology

A somatosensory corticostriatal slice was prepared as described above. Biocytin (2 %) was injected by iontophoresis in the striatum through a patch electrode (200 ms, 2.5 Hz) for 20 minutes (Chang, LoTurco and Nisenbaum, 2000). The slice was incubated for 4 hours at room temperature in ACSF and transferred to 4% paraformaldehyde at 4°C for two days. It was rinsed in PBS containing 0.3 % Triton X-100 (PBS-T), incubated overnight at room temperature in streptavidin-AlexaFluor488 (1:1000 in PBS-T) and mounted using Vectashield mount medium. Stack -acquisition (110 µm) was performed using a LSM 800 microscope (Zeiss). The simulated somatosensory corticostriatal slice was generated using data from the Allen mouse connectivity atlas (https://connectivity.brain-map.org/projection/experiment/cortical_map/293728197). Drd3-Cre_KI196 was the mouse line, eGFP the tracer. Acquisitions of serial two-photon tomography were stacked and the reconstituted brain was

sectioned using the 10° and 60° angles to reproduce the somatosensory corticostriatal slice (Fiji, BigDataViewer). Fluorescence in the striatum and in the corpus callosum (cc) was quantified on 300 µm max projections.

Statistical analysis

All data are expressed as mean ± SEM in the text. Median and 25-75th percentiles are shown in Figures. N and n are the numbers of animals and neurons, respectively. Paired or unpaired non parametric tests, Kruskall-Wallis test for repeated measures followed by Dunn post-hoc test and Šidák correction for multiple comparisons were used. $p < 0.05$ is considered as statistically significant.

Results

A novel preparation for investigating functionally the organization of projections from the barrel cortex to individual SPNs in the DLS

To investigate the spatial organization of sensory projections to SPNs, we prepared parasagittal somatosensory corticostriatal slices, which contained ~ 8 whisker barrels (PND 22-43; Methods; Fig. 1A and Extended Data Fig. 1-1A). In these slices (1-2 per animal), dendrites of pyramidal cells in the barrel cortex and their axonal projections to the DLS ran within the section plane (Fig. 1A,B and Extended Data Fig. 1-1B). Acute slices were prepared from Drd1a-tdTomato hemizygous mice in which D1 receptor expressing neurons are labeled. Based on previous studies, unlabeled neurons in these mice were principally SPNs expressing the D2 receptor (Bertran-Gonzalez et al., 2008; Ade et al., 2011; Enoksson et al., 2012; Thibault et al., 2013; Cao et al., 2018). D1 and D2 SPNs were recorded in the whole-cell voltage–clamp configuration (n = 101 cells, N = 54 mice). Simultaneously, an ultraviolet laser beam was directed at every site of a 29 x 16 pixel grid (2.1 × 1.1 mm, 75 µm spacing) to uncage glutamate over the barrel cortex, excite cortical neurons, and reveal glutamatergic cells presynaptic to the recorded SPN (Fig. 1C,D). When glutamate was uncaged on a cortical neuron innervating the recorded SPN, glutamate uncaging elicited short-lived excitatory postsynaptic currents (EPSCs; < 50 ms duration) (Fig. 1D). We and others have shown that evoked EPSCs are mono-synaptic and that feedforward inhibition cannot occur because only subthreshold synaptic events are elicited (Shepherd et al., 2003; Bureau et al., 2008). In fact, LSPS excited cortical neurons above their firing threshold at a maximal distance of 75 µm from their cell body (Fig. 1E; Extended Data Fig. 1-1C) indicating that the sites where LSPS evoked EPSCs in SPNs contained (or were adjacent to) the cell bodies of cortical neurons that were directly connected to the recorded cell. For each SPN, a so-called input map was assembled from the responses evoked at each uncaging site of the LSPS grid (Fig. 1D, top). Generally, multiple sites in the LSPS grid evoked EPSCs in a

SPN. These ''connected sites'' were either adjacent or separated by non-connected sites in the barrel cortex. When superimposed on the barrel cortex, they principally highlighted the layer (L) 5, below the barrels, and the superficial layers to a lesser extent (Fig. 1F), in agreement with the anatomy of the projection (Wise and Jones, 1977; Cowan and Wilson, 1994; Wall et al., 2013). The region containing the projections was wide in the preparation and shaped like a funnel as the connected sites constituted a band in the cortex that was larger than the positions of the SPNs in the DLS (2.5 mm vs. 1 mm, Fig. 1F).

Innervation of SPNs from the barrel cortex was strikingly discrete, with clusters of connected sites separated by long connectivity gaps (Fig. 1D). We assessed whether this patchy innervation pattern was due to uneven severing of fibers in the slice. We first compared the innervation of SPNs located at different positions in the striatum and found no significant effect on the width of input fields in the barrel cortex (Fig. 1G). Specifically, SPNs with input fields the width of a single cortical column (100-200 µm in this preparation) and those with broader input fields were evenly distributed across the investigated region of DLS (open and solid symbols in Fig. 1G, respectively). Although the width of these input fields varied from 0.075 to 1.6 mm (median, 750 µm), it remained relatively consistent on average across SPN positions within the slice (Fig. 1G). Next, we reversed our approach to determine whether any specific region of the barrel cortex exhibited stronger functional connectivity with the DLS in the preparation. To do so, we superimposed SPN input maps, aligning them on the horizontal axis using a consistent landmark in the slice (see Methods). We observed that within a ~1.5 mm section of the barrel field, each cortical column connected SPNs in a ~700 µm sub-region of the striatum (Fig. 1H). This projection pattern is consistent with the width of axonal arbors in the DLS from neurons in a cortical column (Fig 1B). Thus, projections from a large number of cortical columns were preserved in this preparation, allowing us to investigate the convergence of whisker cortical inputs onto individual SPNs.

Low convergence of projections from the barrel cortex to individual SPNs in the DLS

In general, neurons innervating an SPN were sparse and thinly scattered across the barrel field. First, inputs from an average 2.1 ± 0.1 layers converged on individual SPNs, but these were not necessarily vertically aligned in the LSPS map (examples in Fig. 2A). In fact, a cortical column that innervated an SPN did so by projections from a single layer half of the time (55 % of all data compiled). Moreover, ~ 60% of SPNs received inputs from cells within only one or two cortical columns in the slice (Fig. 2B; see Methods), with an average of 2.7 ± 0.2 columns projecting to each SPN, though some SPNs received input from as many as eight columns. Interestingly, SPNs receiving input from a single column within the slice were often located near others receiving input from multiple columns (Fig. 2C), reinforcing that the

low functional connectivity with columns in the slice was genuine in these cases. When several columns were innervating an SPN, these were either adjacent or separated by connectivity gaps (Fig. 1D, Fig. 2A). To further characterize the somatotopic proximity between cortical inputs received by individual SPNs, we then analyzed their innervation in terms of connectivity clusters. Here, clusters refer to regions in the input map, collapsed in the vertical axis of uninterrupted connectivity (Methods; Fig. 2A,D). We found that SPNs received inputs from 1 to 6 clusters, with an average of 1.9 ± 0.1 clusters (Fig. 2D,E). Cluster width typically corresponded to that of a single cortical column (median, 150 µm) and rarely exceeded two adjacent columns (Fig. 2E,F). For SPNs with multiple connectivity clusters, the distance between those was 265 ± 28 µm, ranging from 75 to 900 µm. Strikingly, 45 % of these input fields (collapsed along the vertical axis) produced no synaptic response upon stimulation, increasing to over 60 % in large input fields, > 1.4 mm (Fig. 2E, bottom). Thus, the input fields spanning > 2 whisker cortical columns exhibited substantial connectivity gaps, often extending across several columns. Altogether, these data suggest a connectivity pattern characterized by small patches of cortical cells presynaptic to a SPN that are distributed across the barrel field.

Loose topographic organization of SPN functional vibrissal innervation

To investigate whether a global organization of the projection could be extracted from these discrete innervation patterns, we once again superimposed LSPS input maps based on histological landmarks and labeled each site in the barrel cortex that provides input according to the corresponding SPN position in the striatum (Fig. 3A). Consistent with its anatomy (Flaherty and Graybiel, 1991; Alloway et al., 1999; Wright et al., 1999; Hooks et al., 2018), the functional vibrissal projection was topographically organized in the the DLS because SPNs located laterally/medially in the dorsal striatum received synaptic inputs whose center of mass was in the lateral/medial part of the barrel cortex (Fig. 3A,B). Given the orientation of the slice (Extended Data Fig. 1-1A), a shift of input from the medial to the lateral region of the barrel cortex corresponds principally to a shift of whisker arcs, towards arcs with higher numbers (e.g. E1 to E8 barrel). But this topographic organization was not as precise as for intracortical projections (Shepherd and Svoboda, 2005; Erlandson et al., 2015), because the connectivity centers of mass of two adjacent SPNs could be 1 mm apart in the barrel cortex (Fig. 3B). Vertically, the vibrissal projection also presented an organization. As predicted by the anatomy (Wise and Jones, 1977; Cowan and Wilson, 1994; Wall et al., 2013), L5a was the principal source of connections to SPNs, as ~ 65 % of them received input from this layer (Fig. 3C). Responses were elicited less frequently when stimulations were in L4, L5b, L2/3 and in L6. We found that 50 % of L5a cells fired action potentials when stimulations were at the bottom of L4, indicating that a fraction of the relatively large bottom L4-inputs were in fact due to

the activation of L5a pyramidal cells (Fig. 1E; Extended Data Fig. 1-1C). In contrast, photo-stimulations in L2/3 never elicited the firing of L5a cells (n = 11; Fig. 1E), indicating that the EPSCs evoked by stimulations in these superficial layers all arose from direct synaptic connections between L2/3 pyramidal cells and SPNs. EPSCs evoked with stimulations in L2/3 to L5b had similar amplitudes (Fig. 3D), suggesting that L5a dominated these other layers thanks to a greater connectivity with SPNs principally. However, L6-EPSCs were smaller compared to L5a-EPSCs (Kruskal-Wallis, H(4) = 16.4, p = 0.0025; Dunn post-hoc test and Šidák correction, p = 0.0015; Fig. 3D). Finally, we investigated the variability of input strength across clusters of connectivity. We found that for SPNs with multiple clusters, a dominant cluster could be clearly identified based on its input, about four times stronger than in adjacent clusters (Fig. 3E). Altogether, these findings indicate two axes of organization for the vibrissal corticostriatal projection: a first one, loose, that is parallel to the axis of barrels and a second more precise that is orthogonal (layers).

Individual SPNs have unique innervation

To understand the local consequences in the DLS of a loose topography combined with sparse innervations, we investigated whether the connectivity clusters of SPNs recorded in the same slice overlapped in the barrel cortex (Fig. 4A). Across all pairs recorded in the same slice (n = 58), the fraction of input sites shared between two cells was generally low, averaging 5.2 ± 1.0 % . Overlap of input sites was most frequently observed when SPNs were less than 100 µm apart (61 % of pairs), but even then, the fraction of shared input sites remained low, 0 to 38 % (mean, 7.7 ± 1.6 %; Fig. 4B). In addition, these input sites were generally not located in the cortical column providing the strongest input to SPNs (25 % of all pairs had shared input in a common dominant whisker cortical column). The fraction of pairs with any overlap in their input maps dropped abruptly to zero when SPNs were distant by more than 250 µm (Fig. 4B). This occurred despite the input fields still intersecting each other. Indeed, the proportion of SPNs pairs sharing a connectivity region in the barrel cortex remained significant, > 40 %, when cells were separated by 250-500 µm (Fig. 4C). Thus, even when DLS SPNs sample inputs from the same region in the barrel cortex, their cortical innervation exhibits almost no redundancy.

D1 and D2 SPNs receive similar input from the barrel cortex

Finally, we investigated whether innervation patterns differed between the two populations of SPNs. As previously reported (Wall et al., 2013), projections to D1 and D2 SPNs were spatially intermingled along the axis of barrels (Fig. 5A,B ; n = 47 and 54, cells respectively). We found that D1 and D2 SPNs had similar input fields: first, their widths were not different (Fig. 5C). In addition, they received input from a

similar number of cortical columns, which were organized in clusters of similar widths (Fig. 5D) (Fig. 5E). Paired analysis of D1 and D2 SPNs recorded in the same slice also showed that their input fields did not significantly differ in width, number of cortical columns or cluster width (p = 0.44 – 0.50 – 0.26, Wilcoxon; Fig. 5C-E). None of these parameters exhibited a clear relationship between subtypes (R = 0.13 – 0.30 – -0.003; p = 0.43 – 0.058 – 0.99, Pearson; Fig. 5C-E). Finally, both types of SPNs received input from each cortical layer in similar proportions (Fig. 5F). Thus, the heterogeneity in patterns of innervation is not due to a difference between SPN subtypes. Overall, there was no difference in the total inputs received by D1 and D2 SPNs (EPSC sum or $EPSC^T$; Fig. 5G). In addition, the principal cluster was similarly dominant over the other clusters (Fig. 5H). However, differences were observed in a layer-specific manner (Fig. 5I). Whereas L5-$EPSC^T$ was similar in D1 and D2 cells, differences were found in layers with the lowest incidence in the LSPS input maps: L2/3-$EPSC^T$ was larger in D2 SPNs (91 ± 36 vs. 23 ± 22 pA, p = 0.005, Mann-Whitney) but L6-$EPSC^T$ was larger in D1 SPNs (37 ± 17 vs. 16 ± 2 pA, p = 0.008).

Discussion

We investigated the organization of functional projections originating in the barrel cortex and targeting projection neurons in the dorsal striatum in a novel preparation. We found overall little input convergence as cortical neurons innervating an SPN were either located in a single cortical column or thinly scattered across the barrel field. Each SPN had a distinct pattern of innervation from the barrel cortex, albeit with occasional overlap for SPNs closely positioned in the DLS. D1 and D2 presented similar patterns of innervations.

Sparse sensory innervation of single SPNs

As previously revealed by tracings of corticostriatal projections, the primary source of innervation of SPNs in this study is the upper part of L5 in the barrel cortex, L5a, although, SPNs are occasionally innervated by cells located in deeper and superficial layers (Wise and Jones, 1977; Reiner et al., 2003; Wall et al., 2013; Guo et al., 2017; Yamashita et al., 2018; Bertero et al., 2022). Given the abundance of cortical axons in the striatum, it has been assumed that a large number of cortical cells innervate each SPN, potentially up to few thousands if synaptic connections were made promiscuously (Kincaid et al., 1998). On the other hand, it has also been reported that neurons in the DLS fire in response to the stimulation of a single body-part in monkeys and rodents *in vivo*, even of a single whisker in some cases (Carelli and West, 1991; Jaeger et al., 1995; Cho and West, 1997). This finding suggested that each striatal neuron is in fact innervated by one small subregion of S1, although feedforward inhibition could

have masked a broader selectivity (Pidoux et al., 2011). Here, the LSPS input maps indicate that connectivity between the barrel cortex and a SPN is indeed low. 60 % of SPNs responded to the stimulation of only one or two whisker cortical columns. Perhaps, these were connected to additional columns not present in the preparation. However, a number of critical findings argues that innervation from the barrel cortex on individual SPNs is genuinely low: i) adjacent SPNs received input from different sites in the barrel cortex, suggesting that actual connections were less than the local potential connections. ii) The connected cortical neurons were scattered along broad horizontal and vertical axes, implying that projections in between were preserved. iii) The cortical columns present in the slice corresponded to different whisker arcs (e.g, E1 to E8), an axis associated with a greater overlap of cortical axons in the striatum (Alloway et al., 1999). iv) The peak of connectivity was with L5a as expected, not with a layer closer to striatum. v) EPSCs were small, suggesting only one or a few cells were presynaptic at each connected site. Altogether, our results suggest that the integration of the vibrissal cortical inputs largely occurs at the population level in the DLS, rather than at the level of individual SPNs. The speckled connectivity pattern of SPNs, arising from the abundant and diffuse cortical innervation in the DLS, suggests that sensory corticostriatal synapses are established through a selective process.

Specific cortical input to individual SPNs

A peculiar feature of the corticostriatal innervation is the imbalance between the number of cortical cells projecting to the striatum and the number of striatal cells, thought to be at a ratio of 10 to 1 (Oorschot, 1996). Based on this ratio and the ultrastructure of the corticostriatal connection, the density of axonal boutons and spines, C. Wilson's group concluded that the probability of an SPN being contacted by one given axon entering the domain of its dendritic arborization was low, 0.04 - 1.4 %, depending on the model. Hence, the chance that two SPNs were innervated by the same cortical axon was even lower according to this model. Consistent with this, here, we found that overlaps between the LSPS input maps of SPNs were rare. This indicates that SPNs primarily integrate distinct cortical inputs originating from the barrel cortex. When overlaps were observed, they occurred only for SPNs located within 250 µm of each other. However, such overlaps involved only a small fraction of their inputs, as the connectivity patterns of nearby SPNs were largely interdigitated. In addition, the input fields continued to intersect significantly beyond 250 µm and up to 500 µm of separation between SPNs. This suggests that SPNs can share a general region of connectivity in the barrel cortex without sharing any specific input sites. The fact that an SPN had to be located within the dendritic arbor of another SPN to share some of its inputs was not predicted by the ultrastructure of corticostriatal connections. In fact, it

predicted the opposite: that two SPNs are more likely to be innervated by the same cortical cell if their dendrites deploy in different striatal subregions, due to the low density of boutons on the cortical cells axon (Kincaid et al., 1998). We attribute this difference to the fact that in our experiments neighboring SPNs were probably innervated by different neurons located at the same stimulation site in the barrel cortex. This may indicate a mechanism by which adjacent cortical neurons (~75 µm, the spacing in the LSPS grid) grow their axon in the same subregion of the striatum. Such a mechanism would permit the emergence of functional clusters in striatum, as those described *in vivo,* that group neurons of close sensory selectivity (Carelli and West, 1991; Jaeger et al., 1995).

Similarities and specificities in the patterns of projection to SPNs of the direct and indirect pathways

Electrophysiological studies have shown that D1 SPNs exhibit larger responses than D2 SPNs to whisker deflections (Reig and Silberberg, 2014; Filipović et al., 2019). Also, the optostimulation of cortical efferents in brain slices showed a bias towards D1 SPNs (Kress et al., 2013; Parker et al., 2016). In our study, we had contrasting results. Taking the projections globally, there was no difference in the innervation of D1 and D2 SPNs, neither in the rate at which cells were connected, nor in the organization of the projection. The principal layer innervating SPNs, L5a, delivered inputs of similar strengths to D1 and D2 SPNs. However, layers with lower incidence in the pattern of innervation showed bias in the amplitude of responses: stimulations in L2/3 induced stronger responses in D2 cells whereas stimulations in L6 activated D1 cells more strongly. We have shown that stimulation in L2/3 activates the L2/3 projection only. Similarly, L6-evoked EPSCs indicate rare L6 projections to striatum, as previously described (Guo et al., 2017; Bertero et al., 2022). However, it is also possible that LSPS at the top of L6 effectively stimulated the proximal dendrites of neurons whose soma was located at the bottom of L5b. This would be consistent with the previous findings that D1 SPNs are more strongly innervated than D2 SPNs by cortical projection neurons of the pyramidal tract (Kress et al., 2013), as these are proportionally more present in deep layer 5 (Ramaswamy and Markram, 2015). The larger L2/3 inputs received by the D2 SPNs is intriguing because of the role of this layer in higher-order integration processes, such as those activated during operant sensory discrimination tasks (Kwon et al., 2016; Han and Helmchen, 2024; Oryshchuk et al., 2024). Moreover, the activity of L2/3 cells during mouse displacement is distinctive, exhibiting a sustained response to ongoing wall touch, as opposed to the transient response observed in L5 (Ayaz et al., 2019). Further investigation is needed to specifically examine projections from the upper and lower cortical layers and how they influence the dynamics of sensory integration in the direct and indirect pathways of the DLS. However, these data illustrate the diversity of paths of sensory integration involving D1 and D2 SPNs.

In conclusion, we found a low and sparse connectivity within the cortical vibrissal projections to individual SPNs. While these projections were topographically organized, the innervation patterns of individual SPNs displayed substantial connectivity gaps and heterogeneity. Since the inputs of each SPN represented only a limited subset of whisker columns, sensory integration must occur at the population level, with each SPN complementing the representations of its neighbors. These observations raise the hypothesis of a selective process underlying the formation of corticostriatal synapses.

References

Ade KK, Wan Y, Chen M, Gloss B, Calakos N (2011) An Improved BAC Transgenic Fluorescent Reporter Line for Sensitive and Specific Identification of Striatonigral Medium Spiny Neurons. Front Syst Neurosci 5:32.

Adibi M (2019) Whisker-Mediated Touch System in Rodents: From Neuron to Behavior. Front. Syst. Neurosci 13:40.

Alexander GE, Crutcher MD (1990) Functional architecture of basal ganglia circuits: neural substrates of parallel processing. Trends Neurosci 13:266–271.

Alloway KD, Crist J, Mutic JJ, Roy SA (1999) Corticostriatal Projections from Rat Barrel Cortex Have an Anisotropic Organization that Correlates with Vibrissal Whisking Behavior. J Neurosci 19:10908–10922.

Alloway KD, Mutic JJ, Hoffer ZS, Hoover JE (2000) Overlapping corticostriatal projections from the rodent vibrissal representations in primary and secondary somatosensory cortex. J Comp Neurol 428:51–67.

Aronoff R, Matyas F, Mateo C, Ciron C, Schneider B, Petersen CCH (2010) Long-range connectivity of mouse primary somatosensory barrel cortex. Eur J Neurosci 31:2221–2233.

Ayaz A, Stäuble A, Hamada M, Wulf M-A, Saleem AB, Helmchen F (2019) Layer-specific integration of locomotion and sensory information in mouse barrel cortex. Nat Commun 10:2585.

Benison AM, Ard TD, Crosby AM, Barth DS (2006) Temporal patterns of field potentials in vibrissa/barrel cortex reveal stimulus orientation and shape. J Neurophysiol 95:2242–2251.

Bertero A, Verrillo L, Apicella AJ (2022) A Novel Layer 4 Corticofugal Cell Type/Projection Involved in Thalamo-Cortico-Striatal Sensory Processing. J Neurosci Off J Soc Neurosci 42:1383–1405.

Bertran-Gonzalez J, Bosch C, Maroteaux M, Matamales M, Hervé D, Valjent E, Girault J-A (2008) Opposing patterns of signaling activation in dopamine D1 and D2 receptor-expressing striatal neurons in response to cocaine and haloperidol. J Neurosci Off J Soc Neurosci 28:5671–5685.

Braitenberg V, Schüz A (1998) Cortex: Statistics and Geometry of Neuronal Connectivity. Berlin, Heidelberg: Springer Berlin Heidelberg. Available at: http://link.springer.com/10.1007/978-3-662-03733-1 [Accessed July 16, 2024].

Bureau I, Shepherd GMG, Svoboda K (2008) Circuit and plasticity defects in the developing somatosensory cortex of FMR1 knock-out mice. J Neurosci Off J Soc Neurosci 28:5178–5188.

Cao J, Dorris DM, Meitzen J (2018) Electrophysiological properties of medium spiny neurons in the nucleus accumbens core of prepubertal male and female Drd1a-tdTomato line 6 BAC transgenic mice. J Neurophysiol 120:1712–1727.

Carelli RM, West MO (1991) Representation of the body by single neurons in the dorsolateral striatum of the awake, unrestrained rat. J Comp Neurol 309:231–249.

Chang SL, LoTurco JJ and Nisenbaum LK (2000) In vitro biocytin injection into perinatal mouse brain: a method for tract tracing in developing tissue. J Neurosci Methods 97:1-6

Cho J, West MO (1997) Distributions of single neurons related to body parts in the lateral striatum of the rat. Brain Res 756:241–246.

Cowan RL, Wilson CJ (1994) Spontaneous firing patterns and axonal projections of single corticostriatal neurons in the rat medial agranular cortex. J Neurophysiol 71:17–32.

de la Torre-Martinez R, Ketzef M, Silberberg G (2023) Ongoing movement controls sensory integration in the dorsolateral striatum. Nat Commun 14:1004.

Enoksson T, Bertran-Gonzalez J, Christie MJ (2012) Nucleus accumbens D2- and D1-receptor expressing medium spiny neurons are selectively activated by morphine withdrawal and acute morphine, respectively. Neuropharmacology 62:2463–2471.

Erlandson MA, Manzoni OJ, Bureau I (2015) The Functional Organization of Neocortical Networks Investigated in Slices with Local Field Recordings and Laser Scanning Photostimulation. PloS One 10:e0132008.

Filipović M, Ketzef M, Reig R, Aertsen A, Silberberg G, Kumar A (2019) Direct pathway neurons in mouse dorsolateral striatum in vivo receive stronger synaptic input than indirect pathway neurons. J Neurophysiol 122:2294–2303.

Flaherty AW, Graybiel AM (1991) Corticostriatal transformations in the primate somatosensory system. Projections from physiologically mapped body-part representations. J Neurophysiol 66:1249–1263.

Flaherty AW, Graybiel AM (1994) Input-output organization of the sensorimotor striatum in the squirrel monkey. J Neurosci Off J Soc Neurosci 14:599–610.

Guo C, Peng J, Zhang Y, Li A, Li Y, Yuan J, Xu X, Ren M, Gong H, Chen S (2017) Single-axon level morphological analysis of corticofugal projection neurons in mouse barrel field. Sci Rep 7:2846.

462 Hooks BM, Papale AE, Paletzki RF, Feroze MW, Eastwood BS, Couey JJ, Winnubst J, Chandrashekar J,
463 Gerfen CR (2018) Topographic precision in sensory and motor corticostriatal projections varies
464 across cell type and cortical area. Nat Commun 9:3549.

465 Jaeger D, Gilman S, Aldridge JW (1995) Neuronal activity in the striatum and pallidum of primates
466 related to the execution of externally cued reaching movements. Brain Res 694:111–127.

467 Kincaid AE, Zheng T, Wilson CJ (1998) Connectivity and Convergence of Single Corticostriatal
468 Axons. J Neurosci 18:4722.

469 Kravitz AV, Freeze BS, Parker PRL, Kay K, Thwin MT, Deisseroth K, Kreitzer AC (2010) Regulation of
470 parkinsonian motor behaviours by optogenetic control of basal ganglia circuitry. Nature
471 466:622–626.

472 Kress GJ, Yamawaki N, Wokosin DL, Wickersham IR, Shepherd GMG, Surmeier DJ (2013) Convergent
473 cortical innervation of striatal projection neurons. Nat Neurosci 16:665–667.

474 Kwon SE, Yang H, Minamisawa G, O'Connor DH (2016) Sensory and decision-related activity propagate in
475 a cortical feedback loop during touch perception. Nat Neurosci 19:1243–1249.

476 Mallet N, Le Moine C, Charpier S, Gonon F (2005) Feedforward inhibition of projection neurons by fast-
477 spiking GABA interneurons in the rat striatum in vivo. J Neurosci Off J Soc Neurosci
478 25:3857–3869.

479 Oorschot DE (1996) Total number of neurons in the neostriatal, pallidal, subthalamic, and substantia
480 nigral nuclei of the rat basal ganglia: a stereological study using the cavalieri and optical disector
481 methods. J Comp Neurol 366:580–599.

482 Oryshchuk A, Sourmpis C, Weverbergh J, Asri R, Esmaeili V, Modirshanechi A, Gerstner W, Petersen CCH,
483 Crochet S (2024) Distributed and specific encoding of sensory, motor, and decision information
484 in the mouse neocortex during goal-directed behavior. Cell Rep 43:113618.

485 Parker PRL, Lalive AL, Kreitzer AC (2016) Pathway-Specific Remodeling of Thalamostriatal Synapses in
486 Parkinsonian Mice. Neuron 89:734–740.

487 Pennartz CMA, Berke JD, Graybiel AM, Ito R, Lansink CS, van der Meer M, Redish AD, Smith KS, Voorn P
488 (2009) Corticostriatal Interactions during Learning, Memory Processing, and Decision Making. J
489 Neurosci Off J Soc Neurosci 29:12831–12838.

490 Peters A (1979) Thalamic input to the cerebral cortex. Trends Neurosci 2:183–185.

491 Pidoux M, Mahon S, Deniau J-M, Charpier S (2011) Integration and propagation of somatosensory
492 responses in the corticostriatal pathway: an intracellular study *in vivo*: Sensory responses in the
493 corticostriatal pathway. J Physiol 589:263–281.

494 Ramaswamy S, Markram H (2015) Anatomy and physiology of the thick-tufted layer 5 pyramidal neuron.
495 Front Cell Neurosci 9 Available at:
496 http://journal.frontiersin.org/Article/10.3389/fncel.2015.00233/abstract [Accessed February 14,
497 2024].

498 Reig R, Silberberg G (2014) Multisensory integration in the mouse striatum. Neuron 83:1200–1212.

499 Reiner A, Jiao Y, Del Mar N, Laverghetta AV, Lei WL (2003) Differential morphology of pyramidal tract-
500 type and intratelencephalically projecting-type corticostriatal neurons and their intrastriatal
501 terminals in rats. J Comp Neurol 457:420–440.

502 Shepherd GMG, Pologruto TA, Svoboda K (2003) Circuit analysis of experience-dependent plasticity in
503 the developing rat barrel cortex. Neuron 38:277–289.

504 Shepherd GMG, Svoboda K (2005) Laminar and columnar organization of ascending excitatory
505 projections to layer 2/3 pyramidal neurons in rat barrel cortex. J Neurosci Off J Soc Neurosci
506 25:5670–5679.

507 Sippy T, Lapray D, Crochet S, Petersen CCH (2015) Cell-Type-Specific Sensorimotor Processing in Striatal
508 Projection Neurons during Goal-Directed Behavior. Neuron 88:298–305.

509 Smith Y, Bevan MD, Shink E, Bolam JP (1998) Microcircuitry of the direct and indirect pathways of the
510 basal ganglia. Neuroscience 86:353–387.

511 Thibault D, Loustalot F, Fortin GM, Bourque M-J, Trudeau L-É (2013) Evaluation of D1 and D2 Dopamine
512 Receptor Segregation in the Developing Striatum Using BAC Transgenic Mice Lee J, ed. PLoS ONE
513 8:e67219.

514 Wall NR, De La Parra M, Callaway EM, Kreitzer AC (2013) Differential innervation of direct- and indirect-
515 pathway striatal projection neurons. Neuron 79:347–360.

516 Wise SP, Jones EG (1977) Cells of origin and terminal distribution of descending projections of the rat
517 somatic sensory cortex. J Comp Neurol 175:129–157.

518 Wright AK, Norrie L, Ingham CA, Hutton EAM, Arbuthnott GW (1999) Double anterograde tracing of
519 outputs from adjacent "barrel columns" of rat somatosensory cortex. Neostriatal projection
520 patterns and terminal ultrastructure. Neuroscience 88:119–133.

521 Yamashita T, Vavladeli A, Pala A, Galan K, Crochet S, Petersen SSA, Petersen CCH (2018) Diverse Long-
522 Range Axonal Projections of Excitatory Layer 2/3 Neurons in Mouse Barrel Cortex. Front
523 Neuroanat 12:33.

524 Znamenskiy P, Zador AM (2013) Corticostriatal neurons in auditory cortex drive decisions during
525 auditory discrimination. Nature 497:482–485.

526

527 **Figure 1. A novel slice preparation for investigating the spatial organization of the somatosensory**
528 **projections to the DLS neurons.**

529 **A**. Left, A somatosensory corticostriatal slice in which projecting cortical cells were retrogradely labeled
530 with biocytin iontophoresis performed in the striatum. Labeled cell bodies of projecting cortical cells are

indicated with green symbols. Right, Example dendritic arbors of cortical cells that were retrogradely labeled .

B, Left, A simulated somatosensory corticostriatal slice generated using data from the Allen Mouse Connectivity Atlas. The brain in which eGFP was expressed in L2/3 pyramidal cells of a few columns of the barrel cortex was reconstructed from serial acquisitions, and virtually re-sectioned (300 µm thick) at the angles used to produce somatosensory corticostriatal slices. Right, focus on the innervation in the striatum.

C. Montage of a corticostriatal slice (left) and layout of the experiment (right). A SPN was recorded in the dorsolateral striatum while cortical neurons were photostimulated with LSPS. The grid of LSPS (blue) was positioned on the barrel cortex. GPe, globus pallidus, external segment; IC, internal capsule; hipp., hippocampus.

D. Top, examples of synaptic input maps for individual SPNs showing one or four clusters of input (SPN 1 and 2, respectively). In the color maps, each pixel of color indicates the peak amplitude of EPSCs detected within a 50 ms window after the stimulus onset. The different cortical layers are represented by solid white vertical lines on the left side of the map. The green boxes at the top of the maps, the clusters of sites in the input maps collapsed in the vertical axis whose stimulation evokes EPSCs. Bottom, EPSC traces evoked at the sites indicated by letters in the maps above. Two repetitions are superimposed (black and orange). Vertical dashed lines, the stimulus onsets (2 ms stimulus).

E. LSPS evoked excitation of two L5a pyramidal neurons recorded in current-clamp mode. LSPS was a 8 x 8 (left) or 24 x 8 (right) 50 µm spacing grid. Cortical neurons are positioned at the center (white triangles). Traces with an action potential are in red. Bottom, Average number of action potentials evoked at every site of the LSPS grid.

F. Overlay of the sites in the barrel cortex (green polygons) where stimulations evoked EPSCs in SPNs (green symbols; n =101 cells, N = 54 mice). The red dashed vertical line is the reference (Refhor in the Methods) used for aligning slices across experiments horizontally.

G. Bottom, Width of the input fields in the barrel cortex for different positions of SPNs in the striatum. Input field is the space encompassing all cortical sites projecting to an SPN. SPNs with an input field the size of a single cortical column (open symbols) or of several cortical columns (solid symbols) are shown. Horizontal bars, distribution of the input field widths. Top, The average width of input fields for 250 µm bins.

H. Bottom, Positions of SPNs in the striatum as a function of the horizontal positions of their connected cortical sites, identified using the LSPS grid. SPNs with an input field the size of a single cortical column (open symbols) or of several cortical columns (solid symbols) are shown. Top, maximal horizontal distance between SPNs for 150 µm bins of connected site positions in the barrel cortex.

Extended data Figure 1-1. (= Supplemental)

A. Left, the corticostriatal slice generated from the Allen mouse brain reference atlas (CutNII custom-angle slice visualization tool; G. Csucs). bf, barrel field. str, striatum. VPL, ventral posterolateral thalamic nucleus. VPM, ventral posteromedial thalamic nucleus. Center, the section angles illustrated on horizontal and longitudinal sections of the brain. Right, the section angle with respect to the orientations of the arcs and rows in the barrel field of the left hemisphere (Allen mouse brain atlas).

B. A simulated somatosensory corticostriatal slice generated using data from the Allen mouse connectivity atlas (https://connectivity.brain-map.org/projection/experiment/cortical_map/293728197). L2/3 was the cell line, eGFP the tracer. The red box identifies the experimental slice with intact projections from the cortex to the striatum. Acquisitions of serial two-photon tomography were stacked in Fiji and the reconstituted brain was sectioned using the angles to produce somatosensory corticostriatal slices (BigDataViewer plugging). Fluorescence in the striatum (blue) and in the corpus callosum (cc, pink) was quantified on 3 max projections (300 µm thick) obtained in the anterior-posterior axis (A-P). **C**. Vertical (left) and horizontal (right) excitation profile of L5 pyramidal cells, in juveniles and adolescents combined (20 and 25 mW stimulation, respectively). Evoked APs were summed along each column (left) or line (right) of the LSPS grid. Solid line, median. In gray, 25-75th percentiles. n = 30, N = 14.
D. Total number of APs evoked in the stimulation grid for L5 (left) and L2/3 (right) pyramidal cells in juvenile (juv, P22-30) and adolescent (ado, P31-41) mice. A higher stimulation intensity was used for adolescent mice (25 mW instead of the standard -std - intensity, 20 mW), so that the total number of APs matched between the two age groups. L5, juv, n = 22, N = 9 ; ado std, n = 22, N = 13; ado high: n = 8, N = 5; L2/3, juv: n = 16, N=3; ado std and high n = 10, N = 2; * $p < 0.001$, Mann-Whitney.

Figure 2. Sparse functional projections from the barrel cortex to individual SPNs in the DLS.
A. Example slice with 3 recordings. The hatched horizontal band is L5a, the polygons are the stimulation sites evoking EPSCs, the boxes on top are the clusters generated from the collapsed input maps, the circles at the bottom the position of the SPNs on the horizontal axis. Recordings are color coded.
B. Fraction of cells receiving inputs from 1 to 8 cortical columns in the barrel area. In inset, median (red) and 25-75th percentiles (box).
n = 101 cells, N = 54 mice.
C. Number of cortical columns innervating individual SPNs. Symbols are cells, lines are slices. Light gray, slices with ≥ 2 recordings. Dark, slices with one recording.
D. Fraction of cells receiving inputs from 1 to 6 clusters of projections in the barrel cortex. In inset, median (red) and 25-75th percentiles (box). Clusters are defined as the ensemble of contiguous sites in the input map, collapsed in the vertical axis, whose stimulation evokes EPSCs (see examples in A, boxes at the top).
E. Top to bottom, Number of clusters, cluster width (expressed in cortical column and µm) and proportion of connectivity gap in the input fields, collapsed along its vertical axis, as a function of the input field width. Gray symbols, cells with ≥ 2 clusters of input. Other symbols, cells with 1 cluster.
F. Width of clusters of inputs, all cells combined (192 clusters). Inset, width of a cluster, median (red) and 25-75th percentiles (box).

Figure 3. Loose topographic organization of the functional vibrissal innervation of SPNs in the DLS
A. Overlay of the sites in the barrel cortex where stimulations evoked EPSCs in SPNs. The colors, yellow to blue, indicate the position of the SPNs (gray circles) along the medio-lateral axis in dorsal striatum (axis at the bottom, 0 is Refhor in the Methods; n = 101, N = 54). Blue shades are for lateral SPNs.
B. Position of the connectivity center of mass (CM) as a function of the SPN position in dorsal striatum R = 0.62 (n = 101, N = 54). Zero on the x and y axis is the position of the vertical dashed line shown in A.

C. Contribution of each cortical layer to the SPN innervations. The 16 rows of the grid correspond to different cortical layers (Layer 2/3: 1-6; L4: 7-9; L5a: 10; L5b: 11-13; L6: 14-16). The horizontal white band is L5a.
D. Amplitude of SPN EPSCs as a function of their laminar origin. Median (red) and 25-75th percentiles (boxes). * Kruskal-Wallis p = 0.0025, Dunn-Šidák posthoc tests, p = 0.0015.
E. EPSC sum obtained in secondary (Adj.) connectivity clusters, relative to the principal cluster EPSC sum . In inset, the same but with the positions, lateral or medial, of the secondary clusters shown. Cells with ≥ 2 clusters, n = 55.

Figure 4. Individual SPNs have unique cortical innervation
A. Four example slices with 2 to 4 recordings. Same as in Fig. 2A.
B. Left, fraction of pairs with overlap in their input maps. Right, fraction of overlap in the input maps as a function of the horizontal distance separating cells.
C. Same as in B for the width of overlap between SPN input fields in the barrel cortex.

Figure 5. D1 and D2 SPNs have similar patterns of innervation from the barrel cortex
A. Overlay of the sites in the barrel cortex where stimulations evoked EPSCs in D1 (blue) or D2 SPNs (red). The shades, light to dark, indicate the position of the SPNs (bottom circles) along the medio-lateral axis in the dorsal striatum (axis at the bottom). D1 cells, n = 47, N = 36; D2 cells, n = 54, N = 37.
B. Position of the connectivity center of mass (CM) as a function of the SPN position in the dorsal striatum (D1, red; D2, blue). R = 0.70 (D1, n = 47, N = 36); R = 0.57 (D2, n = 54, N = 37).
C. Left, D2 SPN input field width as a function of the D1 SPN input field width, in the same slice. The black symbol and lines are the median value and 25-75th percentiles. n = 71 pairs in 28 slices. Large symbols indicate n = 2 to 3 pairs. Right, medians (thick lines) and 25-75th percentiles (boxes) of D1 and D2 input field widths, across all cells. n=101, N = 54.
D. Same as in C for the number of cortical columns
E. Same as in C for the width of connectivity clusters
F. Contribution of each cortical layer to the SPN innervations. The horizontal gray band is L5a.
G. EPSC sum for D1 and D2 SPNs. Outliers were not shown for clarity (1 D1, 2 D2, 1.2-1.5 nA)
H. EPSC sum obtained in secondary (Adj.) connectivity clusters, relative to the principal cluster EPSC sum.
I. Top, D1 and D2 SPN EPSC sum as a function of laminar origin. Cells without inputs are not included. Outliers are not shown for clarity (3 D1, 2 D2, 350-700 pA). * indicates a significant difference (p = 0.005 and p = 0.008; Mann-Whitney). Bottom, fraction of cells with input.

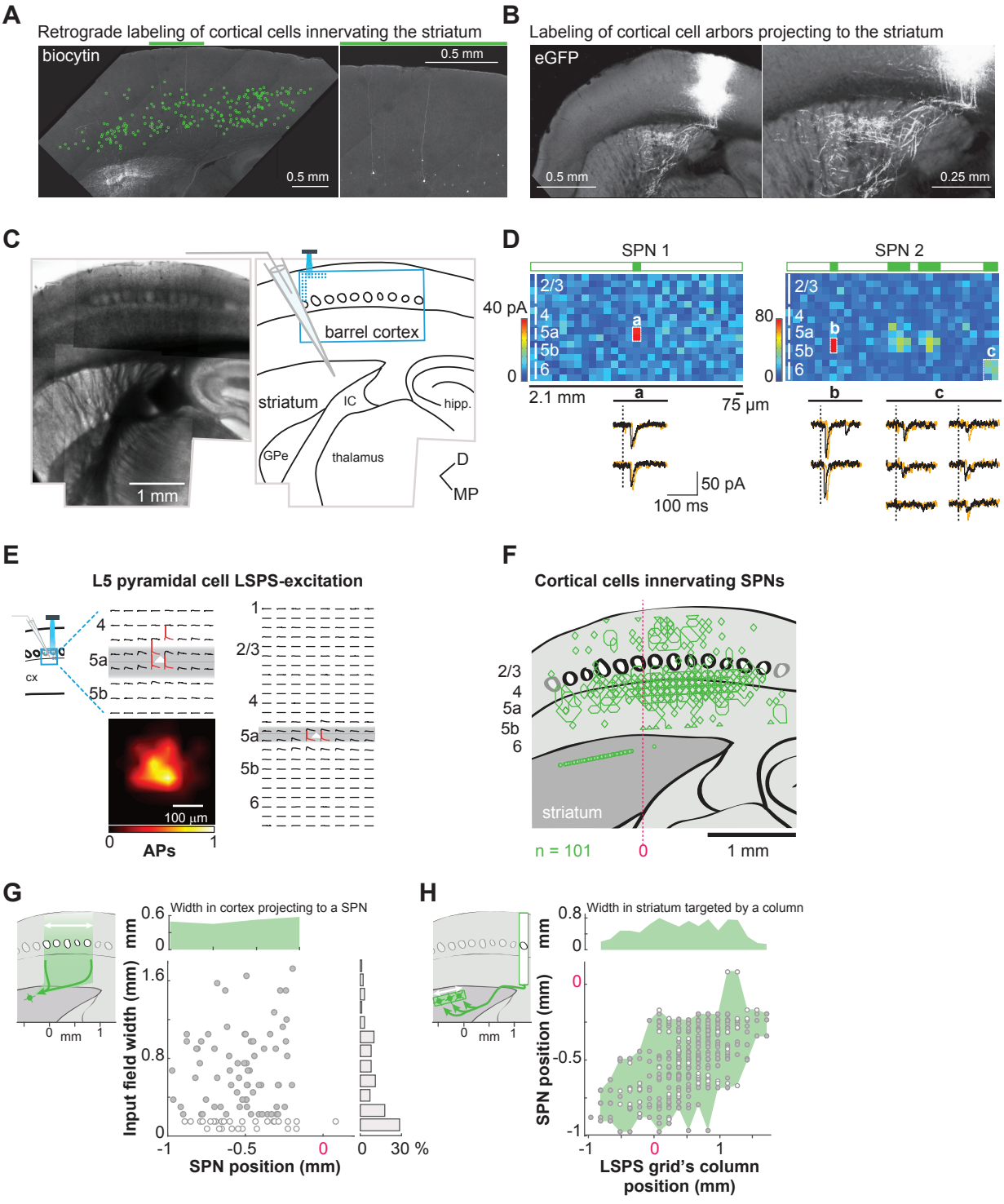
A
Retrograde labeling of cortical cells innervating the striatum
biocytin
0.5 mm
0.5 mm
B
Labeling of cortical cell arbors projecting to the striatum
eGFP
0.5 mm
0.25 mm
C
barrel cortex
striatum
IC
hipp.
GPe
thalamus
D
MP
1 mm
D
SPN 1
SPN 2
40 pA
0
80
0
2/3
4
5a
5b
6
a
b
c
2.1 mm
75 µm
50 pA
100 ms
E
L5 pyramidal cell LSPS-excitation
cx
4
5a
5b
2/3
6
100 µm
0
1
APs
F
Cortical cells innervating SPNs
striatum
n = 101
0
1 mm
G
Width in cortex projecting to a SPN
mm
0.6
0
1.6
0.8
0
Input field width (mm)
-1
-0.5
0
SPN position (mm)
0
30 %
H
Width in striatum targeted by a column
0.8
0
mm
0
-0.5
-1
SPN position (mm)
-1
0
1
LSPS grid's column position (mm)

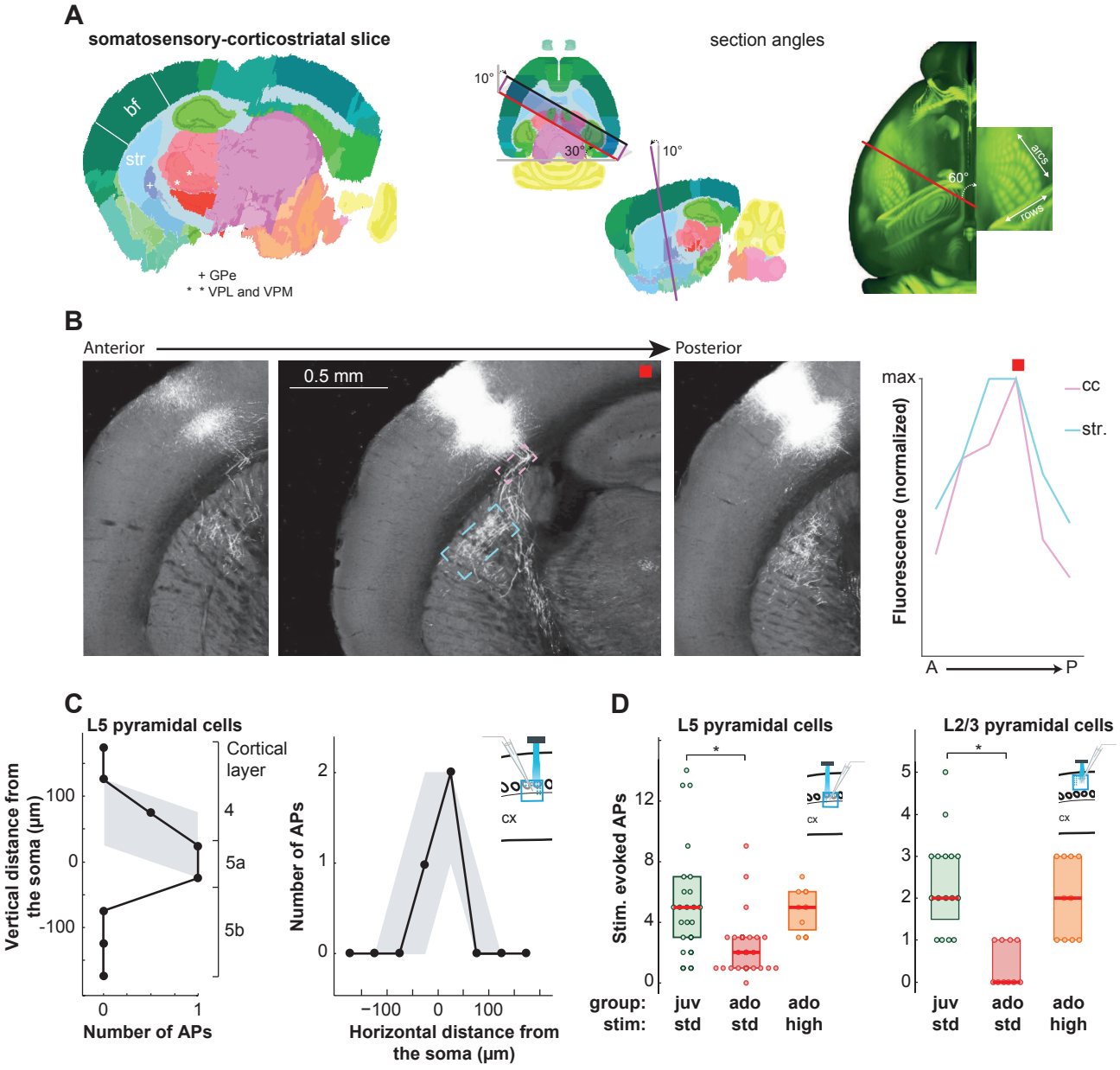

Extended Data Figure 1-1

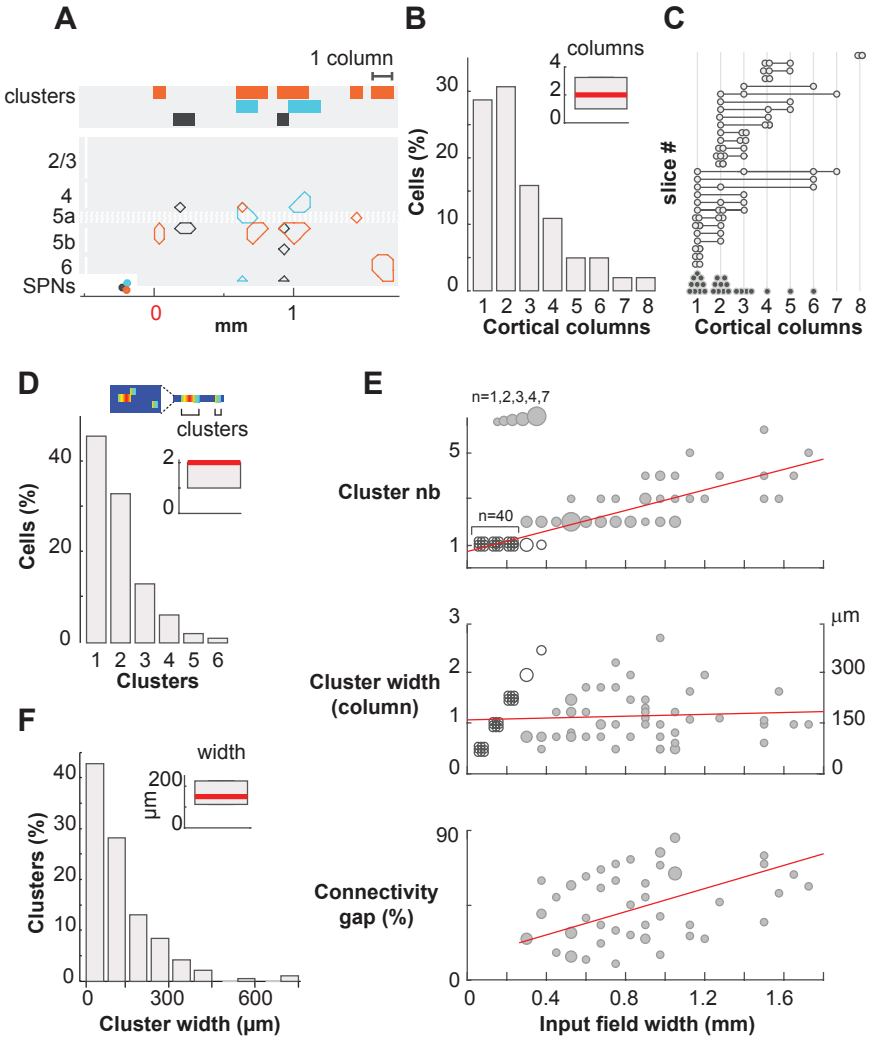
A
1 column
clusters
2/3
4
5a
5b
6
SPNs
0
1
mm
B
columns
Cells (%)
Cortical columns
C
slice #
Cortical columns
D
clusters
Cells (%)
Clusters
E
n=1,2,3,4,7
n=40
Cluster nb
Cluster width (column)
µm
Connectivity gap (%)
Input field width (mm)
F
width
µm
Clusters (%)
Cluster width (µm)

Figure 2

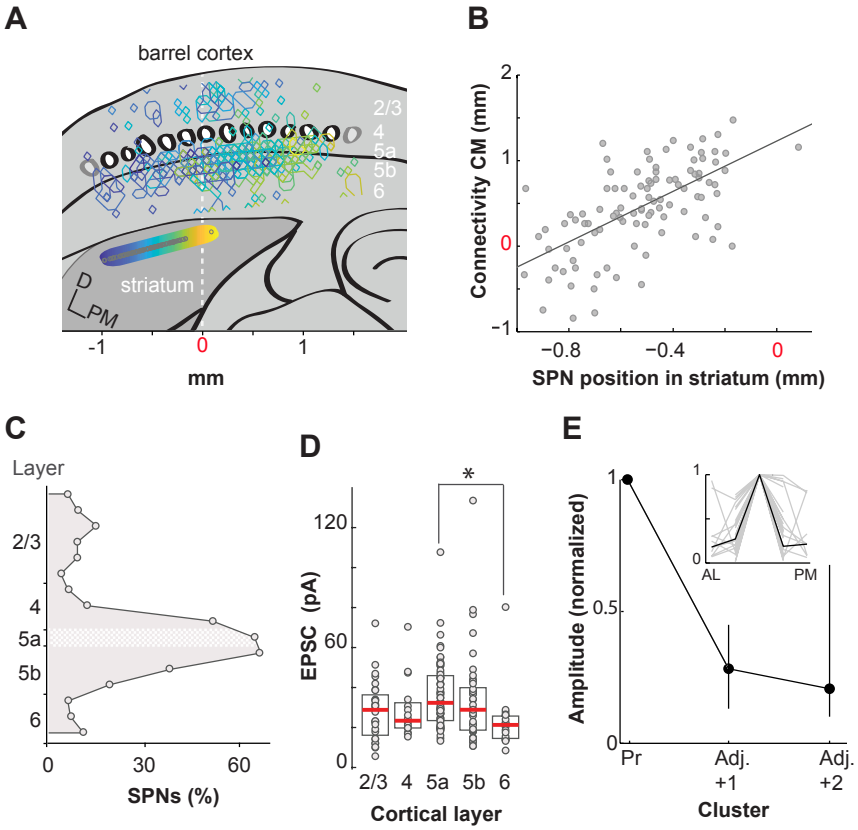
A
barrel cortex
2/3
4
5a
5b
6
striatum
D
L
PM
-1
0
1
mm
B
Connectivity CM (mm)
2
1
0
-1
−0.8
−0.4
0
SPN position in striatum (mm)
C
Layer
2/3
4
5a
5b
6
0
30
60
SPNs (%)
D
EPSC (pA)
120
60
0
*
2/3 4 5a 5b 6
Cortical layer
E
Amplitude (normalized)
1
0.5
0
1
0
AL
PM
Pr
Adj. +1
Adj. +2
Cluster

Figure 3

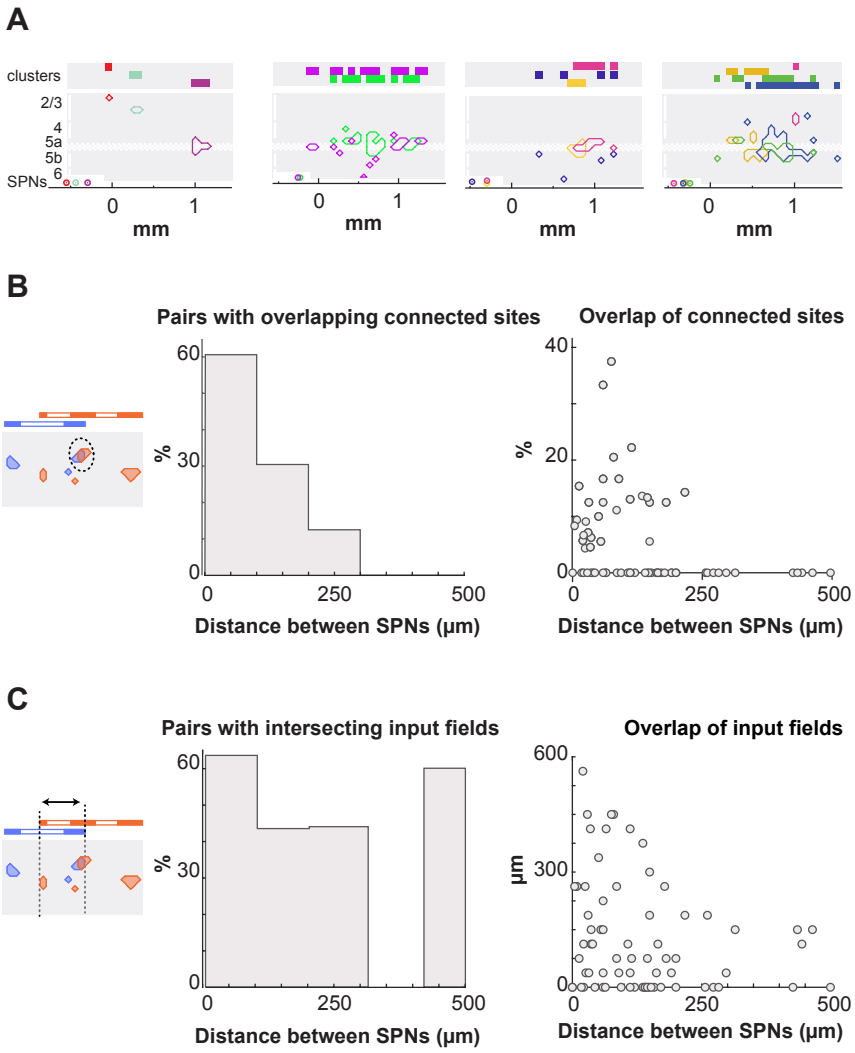
A
clusters
2/3
4
5a
5b
SPNs
6
0
1
mm
B
Pairs with overlapping connected sites
Overlap of connected sites
60
30
0
%
0
250
500
Distance between SPNs (µm)
40
20
C
Pairs with intersecting input fields
Overlap of input fields
600
300
µm

Figure 4

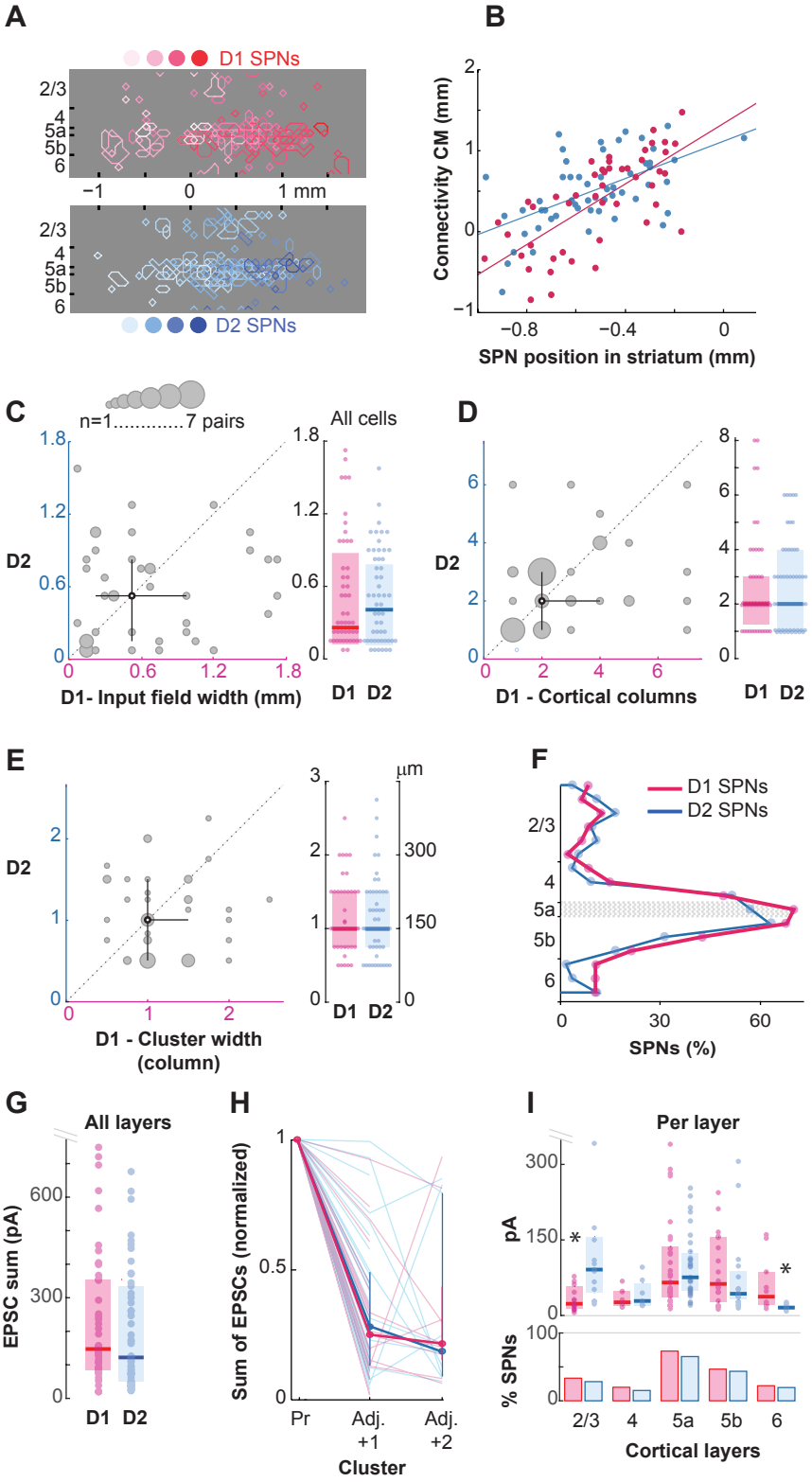
A
D1 SPNs
2/3
4
5a
5b
6
−1
0
1 mm
D2 SPNs
B
Connectivity CM (mm)
SPN position in striatum (mm)
C
n=1.....7 pairs
All cells
D2
D1- Input field width (mm)
D1 D2
D
D1 - Cortical columns
E
D1 - Cluster width (column)
µm
F
SPNs (%)
G
All layers
EPSC sum (pA)
H
Sum of EPSCs (normalized)
Pr
Adj. +1
Adj. +2
Cluster
I
Per layer
pA
% SPNs
Cortical layers

Figure 5

3.0.1 Supplementary: IT and PT innervation of SPNs

As described in the introduction, different innervation of D1 and D2 SPNs by pyramidal tract (PT) and intra-telencephalic (IT) CS projections have been described both anatomically (Lei *et al.* 2004; Reiner *et al.* 2003; Reiner 2010; Deng *et al.* 2015) and functionally (Kress *et al.* 2013; Ding *et al.* 2008; Takada *et al.* 2013). Here, we took advantage of the fact that IT and PT cells can be distinguished based on their electrophysiological profile. Regular Spiking (RS) neurons are IT types, and intrinsic bursting (IB) cells correspond to PT (Harris & Shepherd 2015; Petersen 2019). In line with previous findings (Harris & Shepherd 2015; Petersen 2019), we confirmed that IT neurons are predominantly located in L5a (RS neurons), while L5b contains a combination of both IT and PT cells (RS and IB).

We developed a stimulation protocol that selectively triggered PT neurons while leaving IT neurons inactive. This strategy allowed us to isolate the contribution of PT neurons to the innervation of D1 and D2 SPNs.

When only PT neurons were activated, approximately 10% of the original inputs to single SPNs were maintained, although there was considerable variability among individual cells. Notably, half of the SPNs lost all input when only PT neurons were engaged, while two D1 SPNs showed no reduction in their input. Overall, D1 SPNs tended to retain more connections from PT neurons compared to D2 SPNs, which exhibited a more pronounced decrease in inputs when IT contributions were eliminated.

These findings align with previous observations by Kress *et al.* 2013, suggesting that D1 SPNs may receive more robust innervation from PT neurons than D2 SPNs.

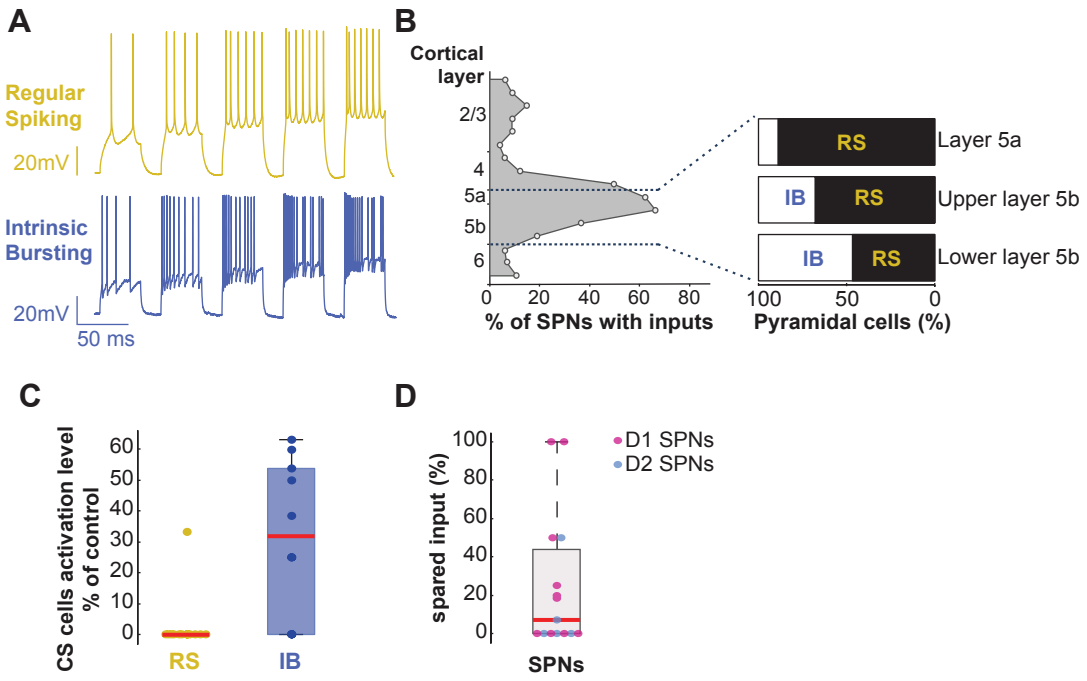

Figure 3.1: Different implication of IT and PT neurons in SPNs innervation.
A) Representative examples of the different firing profile of RS (IT) cells versus IB (PT) cells. **B**) L5a is primarily composed of IT cells whereas L5b contains both IB and RS cells. **C**) Excinction of evoked action potential with a decrease in stimulation intensity (n=14 RS; n=10 IB).**D**) Spared input: comparing the number of sites in the barrel cortex where the stimulation evoked an EPSCs before and after decreasing the stimulation intensity (n=15 cells, n=10 D1 SPNs; n=5 D2 SPNs).

CHAPTER 4

Study 2: Changes in Corticostriatal Circuits Following Learning

The second aim of this thesis is to explore how corticostriatal (CS) projections contribute to lateralized sensorimotor behavior, linking sensory cues to specific motor outputs. In particular, we examined how CS inputs to D1 and D2 spiny projection neurons (SPNs) are modulated by sensorimotor learning in a task requiring lateralized (contraversive and ipsiversive) turning to receive rewards. We hypothesized that in the striatum contralateral to the rewarded turn direction, sensory cortical input would increase to D1 SPNs, promoting movement, and/or decrease to D2 SPNs, reducing movement inhibition.

Lateralized foraging induces unexpected asymmetric corticostriatal plasticity

Kenza Amroune[1], Maud Schaffhauser[1], Thomas Morvan[1], Ingrid Bureau[1,+], and David Robbe[1,*,+]

[1]Aix-Marseille Université, INSERM, INMED, Marseille, 13009, France

[*]david.robbe@inserm.fr

[+]these authors contributed equally to this work

ABSTRACT

During foraging, animals can maximize their reward rate by progressively performing reward-oriented actions at increasing speed and with decreasing variability. The dorsolateral striatum (DLS) is critical for this process, potentially through opponent changes in the strength of cortical inputs on the two main types of striatal projection neurons (D1- and D2-SPNs). To test this hypothesis, and taking in account that unilateral selective perturbations of D1-SPNs or D2-SPNs induce orienting movements in opposite directions, we examined whether mice trained in a lateralized foraging task display asymmetrical changes in the strength of cortical input on these two types of neurons. Mice were required to make unidirectional turns along the walls of square towers in complete darkness to obtain drops of water. Across foraging sessions, the speed and stereotypy of reward-oriented turns rapidly increased. Whisker trimming in well-trained mice altered the kinematics of these actions, underscoring the contribution of sensory inputs in optimal foraging performance. Ex vivo patch-clamp recordings in the DLS and glutamate uncaging in the barrel cortex were combined to map the location of presynaptic cortical neurons connected to individual SPNs while recording the strength of monosynaptically connected pairs. Compared to naive animals, there were no significant changes in the functional connectivity of D1 or D2-SPNs in the contraversive hemisphere of well-trained mice, even though we observed an increased excitability of cortical pyramidal neurons. The ipsiversive hemisphere, which was less stimulated during foraging, showed no increase in cortical excitability but an increase in the strength of cortical inputs to SPNs. These findings reveal an unexpected hemispheric asymmetry in corticostriatal functional connectivity during automatization of a lateralized foraging task that may represent an homeostatic adaptation to normalize striatal activity during lateralized foraging.

Introduction

Animals modify the way they execute actions leading to rewards as they learn to associate specific sequences of movements with the systematic obtention of a particular reward within a given environment. This modification occurs both in time (actions are performed faster) and in space (movements become more stereotyped and kinematically optimized) and reflects the animals natural tendency to maximize reward capture rates as familiarity with the environment grows. A wide range of evidence supports a critical role of the dorsal striatum (DS) in enabling reward rate maximization. Many studies have provided evidence that the DS activity is critical for controlling the kinematics of reward-oriented movements (Panigrahi *et al.* 2015; Rueda-Orozco & Robbe 2015; Yttri & Dudman 2016; Sales-Carbonell *et al.* 2018; Jurado-Parras *et al.* 2020; Dhawale *et al.* 2021; Mizes *et al.* 2023; Monteiro *et al.* 2023; Park *et al.* 2023). Additionally, striatal neuronal activity changes as animals progressively automatize reward-oriented behavior (Barnes *et al.* 2005; Jin & Costa 2010; Rueda-Orozco & Robbe 2015; Sippy, Lapray, *et al.* 2015; Sippy, Chaimowitz, *et al.* 2021; Peters *et al.* 2021; Zareian *et al.* 2023) and coordinated neural activity emerges across the cortex and striatum during the learning (Koralek, Costa, *et al.* 2013; Lemke, Ramanathan, Guo, *et al.* 2019). Several studies have shown that the plasticity of excitatory cortico-striatal (CS) synapses is necessary for the learning and automatization of reward-oriented actions (Santos *et al.* 2015; Koralek, Jin, *et al.* 2012; Jin & Costa 2010; Lemke, Ramanathan, Darevksy, *et al.* 2021), but whether such changes affect similarly the two main types of projection neurons in the dorsal striatum is not known.

SPNs can be broadly divided into two main populations: D1-SPNs, which express dopamine D1 receptors, and D2-SPNs, which express dopamine D2 receptors (Kreitzer & Malenka 2008). These neurons project to distinct targets within the basal ganglia, forming two functionally opposing pathways: the direct pathway (D1-SPNs), known to facilitate movement, and the indirect pathway (D2-SPNs), which suppresses it (Mink 1996; Kravitz *et al.* 2010 but see Bonnavion *et al.* 2024). The opponent modulation of movement by D1- and D2-SPNs is well established in the context of locomotion and orienting-movements: unilateral activation of D1-SPNs induces contraversive turns (i.e., opposite to the activated hemisphere), while activation of D2-SPNs produces ipsiversive (same side) turns. Conversely, inhibition of D1-SPNs results in ipsiversive turns, and inhibition of D2-SPNs

leads to contraversive turns (Kravitz *et al.* 2010; Tecuapetla *et al.* 2014; Bay Kønig *et al.* 2019). These findings suggest that lateralized behavior is associated with distinct activation levels of D1- and D2-SPNs (Cruz *et al.* 2022), which may be driven by asymmetrical cortical input strengths to each population. If this simple but straightforward model was correct, highly stereotyped and lateralized sensory-guided reward-oriented actions could therefore reflect an imbalance in CS inputs driving the activity of D1 and D2 SPNs, with an increased number/strength of projections to D1 SPNs and/or fewer to D2 SPNs in the hemisphere contralateral to the actions performed (e.g., increase in D1 vs D2 connectivity ratio in the left hemisphere in mice performing rightward/clockwise turns). Although this hypothesis has never been tested, one week of practice in the accelerating rotarod has been shown to induce pathway-specific change in synaptic transmission (Yin *et al.* 2009) and repetitive positive reinforcements triggered by intracranial self-stimulation of the nigrostriatal system potentiate synaptic transmission between the cortex and the dorsal striatum, in a dopamine dependent manner (Reynolds & Wickens 2002). More recently, studies have shown that learning reward-oriented behaviors induces plasticity of the cortico-striatal synaptic transmission (Xiong *et al.* 2015; Hwang *et al.* 2022). Still, whether opponent changes in the strength of cortical inputs on D1- et D2-SPNs develop following learning of a lateralized reward-oriented action, as expected from the modulation of turning behavior by SPNs, is not known.

We recently characterized features of the functional connectivity between the barrel cortex and SPNs and found no major difference in the way this sensory region contacted D1- or D2-SPNs in naive non-trained mice (Amroune *et al.* 2024). To directly probe whether the spatiotemporal optimization of reward-oriented actions leads to opponent changes in connectivity between sensory cortex and D1/D2-SPNs, we designed a foraging task in which mice were required to make 90-degree unidirectional turns along walls of squared towers to obtain water rewards. We hypothesized that task learning would induce opposite changes in the strength of inputs originating from the barrel cortex toward SPN, with an increase in inputs to D1-SPNs and/or a decrease in inputs to D2-SPNs in the hemisphere contraversive to the rewarded direction. Within a few training sessions, water-restricted mice rapidly performed the task proficiently, showing a selective increase in the number of rewarded turns and in their speed and stereotypy. The speed and stereotypy of reward-oriented turns were reduced following trimming of the whiskers, confirming their contribution to task performance. We tested if these behavioral changes were associated with synaptic modifications

in corticostriatal projections by recording the functional inputs from the barrel cortex (S1) to D1- and D2-SPNs in the dorsolateral striatum (DLS) in ex-vivo preparation from naive or well-trained mice. Contrary to what could have been expected from an opponent plasticity of cortical inputs on D1/D2 neurons following learning of a lateralized sensory-guided movements, we found no significant differences in the number or strength of cortical inputs to D1- or D2-SPNs between trained and naive animals in the contralateral hemisphere (relative to sensory stimulation), although excitability of pyramidal neurons in the barrel cortex was increased. The ipsiversive hemisphere, which was less stimulated during unilateral foraging, showed no increase in cortical excitability but an increase in the number and strength of cortical inputs to SPNs. Our study indicates that, although the automatization of a lateralized reward-oriented movements leads to an increased cortical excitation in the hemisphere contralateral to the side of body receiving sensory stimulation, opposite changes in cortical connectivity to D1 and D2 SPNs were not observed, at least in the context of our sensory guided foraging task.

Results

Schematic of the 4-Towers Foraging Task and Representative Example

We developed a foraging task where freely moving mice could obtain water rewards delivered by water spouts protruding from the walls of 4 squared towers (Schaffhauser *et al*, in prep). Specifically, rewards were only delivered when water-restricted mice performed counterclockwise (CCW) turns along the walls of the towers (e.g., from the east spout to north spout protruding from a given tower, Fig. 1A). Each time a mouse started to turn around a given tower, a maximum number of consecutive rewarded turns was randomly selected between 4 and 12. Once a mouse reached this number (i.e., without leaving to harvest another tower), water drops were not delivered even if the mice performed additional turns in the CCW direction. Mice were free to change towers before the maximum number of rewarded turns was reached and a new maximum number of consecutive rewarded turns was set each time the mice started to harvest a tower (Fig 1A) To encourage thigmotaxis, the task was conducted in complete darkness.

During the first session, mice primarily ran along the external walls of the arena (Fig. 1B, Left). As expected, across foraging sessions they spent progressively more time around the tower over

training (Fig. 1B, Right). To quantify this change in behavior, we detected the movements of mice from one water spout to the next around a tower (turn around tower, TAT; methods ; Fig. 1C). Across sessions, mice performed more and more TAT in the rewarded direction, but not in the non-rewarded one (Fig. 1C). Moreover, when overlaying all the CCW reward-oriented runs within each session (Fig. 1D), we observed an increase in their stereotypy, (i.e., decrease in trajectory variability). Finally, examining the speed profiles of the turns in the rewarded direction revealed a prominent increase across sessions and confirmed the increased stereotypy of the run in the time domain. Altogether the increase in number, stereotypies and speeds of reward-oriented quarter of turns is congruent with this mouse maximizing its capture rate across sessions.

Selective Increase in Speed and Stereotyped Movements in Rewarded Direction

We next examined how the behavioral changes observed in a single mouse were robust across a significant number of animals (Figure 2, N=17, 6 female). Task performance was quantified across all sessions performed by the mice (range of sessions performed: 1519, only the first 15 sessions are presented). We observed the same behavioral changes at the population level as in Figure 1, namely an increase in proportion and number of reward-oriented turns (Fig. 2A-B), speed of execution (Fig 2C), and trajectory stereotypy (Fig. 2D). Altogether, these results show that mice subjected to this foraging protocol quickly developed lateralized reward-oriented full-body movements that presented the spatiotemporal characteristics of an automatized action (rapid and stereotyped).

As we hypothesized that the functional connectivity between the barrel cortex and striatum changes as animals automatized reward-oriented turns, we first verified that animals rely on their whiskers to execute these turns. For this, we bilaterally trimmed the whiskers of mice (N=6, methods) after 12 or 14 foraging sessions. When comparing the kinematics of CCW turns in the session preceding and following whisker trimming (see Method), reward-oriented turns were slower (Fig. 3A, B, $p = 0.028$, Wilcoxon), and more variable (Fig. 3C, D, $p = 0.028$, Wilcoxon). These alterations were not paralleled by a decrease in the number of reward-oriented turns nor an increase in the number of turns in the wrong direction (clockwise non reward). Finally, sham manipulation (see Method) did not induce comparable effects (not shown). These results indicate that mice use whisker-derived

sensory feedback to constrain the kinematics of their automatized reward-oriented turns along the walls of the tower.

CS Inputs to D1 and D2 SPNs Following Lateralized Learning

To explore if the behavioral changes observed following learning were associated with changes in CS projections to D1 and D2 SPNs, we mapped functional CS monosynaptic connections using a newly developed parasagittal ex-vivo slice preparation preserving the connectivity between a large chunk of the barrel cortex and DLS SPNs neurons (Amroune *et al.* 2024). We combined patch-clamp recordings of Drd1+ and Drd1- DLS SPNs in whole-cell voltage-clamp configuration with glutamate uncaging through laser scanning photostimulation (LSPS), allowing us to determine the location and strength of presynaptic inputs to individual SPNs. Glutamate was uncaged over a 29×16 pixel grid (2.1 × 1.1 mm, 75 μm spacing) to stimulate presynaptic cortical neurons, revealing glutamatergic inputs to the recorded SPN. Each uncaging site generated an input map, displaying the spatial distribution and strength of cortical inputs to D1- and D2-SPNs (Fig. 4A, Right). We search for potential changes in CS projections to D1- and D2-SPNs by examining three parameters contributing to cortico-striatal connectivity: the cortical field width, contributing cortical columns, and EPSC strength (*cf.* Schema).

Despite extensive task training and the observed behavioral lateralization and stereotypy, no significant changes in the number or strength of corticostriatal inputs to either D1- or D2-SPNs were observed between naive and trained animals (Fig. 4B-E). Further laminar analysis of the input distribution across cortical layers (layers 2/3, 4, 5a, 5b, and 6) also showed no significant change in the overall EPSC (excitatory postsynaptic current) sum across layers for D1 and D2 neurons (Fig. 4F-G). Similarly, the proportion of cells receiving input from each cortical layer remained consistent between naive and trained animals (Fig. 4H-I), with a major contribution of upper Layer 5 (50%) and a smaller one from the superficial layer (20% from layer 2/3), as previously described (Wise & Jones 1977; Reiner *et al.* 2003; Wall *et al.* 2013; Yamashita, Vavladeli, *et al.* 2018). These results indicate that the overall organization of corticostriatal inputs to both types of SPNs remains unchanged following the acquisition of a lateralized task.

Increased Cortical Excitation and Interhemispheric Asymmetry in CS Connectivity

One possibility is that functional connectivity is unchanged but that cortical neurons become more excitable. We investigated the excitation of Layer 5 (L5) pyramidal neurons, as they were the primary source of CS projections in our experiments (Fig. 4L-M , Fig. 5H). To characterize their excitation profiles, we recorded action potentials (APs) in current-clamp mode while using glutamate uncaging across an 8 × 8 grid to stimulate the soma and dendrites (Fig. 5A,B; 50 µm grid spacing, 350 × 350 µm area). Interestingly, trained animals displayed a significantly higher number of uncaging-evoked APs in L5 pyramidal neurons compared to naive animals ($p = 0.003$; Fig. 5C).

To examine whether the increase in cortical excitation was caused by increased contralateral whisker stimulation during the lateralized foraging task rather than reflecting a general change in motivational state, we examined whether it was also present in the less-stimulated ipsiversive hemisphere (Fig. 6). Our ex-vivo preparation, which maintains the connectivity between barrel cortex and DLS, requires a mediolateral angle precluding the investigation of the CS connectivity in the left and right hemispheres of the same animal. We therefore trained a subset of mice to perform clockwise turns and recorded from slices taken from the same hemisphere as above, now ipsilateral to the walls of the towers when mice turn around them. We found that L5 pyramidal neurons in the ipsiversive hemisphere exhibited significantly lower excitation than those in the contraversive hemisphere ($p = 0.037$; Fig. 6A). Next, we assessed whether this asymmetry in cortical excitation impacted CS circuits in both hemispheres. Surprisingly, CS inputs in the ipsiversive hemisphere had wider field width (Fig. 6B, $p = 0.001$), with a greater number of whisker-cortical columns contributing to these inputs (Fig. 6C, $p = 0.004$). However, the strength of individual connections remained similar between the two hemispheres (Fig. 6D-E). Thus the observed increase in total EPSC sum in the ipsiversive hemisphere (Fig. 6F, $p = 0.015$) reflects an increased number of CS connections rather than a change in individual synaptic strength. Additionally, we noted greater variability in the total EPSC sum in the ipsiversive hemisphere, indicating more heterogeneity in input strength (Fig. 6G, $p = 0.001$). This increase in the sum of the EPSP is particularly prominent in layer Va and Vb, which are the primary sources of input to SPNs. When examining the contributions of specific cortical layers to the overall strength of CS innervation, no significant differences emerged between

the hemispheres (Fig. 6H). However, SPNs in the ipsiversive hemisphere received more inputs from upper Layer 5 (86% vs. 57%) and superficial Layer 2/3 (39% vs. 19%), as shown in Fig. 6I. Those unexpected results suggest that the ipsiversive hemisphere, while not over-stimulated during lateralized foraging, undergoes important changes leading to an overall increase in CS connectivity to individual SPNs.

Discussion

In this study, we developed an original foraging task to test whether learning to perform a lateralized sensory-guided action to obtain rewards is associated with an increased (decreased) strength in functional connectivity between the sensory cortex and D1-SPNs (D2-SPNs). All the mice that were subjected to our foraging protocol developed highly automatized (i.e., fast and stereotyped in time and space) and lateralized (i.e., counterclockwise) reward-oriented movements, allowing them to quickly obtain drops of water. Critically, the kinematics changes were altered following whisker trimming showing that mice used their whisker to optimize the kinematics of their movements. *Ex-vivo*, we quantified the pattern of monosynaptic connectivities between the barrel cortex and D1- or D2-SPNs by combining glutamate uncaging with LSPS and patch-clamp recording, an approach that allow to quantify both the localization of presynaptic cortical neurons (horizontally across several barrels and vertically across all cortical layers) and the strength of the evoked monosynaptic responses. When comparing CS connectivity patterns (input map and strength) between brain slices obtained from animals either trained at least in 15 foraging sessions or untrained, no significant differences were observed. Still, we observed increased excitation of the striatal-projecting layer V barrel cortex neurons in the hemisphere predominantly "stimulated" during the task (i.e., the hemisphere contralateral to the towers walls when the mice performed rewarded turns). No such increase was observed in the ipsilateral barrel cortex (i.e, the hemisphere less "stimulated"). Surprisingly, this lower excitation of cortical neurons in the less-stimulated brain hemisphere was accompanied by an increase in the connectivity coupling between barrel cortex and SPNs. Altogether our study failed to show the expected opponent change in CS connectivity on D1- and D2-SPNs in mice having learned a task requiring them to perform lateralized sensory-guided turns. It however reveals that sensory overstimulation of one side of the body leads to an unexpected form of hemispheric adaptation suggestive of an inter-

hemispheric homeostatic process that maintains similar levels of activity in the left and right striatum.

Building on the well-known opposite modulation of orienting movements following unilateral perturbation of D1-SPNs and D2-SPNs, we tested the straightforward hypothesis that overtraining mice to perform sensory-guided turns in a single direction by following walls would lead to increased (or decreased) corticostriatal connectivity in D1-SPNs (or D2-SPNs) compared to naïve mice. However, no such changes were observed, as both groups of animals displayed similar corticostriatal connectivity in both cell types. Clearly, an absence of evidence should not be taken as evidence refuting the original hypothesis. We will discuss the potential pitfalls of our experimental approaches. Our aim is threefold: first, to expose the challenges in linking behavioral and synaptic levels of understanding; second, to argue that it is too early to interpret this negative result as favoring the so-called co-activation hypothesis of SPNs functions, and third, to highlight an expected modulation of CS connectivity following extensive asymmetrical foraging that may represent a form of homeostatic plasticity.

When considering the reasons for the absence of opponent changes in CS strength, a first potential issue is whether our training protocol was strong enough to induce plasticity and whether our method to study corticostriatal functional connectivity is sufficiently sensitive to detect plastic changes. Our data argue against these concerns, as training not only induced detectable changes in the excitation of cortical neurons projecting to the DLS in the contralateral hemisphere (relative to whisker stimulation) but also increased connectivity in the less-stimulated hemisphere. Thus, the expected effect could, in principle, have occurred, and the issue with our study is not that no changes were detected but rather that they were not the expected one. Still our sampling of patched neurons was very low (on average four neurons per animal; two D1 SPNs and two D2 SPNs) in a given animal. Given the variability in input map and EPSC amplitudes observed in naive and trained animals it would have been unrealistic and dangerous to examine whether a difference in connectivity on D1- and D2-SPN correlated with certain aspects of the foraging performance (e.g., stereotypy).

Another potential limitation of our experimental strategy is that, although we quantified clear changes in kinematics (and found no correlation with D1-SPN vs. D2-SPN differences), we did

not test learning at the behavior level. Indeed, two mice could exhibit similar kinematics reflecting similar motivation but they may differ in learning, which might only manifest when challenging the animals to switch from CCW to CW turns. This would have required testing the animals in a last session in which the rewarded direction would have been switched, which unfortunately might also have affected learning and potential synaptic changes. This type of paradox highlights the difficulty in testing changes in functional connectivity using ex-vivo preparation from trained animals. Obviously, there are also all kinds of behavioral paradigms we could have tested beyond a simplistic learned vs not-learned conditions. For instance, an increase in functional connectivity on D2-SPNs might have been observed had we trained animals in a highly uncertain environment (Dunovan & Verstynen 2016; Geramita *et al.* 2024). Another potential issue is that most of the changes may have occurred earlier in learning, although there is evidence for a role of the DLS in constraining the kinematics of reward-oriented movements and orienting-choice after extensive task training (Tai *et al.* 2012; Rueda-Orozco & Robbe 2015; Dhawale *et al.* 2021; Cruz *et al.* 2022; Mizes *et al.* 2023) and plasticity of the corticostriatal synaptic transmission has been observed after several days of training in the accelerating rotarod and week-s of training in a sensory-guided decision and a reaching task (Yin *et al.* 2009; Xiong *et al.* 2015; Hwang *et al.* 2022). A more realistic pitfall, that was difficult to anticipate, is that even if the task required the animals to make CCW turns, reaching the next water spout in the CCW direction required them to make a first CW initial movement because their animals head pointed toward the center of the tower. Thus, we can't rule out that changes might have been observed if the animals did not have to generate a CW-CCW sequence of body orientations.

To track changes in both the spatial organization and synaptic of strength of barrel cortex neurons connected to single SPN, we used single-spike cortical stimulation. This approach may not fully capture the nuanced dynamics of synaptic plasticity that occur during learning. For instance, changes in burst-induced synaptic responses, or other functional properties might not be apparent with our method (e.g., intrinsic excitability of SPN). Furthermore, in vivo functional coupling might be strongly constrained by high tonic levels of dopamine, especially during foraging (Niv *et al.* 2007; Hamid *et al.* 2016). Altogether, there are many reasons that could account for the fact that we did not see the expected opponent changes in functional coupling, precluding us to conclude that

those changes are in agreement with models that consider that balanced co-activation of D1- and D2-SPN are responsible for motor/decision function of the striatum (Klaus *et al.* 2017; Barbera *et al.* 2016; Cui *et al.* 2013; Parker *et al.* 2016). Future investigation should therefore take into account these kinds of pitfalls to further advance our understanding of the respective function of these two populations of neurons.

Although we did not observe detectable changes in CS projections to D1- and D2-SPNs in the contralateral DLS of mice that were subjected to extensive practice of a lateralized foraging task, we did find an increased excitation in cortical L5 pyramidal neurons – the primary source of cortical inputs to the striatum (Wise & Jones 1977; Reiner *et al.* 2003; Shepherd 2013; Wall *et al.* 2013). Specifically, more spikes were evoked by glutamate uncaging in cortical neurons taken from trained animals, compared to naive animals. This heightened excitation aligns with previous findings indicating that sensorimotor learning enhances cortical activity in associated sensory regions involved in task-related processing (O'Connor *et al.* 2010; Sachidhanandam *et al.* 2013; Yamashita & Petersen 2016). Following sensorimotor learning, in vivo recording in the DLS have highlight an increase in CS activity (Xiong *et al.* 2015), as well as a heightened membrane response in SPNs (Sippy, Chaimowitz, *et al.* 2021), leading to the hypothesis that learning might strengthen CS inputs to SPNs. While we did not find direct changes in the strength or number of CS connections, the increased excitation in L5 suggests an enhanced cortical activity that could still lead to more effective activation SPNs in the DLS. Future studies should investigate whether this increased excitation is selective for cortical neurons projecting on D1-or D2-SPNs. Therefore, functional changes at the cortical level may be driving the behavioral adaptations and striatal activity changes observed after motor learning (Xiong *et al.* 2015; Sippy, Chaimowitz, *et al.* 2021). This increase in pyramidal neuron excitation was specific to the hemisphere that was primarily stimulated during our lateralized foraging task (i.e., cortical excitation in the ipsilateral hemisphere was reduced compared to contralateral one ; Fig. 6). Unexpectedly, we observed an increase in CS functional coupling in slices taken from this less-stimulated hemisphere. This heightened CS connectivity in the ipsilateral DLS may be a form of compensatory plasticity or a homeostatic adaptation, to normalize CS activity between hemispheres. The concept of homeostatic plasticity suggests that neural circuits can maintain stable activity by adjusting synaptic strengths to counterbalance changes in network

activity (Turrigiano 2008; Wen & Turrigiano 2024). Therefore, increasing CS inputs to SPNs in the ipsiversive hemisphere might help stabilize striatal activity across both hemispheres. One possible explanation for our findings is that the contraversive hemisphere, actively engaged in task performance, relies on enhanced cortical excitability to modulate the kinematics of reward-oriented movements, while the ipsiversive hemisphere compensates by increasing its synaptic input to maintain overall neural balance during other exploratory movements. These findings suggest that lateralized motor learning involves not only changes within the associated hemisphere but also compensatory adjustments in the ipsilateral one, indicating a more nuanced understanding of corticostriatal plasticity than previously thought.

In summary, our study reveals unexpected patterns of corticostriatal plasticity during lateralized motor learning, marked by hemispheric asymmetry and the absence of significant changes in CS inputs to D1- and D2-SPNs in the actively engaged hemisphere. We propose that these findings may involve homeostatic adjustments between hemispheres to maintain balanced excitation levels across the two DLS. Future research should focus on exploring the mechanisms and function of this hemispheric asymmetry.

Methods

Animals

A total of 37 hemizygous B6.Cg-Tg(Drd1a-tdTomato)6Calak/J mice (JAX stock #016204; (Ade *et al.* 2011) were used, both males and females (postnatal day [PND] 30–45). They were housed in groups of 2–3 mice on ventilated racks controlled by temperature (21 °C). A 12 h–12 h light/dark cycle was maintained, and all experiments were carried out during the dark phase. Food was available *ad libitum* in their home cage, but mice had to perform the behavioral task described below to obtain water. Body weight was measured twice a day, before and after behavioral experiments. All experiments were performed under the European Union Directive (European Community Directive 86/609/EEC) and approved by the national ethics committee (Ministère de l'enseignement supérieur et de la recherche, France, Authorization # 46285).

Task Apparatus

The experimental apparatus consists of a square arena (83 cm per side) with four square towers positioned at the center of each quadrant (Northwest, Northeast, Southwest, and Southeast). Each tower (15 cm in length and 10 cm in height) has four external faces, each equipped with a water spout located 2 cm above the floor. The spouts extend 2 cm outward from the walls and are connected to water reservoirs housed within the towers.

Water delivery (2–5 μL per droplet) is controlled by solenoid valves (VAC–20 PSIG, Parker), with each tower having four independently controlled valves. In total, the arena contains 16 valves (4 towers $\times$ 4 valves) programmed to dispense water droplets based on the animals' behavior. The arena floor is made of transparent plexiglass, elevated 140 cm above the ground, allowing real-time tracking of the mice's movements by a camera placed beneath the apparatus. The camera captures the position of the mouse, defined as the centroid of its body, using a background subtraction method implemented via OpenCV.

The data recording and apparatus control are fully automated through custom Python-based software running on a PC, which communicates with a Raspberry Pi that controls the solenoid valves. The task structure is designed to allow mice to obtain water by running around the towers. Water droplets are delivered when the mice cross boundaries between predefined regions of interest (North, East, South, West trapezes) surrounding each tower's spouts. The water delivery is triggered when the mouse completes a quarter turn around a tower, either in a clockwise or counterclockwise direction, depending on the task protocol.

This delivery system can be adjusted based on various parameters, including the direction of movement (e.g., drops of water may be delivered for a given running direction such as clockwise or counterclockwise, or both), specific tower locations, and the animals' interaction history with each tower.

Behavioral task

In this version of the task, mice can obtain rewards by turning around the 4 towers with two following constraints: 1) only one direction is rewarded, and 2) once a mouse starts exploiting a tower, a maximum number of consecutive drops is randomly drawn (between 4 and 12, corresponding to one and three full turns) after which the current tower stops delivering reward, and the mouse must

leave to exploit one of the three equivalent towers.

The protocol is as follows: Prior to training, mice were handled 2–3 times per day for 30 minutes, for 3 days. Following handling, the mice were familiarized with the arena through 1 session of 12 minutes (free exploration). After the familiarization session, the mice were weighed and placed on water restriction. The next day, training began, and each quarter turn made in a specific direction (either clockwise or counterclockwise) around a tower was rewarded. This initial learning phase (Phase 1, free exploitation) was carried out over 2 days (2–3 sessions of 12 minutes, 5 hours apart). Throughout the training, animals were trained in a single fixed direction to promote highly stereotyped behaviors.

However, to encourage the exploitation of several towers during sessions, following the initial 2 days of learning, the number of consecutive rewards available around a tower was randomly set between 4 and 12. This protocol was applied for 10 days. During weekends, water restriction was interrupted. All experiments were performed in darkness.

Mice were weighed each morning before the first training session. Water droplet size was adjusted (ranging from 2 to 5 μL) depending on the number of rewards obtained. Care was taken to ensure their growth curve was maintained.

After a few training days (3–5 days), mice were able to achieve a stable level of performance characterized by a high percentage of turns in the rewarded direction. Electrophysiological recordings were conducted either in task-naive animals that had not undergone the task or in mice that had reached a reliable level of performance, typically after 6 to 10 days of training. Following their last training session, water was reintroduced in the cages, and the brain slice preparation was performed the following day.

Due to the corticostriatal slice preparation for electrophysiological experiments (see section), only the left hemisphere was kept. In order to study corticostriatal projections in the ipsiversive and contraversive hemisphere, mice were trained to perform either clockwise (CW) turns (contraversive) or counterclockwise (CCW) turns (ipsiversive), as electrophysiological experiments were always performed in the left hemisphere.

Whisker Trimming

Whisker trimming was performed on 6 mice once task performance had stabilized. Mice completed a morning session (session 12 for 3 mice or session 14 for the other 3), which was followed by bilateral whisker trimming with scissors under isoflurane anesthesia (5 minutes of exposure). The sham group underwent identical isoflurane exposure without trimming. Five hours after sensory deprivation, an afternoon session was conducted. Behavioral parameters were compared before and after trimming to assess changes induced by sensory deprivation.

Brain slices preparation and electrophysiology

One day after their last session, mice were deeply anesthetized with isoflurane (4%) before cervical dislocation and decapitation. Parasagittal corticostriatal slices were prepared as previously described (Amroune *et al.* 2024). Due to the angle to preserve corticostriatal projections, only the left hemisphere of the brain was used for electrophysiological experiments. Slices used for LSPS contained barrels in the L4 of cortex, the globus pallidus, its external segment (GPe), the internal capsule, the ventral posteromedial nucleus of thalamus, and the anterior hippocampus. Approximately 8 barrels (5–13) were visible in the slice.

SPNs 50–150 μm deep in the slice were visualized under infrared and fluorescent lights in a BX61WI microscope (Olympus) and patched with borosilicate electrodes (3–6 MΩ) and recorded in the voltage-clamp whole-cell configuration using a Multiclamp 700A amplifier (Axon Instrument, Molecular Devices). The holding membrane potential was –80 mV.

The intracellular solution contained (in mM): 128 Cs-methylsulfate, 4 $MgCl_2$, 10 HEPES, 1 EGTA, 4 Na_2ATP, 0.4 Na_2GTP, 10 Na-phosphocreatine, 3 ascorbic acid; pH 7.25; 290–300 mOsm. Cells in L5 and L2/3 of the barrel cortex were recorded in the current-clamp mode, with an intracellular solution in which Cs-methylsulfate was replaced by K-methylsulfate. All experiments were performed at room temperature (21℃).

LSPS with glutamate uncaging

LSPS was performed as described previously (Bureau *et al.* 2006). Recirculating (2 mL/min) ACSF solution contained (in mM): 0.2 MNI-caged glutamate (Tocris), 0.005 CPP [()–3–(2–carboxypiperazin–4–yl) propyl–1–phosphonic acid], 4 $CaCl_2$, and 4 $MgCl_2$. Focal photolysis of caged glutamate was achieved using a 2 ms pulse from a pulsed UV (355 nm) laser (DPSS Lasers Inc.) through a

0.16 NA 4× objective (Olympus). A 20 mW pulse was used for stimulating cortical neurons in the contraversive hemisphere, while a 25 mW pulse was employed for naive animals and for stimulation in the ipsiversive hemisphere to maintain excitation of cortical neurons at comparable levels.

The stimulus pattern for mapping the corticostriatal projections was 464 positions spaced by 75 μm on a 29×16 grid (2.1 × 1.1 mm) over barrel cortex. The corticostriatal slice and the LSPS grid were oriented in such a way that layer 5a was laid out horizontally. UV stimuli were applied every 700 ms and their successive positions on the LSPS grid were such as to maximize the time between stimulations of neighboring sites. Electrophysiological traces consisted of 100 ms baseline, a 450 ms window followed by a $-5\,\mathrm{mV}/100\,\mathrm{ms}$ test pulse. A minimum of 2 and up to 4 stimulations were performed at each site at several minutes intervals.

Custom software for instrument control and acquisition (Suter et al. 2010) was written in Matlab (Mathworks). Excitation profiles of pyramidal neurons were generated under similar conditions except that cells were recorded in current-clamp mode and glutamate was uncaged on a smaller 8×8 grid covering their soma and dendrites (50 μm spacing; 350 × 350 μm).

Analysis of LSPS data

Synaptic input maps of neurons were constructed by taking the peak amplitude of EPSCs detected in a 50 ms time window starting at stimulation onset for each position in the LSPS grid. Measures were averaged across repetitions of stimulations (2–4). The threshold for EPSC detection was 3 standard deviations from baseline or $9.2 \pm 0.4\,\mathrm{pA}$. To disambiguate evoked responses from spontaneous activity, synaptic responses occurring less than 2 times across repetitions of maps were set to zero. Averaged maps were superposed taking L5a as a reference in the vertical axis and the junction of the GPe, dorsal striatum, and internal capsule as a reference in the horizontal axis (Refhor).

To detect clusters and the center of mass of inputs in the LSPS map, we used the binary version of the map reporting the location of connected and non-connected sites (i.e., yielding EPSCs or none in the recorded SPN) and stacked it along its vertical axis. A cluster of inputs comprised 1 or more consecutive connected sites in the stacked map that was framed by 1 or more non-connected sites. Thus, a cluster here may include connected sites that were not adjacent on the vertical axis in the original map, and may combine synaptic inputs from different layers.

The number of cortical columns was estimated based on the number of consecutive connected sites (ConsSites) in the stacked map and the mean width of a barrel in the slice, $150\,\mu$m, which is equal to 2 connected sites in the map. Hence, the number of cortical columns $= \sum(\lceil \text{ConsSites}/2 \rceil)$. Traces from current clamp recordings were analyzed in a 50 ms time window at stimulus onset to count the number of action potentials (APs) elicited upon glutamate uncaging at every site and in the entire stimulation grid.

Statistical Analysis

Median and 25-75th percentiles are shown in the Figures. N and n are the numbers of animals and neurons, respectively. Statistical analyses were performed with Python scripts using permutation tests (n = 10000 iterations), and Wilcoxon signed ranks test for paired comparison. Results were considered statistically significant for a p-value < 0.05, except for multiple comparisons where we divided 0.05 by the number of comparisons.

References

1. Ade, K. K., Wan, Y., Chen, M., Gloss, B. & Calakos, N. An Improved BAC Transgenic Fluorescent Reporter Line for Sensitive and Specific Identification of Striatonigral Medium Spiny Neurons. eng. *Frontiers in Systems Neuroscience* **5,** 32. ISSN: 1662-5137 (2011).
2. Amroune, K., Fontolan, L., Robbe, D. & Bureau, I. *Sparse and specific somatosensory functional innervation of dorsolateral striatal neurons* working paper or preprint. May 2024.
3. Barbera, G. *et al.* Spatially Compact Neural Clusters in the Dorsal Striatum Encode Locomotion Relevant Information. eng. *Neuron* **92,** 202–213. ISSN: 1097-4199 (Oct. 2016).
4. Barnes, T. D., Kubota, Y., Hu, D., Jin, D. Z. & Graybiel, A. M. Activity of striatal neurons reflects dynamic encoding and recoding of procedural memories. en. *Nature* **437,** 1158–1161. ISSN: 0028-0836, 1476-4687 (Oct. 2005).

5. Bay Kønig, A., Ciriachi, C., Gether, U. & Rickhag, M. Chemogenetic Targeting of Dorsomedial Direct-pathway Striatal Projection Neurons Selectively Elicits Rotational Behavior in Mice. en. *Neuroscience* **401,** 106–116. ISSN: 03064522 (Mar. 2019).

6. Bonnavion, P. *et al.* Striatal projection neurons coexpressing dopamine D1 and D2 receptors modulate the motor function of D1- and D2-SPNs. en. *Nature Neuroscience* **27,** 1783–1793. ISSN: 1097-6256, 1546-1726 (Sept. 2024).

7. Bureau, I., von Saint Paul, F. & Svoboda, K. Interdigitated paralemniscal and lemniscal pathways in the mouse barrel cortex. eng. *PLoS biology* **4,** e382. ISSN: 1545-7885 (Nov. 2006).

8. Cruz, B. F. *et al.* Action suppression reveals opponent parallel control via striatal circuits. en. *Nature* **607,** 521–526. ISSN: 0028-0836, 1476-4687 (July 2022).

9. Cui, G. *et al.* Concurrent activation of striatal direct and indirect pathways during action initiation. en. *Nature* **494,** 238–242. ISSN: 0028-0836, 1476-4687 (Feb. 2013).

10. Dhawale, A. K., Wolff, S. B. E., Ko, R. & Ölveczky, B. P. The basal ganglia control the detailed kinematics of learned motor skills. en. *Nature Neuroscience* **24,** 1256–1269. ISSN: 1097-6256, 1546-1726 (Sept. 2021).

11. Dunovan, K. & Verstynen, T. Believer-Skeptic Meets Actor-Critic: Rethinking the Role of Basal Ganglia Pathways during Decision-Making and Reinforcement Learning. *Frontiers in Neuroscience* **10.** ISSN: 1662-453X (Mar. 2016).

12. Geramita, M. A., Ahmari, S. E. & Yttri, E. A. *Striatal indirect pathway mediates hesitation* en. Sept. 2024.

13. Hamid, A. A. *et al.* Mesolimbic dopamine signals the value of work. en. *Nature Neuroscience* **19,** 117–126. ISSN: 1097-6256, 1546-1726 (Jan. 2016).

14. Hwang, F.-J. *et al.* Motor learning selectively strengthens cortical and striatal synapses of motor engram neurons. eng. *Neuron* **110,** 2790–2801.e5. ISSN: 1097-4199 (Sept. 2022).

15. Jin, X. & Costa, R. M. Start/stop signals emerge in nigrostriatal circuits during sequence learning. en. *Nature* **466,** 457–462. ISSN: 0028-0836, 1476-4687 (July 2010).

16. Jurado-Parras, M.-T. *et al.* The Dorsal Striatum Energizes Motor Routines. eng. *Current biology: CB* **30,** 4362–4372.e6. ISSN: 1879-0445 (Nov. 2020).

17. Klaus, A. *et al.* The Spatiotemporal Organization of the Striatum Encodes Action Space. eng. *Neuron* **95,** 1171–1180.e7. ISSN: 1097-4199 (Aug. 2017).

18. Koralek, A. C., Costa, R. M. & Carmena, J. M. Temporally Precise Cell-Specific Coherence Develops in Corticostriatal Networks during Learning. en. *Neuron* **79,** 865–872. ISSN: 08966273 (Sept. 2013).

19. Koralek, A. C., Jin, X., Long, J. D., Costa, R. M. & Carmena, J. M. Corticostriatal plasticity is necessary for learning intentional neuroprosthetic skills. eng. *Nature* **483,** 331–335. ISSN: 1476-4687 (Mar. 2012).

20. Kravitz, A. V. *et al.* Regulation of parkinsonian motor behaviours by optogenetic control of basal ganglia circuitry. eng. *Nature* **466,** 622–626. ISSN: 1476-4687 (July 2010).

21. Kreitzer, A. C. & Malenka, R. C. Striatal Plasticity and Basal Ganglia Circuit Function. en. *Neuron* **60,** 543–554. ISSN: 08966273 (Nov. 2008).

22. Lemke, S. M., Ramanathan, D. S., Darevksy, D., *et al.* Coupling between motor cortex and striatum increases during sleep over long-term skill learning. en. *eLife* **10,** e64303. ISSN: 2050-084X (Sept. 2021).

23. Lemke, S. M., Ramanathan, D. S., Guo, L., Won, S. J. & Ganguly, K. Emergent modular neural control drives coordinated motor actions. eng. *Nature Neuroscience* **22,** 1122–1131. ISSN: 1546-1726 (July 2019).

24. Mink, J. W. The basal ganglia: focused selection and inhibition of competing motor programs. eng. *Progress in Neurobiology* **50,** 381–425. ISSN: 0301-0082 (Nov. 1996).

25. Mizes, K. G. C., Lindsey, J., Escola, G. S. & Ölveczky, B. P. Dissociating the contributions of sensorimotor striatum to automatic and visually guided motor sequences. eng. *Nature Neuroscience* **26,** 1791–1804. ISSN: 1546-1726 (Oct. 2023).

26. Monteiro, T. *et al.* Using temperature to analyze the neural basis of a time-based decision. eng. *Nature Neuroscience* **26,** 1407–1416. ISSN: 1546-1726 (Aug. 2023).

27. Niv, Y., Daw, N. D., Joel, D. & Dayan, P. Tonic dopamine: opportunity costs and the control of response vigor. en. *Psychopharmacology* **191,** 507–520. ISSN: 0033-3158, 1432-2072 (Mar. 2007).

28. O'Connor, D. H. *et al.* Vibrissa-based object localization in head-fixed mice. eng. *The Journal of Neuroscience: The Official Journal of the Society for Neuroscience* **30,** 1947–1967. ISSN: 1529-2401 (Feb. 2010).

29. Panigrahi, B. *et al.* Dopamine Is Required for the Neural Representation and Control of Movement Vigor. en. *Cell* **162,** 1418–1430. ISSN: 00928674 (Sept. 2015).

30. Park, J. *et al. Conjoint specification of action by neocortex and striatum* en. Oct. 2023.

31. Parker, P. R. L., Lalive, A. L. & Kreitzer, A. C. Pathway-Specific Remodeling of Thalamostriatal Synapses in Parkinsonian Mice. eng. *Neuron* **89,** 734–740. ISSN: 1097-4199 (Feb. 2016).

32. Peters, Fabre, J. M. J., Steinmetz, N. A., Harris, K. D. & Carandini, M. Striatal activity topographically reflects cortical activity. en. *Nature* **591,** 420–425. ISSN: 0028-0836, 1476-4687 (Mar. 2021).

33. Reiner, A., Jiao, Y., Del Mar, N., Laverghetta, A. V. & Lei, W. L. Differential morphology of pyramidal tract-type and intratelencephalically projecting-type corticostriatal neurons and their intrastriatal terminals in rats. eng. *The Journal of Comparative Neurology* **457,** 420–440. ISSN: 0021-9967 (Mar. 2003).

34. Reynolds, J. N. & Wickens, J. R. Dopamine-dependent plasticity of corticostriatal synapses. en. *Neural Networks* **15,** 507–521. ISSN: 08936080 (June 2002).

35. Rueda-Orozco, P. E. & Robbe, D. The striatum multiplexes contextual and kinematic information to constrain motor habits execution. en. *Nature Neuroscience* **18,** 453–460. ISSN: 1097-6256, 1546-1726 (Mar. 2015).

36. Sachidhanandam, S., Sreenivasan, V., Kyriakatos, A., Kremer, Y. & Petersen, C. C. H. Membrane potential correlates of sensory perception in mouse barrel cortex. en. *Nature Neuroscience* **16,** 1671–1677. ISSN: 1097-6256, 1546-1726 (Nov. 2013).

37. Sales-Carbonell, C. *et al.* No Discrete Start/Stop Signals in the Dorsal Striatum of Mice Performing a Learned Action. en. *Current Biology* **28,** 3044–3055.e5. ISSN: 09609822 (Oct. 2018).

38. Santos, F. J., Oliveira, R. F., Jin, X. & Costa, R. M. Corticostriatal dynamics encode the refinement of specific behavioral variability during skill learning. en. *eLife* **4,** e09423. ISSN: 2050-084X (Sept. 2015).

39. Shepherd, G. M. G. Corticostriatal connectivity and its role in disease. eng. *Nature Reviews. Neuroscience* **14,** 278–291. ISSN: 1471-0048 (Apr. 2013).

40. Sippy, T., Chaimowitz, C., Crochet, S. & Petersen, C. C. H. Cell Type-Specific Membrane Potential Changes in Dorsolateral Striatum Accompanying Reward-Based Sensorimotor Learning. en. *Function* **2,** zqab049. ISSN: 2633-8823 (Oct. 2021).

41. Sippy, T., Lapray, D., Crochet, S. & Petersen, C. C. H. Cell-Type-Specific Sensorimotor Processing in Striatal Projection Neurons during Goal-Directed Behavior. eng. *Neuron* **88,** 298–305. ISSN: 1097-4199 (Oct. 2015).

42. Tai, L.-H., Lee, A. M., Benavidez, N., Bonci, A. & Wilbrecht, L. Transient stimulation of distinct subpopulations of striatal neurons mimics changes in action value. en. *Nature Neuroscience* **15,** 1281–1289. ISSN: 1097-6256, 1546-1726 (Sept. 2012).

43. Tecuapetla, F., Matias, S., Dugue, G. P., Mainen, Z. F. & Costa, R. M. Balanced activity in basal ganglia projection pathways is critical for contraversive movements. eng. *Nature Communications* **5,** 4315. ISSN: 2041-1723 (July 2014).

44. Turrigiano, G. G. The Self-Tuning Neuron: Synaptic Scaling of Excitatory Synapses. en. *Cell* **135,** 422–435. ISSN: 00928674 (Oct. 2008).

45. Wall, N. R., De La Parra, M., Callaway, E. M. & Kreitzer, A. C. Differential innervation of direct- and indirect-pathway striatal projection neurons. eng. *Neuron* **79,** 347–360. ISSN: 1097-4199 (July 2013).

46. Wen, W. & Turrigiano, G. G. Keeping Your Brain in Balance: Homeostatic Regulation of Network Function. en. *Annual Review of Neuroscience* **47,** 41–61. ISSN: 0147-006X, 1545-4126 (Aug. 2024).

47. Wise, S. P. & Jones, E. G. Cells of origin and terminal distribution of descending projections of the rat somatic sensory cortex. eng. *The Journal of Comparative Neurology* **175,** 129–157. ISSN: 0021-9967 (Sept. 1977).

48. Xiong, Q., Znamenskiy, P. & Zador, A. M. Selective corticostriatal plasticity during acquisition of an auditory discrimination task. en. *Nature* **521,** 348–351. ISSN: 0028-0836, 1476-4687 (May 2015).

49. Yamashita, T. & Petersen, C. C. Target-specific membrane potential dynamics of neocortical projection neurons during goal-directed behavior. en. *eLife* **5,** e15798. ISSN: 2050-084X (June 2016).

50. Yamashita, T., Vavladeli, A., *et al.* Diverse Long-Range Axonal Projections of Excitatory Layer 2/3 Neurons in Mouse Barrel Cortex. eng. *Frontiers in Neuroanatomy* **12,** 33. ISSN: 1662-5129 (2018).

51. Yin, H. H. *et al.* Dynamic reorganization of striatal circuits during the acquisition and consolidation of a skill. eng. *Nature Neuroscience* **12,** 333–341. ISSN: 1546-1726 (Mar. 2009).

52. Yttri, E. A. & Dudman, J. T. Opponent and bidirectional control of movement velocity in the basal ganglia. eng. *Nature* **533,** 402–406. ISSN: 1476-4687 (May 2016).

53. Zareian, B., Lam, A. & Zagha, E. Dorsolateral Striatum is a Bottleneck for Responding to Task-Relevant Stimuli in a Learned Whisker Detection Task in Mice. eng. *The Journal of Neuroscience: The Official Journal of the Society for Neuroscience* **43,** 2126–2139. ISSN: 1529-2401 (Mar. 2023).

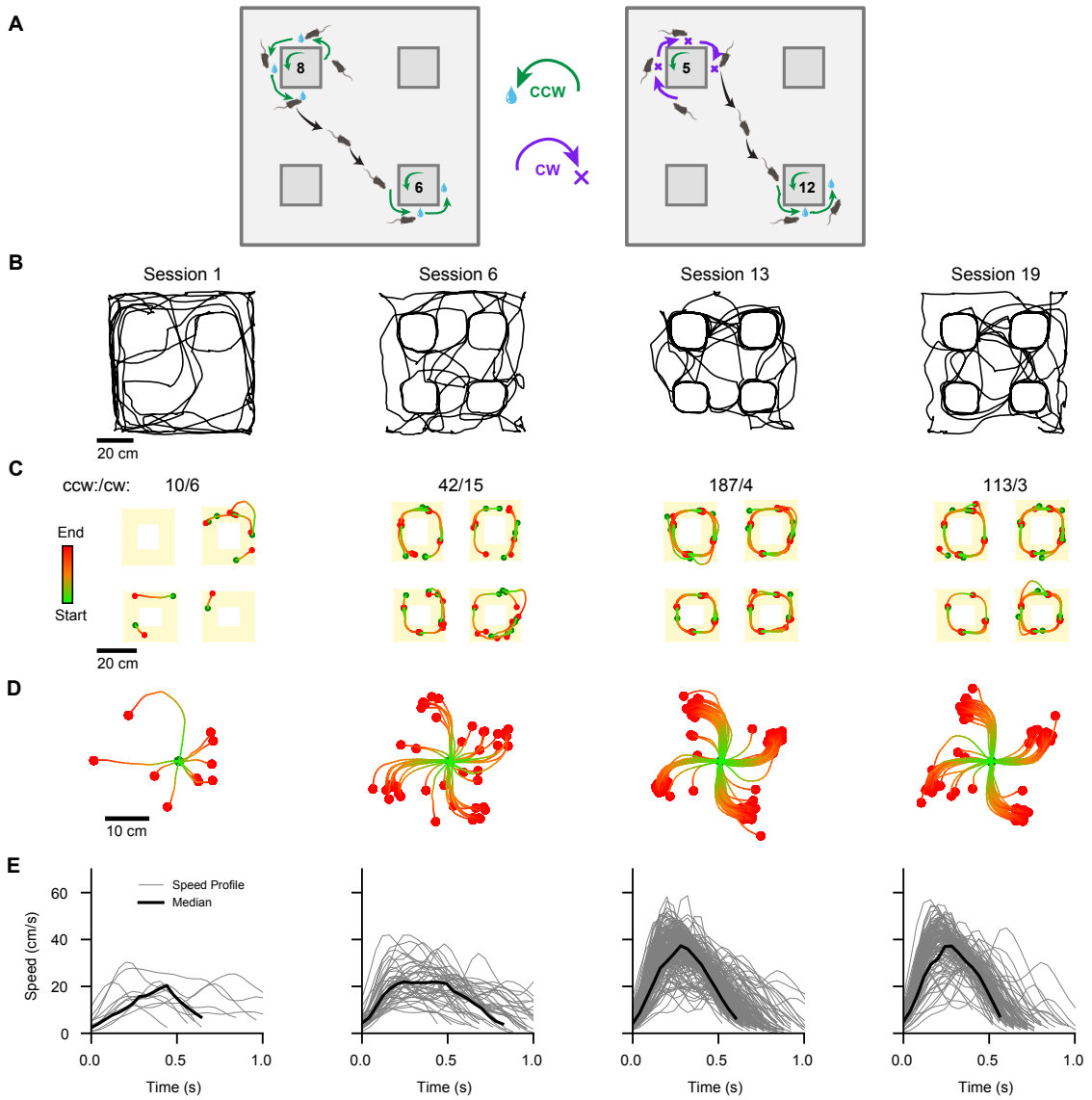

Figure 1. Increased efficiency of a single mouse in the 4 towers foraging task
A. Schematic of the task design. Counterclockwise (CCW) turns (green) around towers are rewarded with water, while clockwise (CW) turns (violet) are not rewarded. The number of maximum consecutive reward for each tower is randomly picked between 4 and 12 consecutive quarter turns rewarded (8 and 6 in the first example, 5 and 12 in the second).
B. Representative trajectories of a single animal during four different sessions (Sessions 1, 6, 13, and 19). Trajectories show movement paths during the first four minutes of each session.
C. Up: Number of CCW and CW turns for each session. Bottom: Representation of CCW and CW turns around the 4 towers (yellow) for the same mouse and sessions as in (B). Turns trajectories are color-coded, with green indicating the start and red the end of the movement.
D. Overlay of all the CCW trajectories around towers from a single session, turns trajectories are color-coded, with green indicating the start and red the end of the movement (same as in B and C).
E. Speed profiles of CCW turns across the same sessions as shown in (B), (C), and (D). Black line represents the median speed of CCW turns for each session.

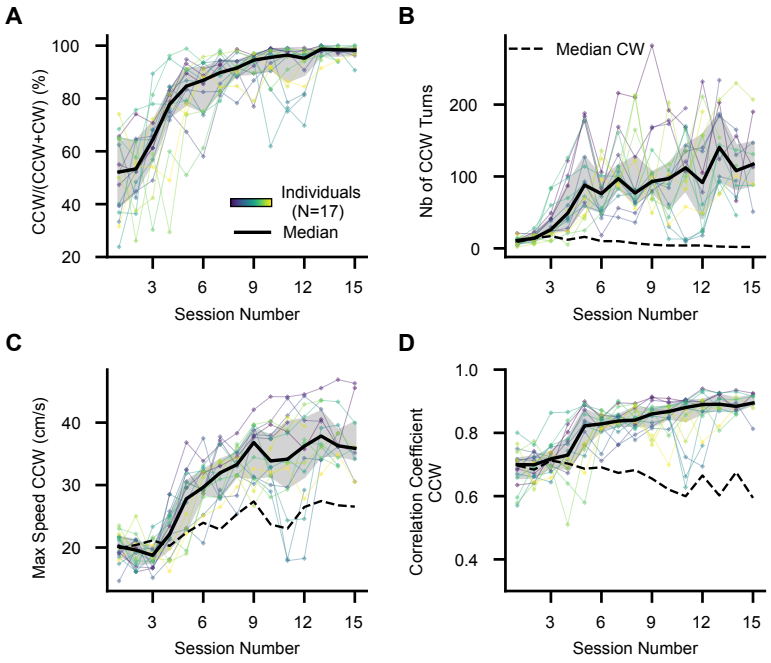

Figure 2. Improved task proficiency and stereotyped turning behavior
A. Percentage of CCW turns (%) across sessions for individual mice (N=17). Each colored line represents a single mouse, while the black line indicates the median across animals. The grey shaded area denotes the interquartile range (25th to 75th percentile).
B. Absolute number of CCW turns per session. Each colored line represents a single mouse, and the solid black line indicates the median with the grey area representing the interquartile range (25th to 75th percentile). The median number of CW turns across sessions is represented in dashed black.
C. Speed of CCW turns across sessions. The median maximum speed (cm/s) of CCW turns is shown for each mouse over sessions. The black line indicates the median speed across animals, and the grey shaded area represents the interquartile range (25th to 75th percentile). The median speed of CW turns across sessions is represented in dashed black.
D. Correlation of CCW turns trajectories across session. The median correlation of CW turns across sessions is represented in dashed black.

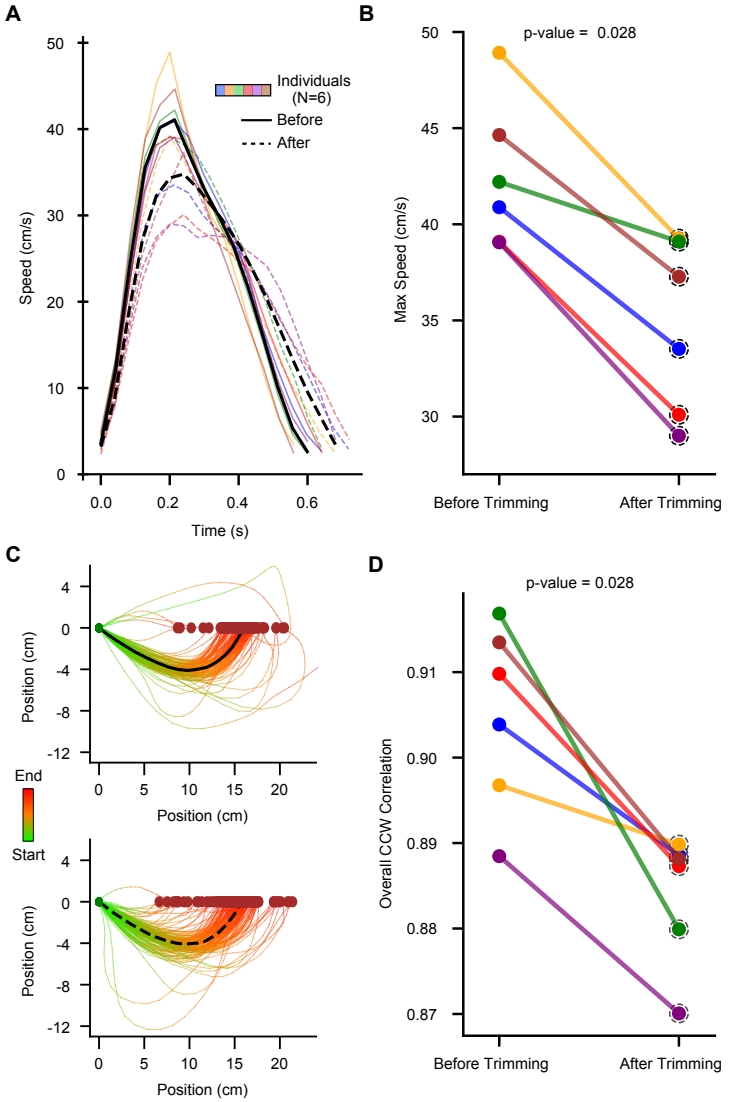

Figure 3. Foraging kinematics alteration following whisker trimming
A. CCW turns median speed profiles before and after whisker trimming for six mice. Solid lines represent speed before trimming, and dashed lines represent speed after trimming. Each mouse is represented by a different color.
B. Median max speed of CCW turns for individual mice before and after trimming. Each colored line represents an individual, with dashed circles highlighting statistically significant reductions in speed (Wilcoxon signed ranks test, p = 0.028).
C Representative trajectories for one mouse before (C) and after (D) whisker trimming. Trajectories are aligned at the starting point and color-coded from green (start) to red (end).
D. Overall median correlation between pairs of CCW turns before and after whisker trimming, indicating a significant increase in variability after trimming (Wilcoxon signed ranks test, p = 0.028). Lines represent individual mice, with colors matching (A) and (B).

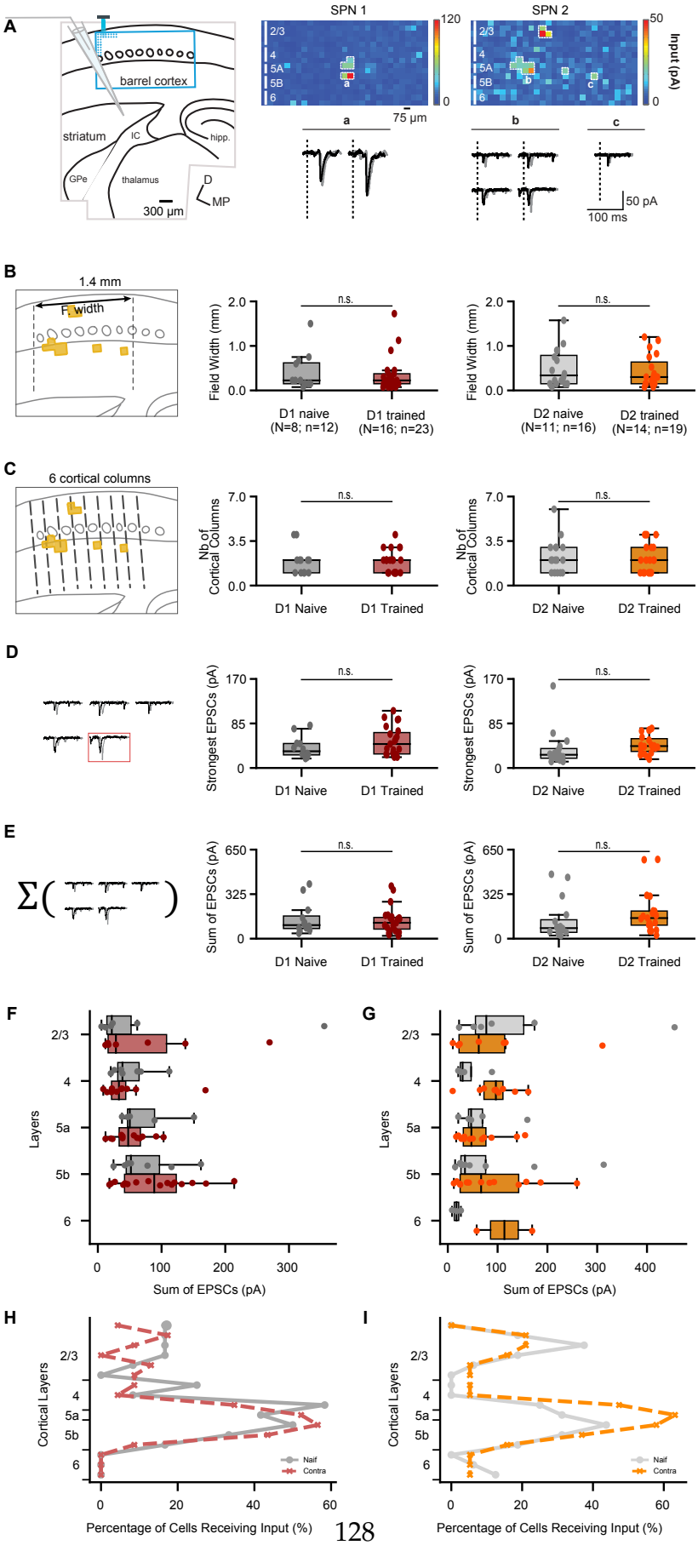
A
barrel cortex
striatum
IC
hipp.
GPe
thalamus
300 µm
D
MP
SPN 1
SPN 2
2/3
4
5A
5B
6
120
0
50
Input (pA)
75 µm
a
b
c
50 pA
100 ms
B
1.4 mm
F width
Field Width (mm)
n.s.
D1 naive (N=8; n=12)
D1 trained (N=16; n=23)
D2 naive (N=11; n=16)
D2 trained (N=14; n=19)
C
6 cortical columns
Nb of Cortical Columns
D1 Naive
D1 Trained
D2 Naive
D2 Trained
D
Strongest EPSCs (pA)
E
Σ( )
Sum of EPSCs (pA)
F
G
Layers
Sum of EPSCs (pA)
H
I
Cortical Layers
Naif
Contra
Percentage of Cells Receiving Input (%)

Figure 4. No differences between naïve and trained animals in the number and strength of corticostriatal inputs to D1/D2 SPNs

A. Left: Layout of the experiment. A SPN was recorded in the dorsolateral striatum while cortical neurons were photostimulated with LSPS. The grid of LSPS (blue) was postionned on the barrel cortex. GPe, globuls pallidus, external segment; IC, internal capsule; hipp., hippocampus. Top Section (Right Upper): Synaptic input maps for two individual SPNs, labeled SPN 1 and SPN 2. SPN 1 shows a single cluster of input, whereas SPN 2 exhibits four distinct clusters. Each color pixel represents the peak amplitude of excitatory postsynaptic currents (EPSCs) within a 50 ms window following stimulus onset. Cortical layers are marked with solid white lines on the left side of each map, and inputs are highlighted with white dashed borders around relevant pixels. Bottom: Example EPSCs recorded from the two SPNs. Responses were evoked by the photorelease of glutamate at the sites indicated by letters a-c in the maps shown above. Two repetitions are superposed (black and gray). Stimulus onsets are indicated by the vertical dashed lines (2 ms duration).
B-E. No significant changes in the CS innervation of D1 or D2 SPNs after learning(D1, n=12 cells in N=8 mice ; D2, n=16, N=11), in Field width (mm, B); number of cortical columns (C); strongest excitatory postsynaptic currents (EPSCs, D) and sum of EPSCs (E).
F-I. Laminar input distribution. The sum of EPSCs to individual SPNs as a function of their laminar origin (F-G). Panel H-I shows the contribution of each cortical layer to the SPN innervations. The 16 rows of the grid correspond to different cortical layers (Layer 2/3: 1-6; L4: 7-9; L5a: 10; L5b: 11-13; L6: 14-16).

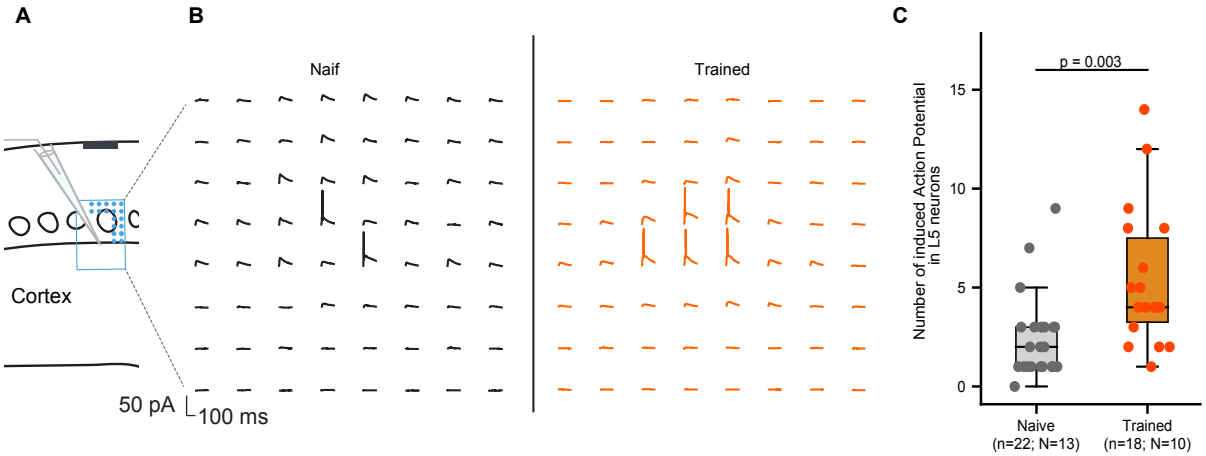

Figure 5. Increased excitation of cortical layer 5 neurons in the contralateral hemisphere, after training
A. Experimental layout showing cortical Layer 5 (L5) neuron recordings in the barrel cortex, while glutamate is uncaged around its soma and dendrites.
B. Representative traces of action potentials (APs) evoked by glutamate uncaging in Layer 5 (L5) neurons of the barrel cortex, recorded in naive and trained animals.The scale bar represents 100 ms and 50 pA.
C. The number of evoked action potentials by glutamate uncaging in L5 neurons for naive (n=21) and trained (n=18) conditions. Each dot represents a cell. Trained animals show a significantly higher number of evoked APs compared to naive animals (p = 0.003).

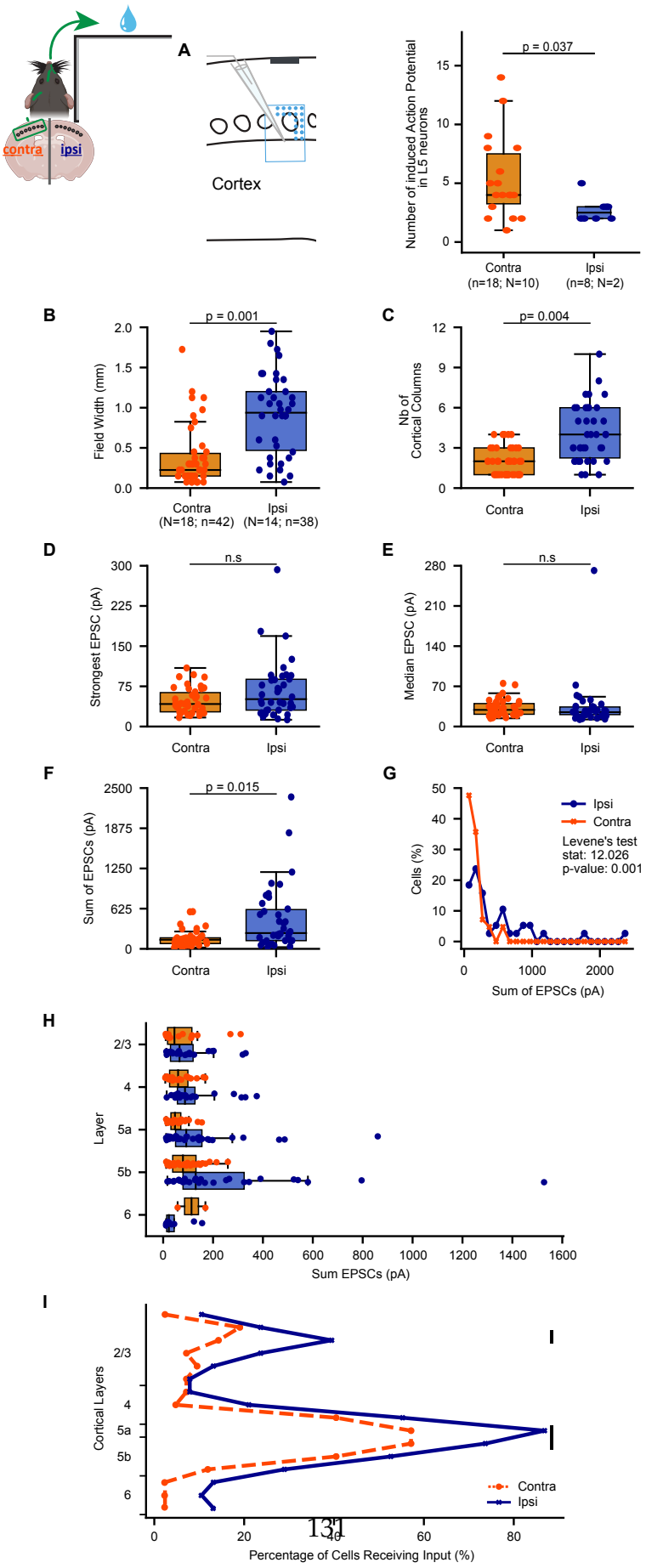
A
contra
ipsi
Cortex
Number of induced Action Potential in L5 neurons
p = 0.037
Contra (n=18; N=10)
Ipsi (n=8; N=2)
B
p = 0.001
Field Width (mm)
Contra (N=18; n=42)
Ipsi (N=14; n=38)
C
p= 0.004
Nb of Cortical Columns
Contra
Ipsi
D
n.s
Strongest EPSC (pA)
Contra
Ipsi
E
n.s
Median EPSC (pA)
Contra
Ipsi
F
p = 0.015
Sum of EPSCs (pA)
Contra
Ipsi
G
Ipsi
Contra
Levene's test
stat: 12.026
p-value: 0.001
Cells (%)
Sum of EPSCs (pA)
H
Layer
2/3
4
5a
5b
6
Sum EPSCs (pA)
I
Cortical Layers
Contra
Ipsi
Percentage of Cells Receiving Input (%)

Figure 6. Increased functional connectivity between barrel cortex and SPN in the ipsilateral hemisphere after lateralized foraging
A. Left: Experimental layout showing cortical Layer 5 (L5) neuron recordings in the barrel cortex, while glutamate is uncaged around its soma and dendrites. Right: The number of evoked action potentials by glutamate uncaging in L5 neurons for trained contraversive (n=18) and ipsiversive (n=8) conditions. Each dot represents a cell. The trained contraversive animals show a significantly higher number of evoked APs compared to ipsiversive animals ($p = 0.037$).
B-C. Field width and number of cortical columns receiving input. Field width (mm) and the number of cortical columns with synaptic input are compared between contralateral (Contra, n=42, N=18) and ipsilateral (Ipsi, n=38, N=14) hemispheres in trained mice. Panel A shows that the field width is significantly larger in the ipsilateral hemisphere ($p = 0.001$). Panel B indicates that the number of cortical columns receiving input is also significantly greater in the ipsilateral hemisphere ($p = 0.004$).
D-E. Strength and median of EPSCs. The strongest excitatory postsynaptic currents (EPSCs) are shown in panel C, with no significant difference between ipsilateral and contralateral hemispheres ($p = 0.2991$). D. the median of EPSCs has no significant differences between both hemispheres ($p = 0.2001$).
F-G. Sum of EPSCs and its distribution. Panel E shows the sum of EPSCs, with significant differences between hemispheres ($p = 0.01485$). Panel F shows the distribution of sum of EPSCs, representing the difference in the variance between the 2 groups ((Levene test) : $p = 0.0008$)).
H-I. Laminar input distribution. The sum of EPSCs to individual SPNs as a function of their laminar origin (G). Panel H shows the contribution of each cortical layer to the SPN innervations. The 16 rows of the grid correspond to different cortical layers (Layer 2/3: 1-6; L4: 7-9; L5a: 10; L5b: 11-13; L6: 14-16). Vertical black lines indicate significant differences between the two groups.

Acknowledgements

This work was supported by funding from the Institut National de la Santé et de la Recherche Médicale and a grant from the Agence Nationale de la Recherche (Corticostriatal, ANR-20-CE16-0002). K. Amroune is supported by fellowships from the Ministère de l'Enseignement Supérieur et de la Recherche and from the French government under the "France 2030" program via A*Midex (Initiative d'Excellence d'Aix-Marseille Université, AMX-19-IET-004) and ANR funding (ANR-17-EURE-0029). T. Morvan is supported by XX. We thank the staff at the animal and genotyping facilities of INMED, Robert Martinez for help with the setup, and the members of the CBGB group for their help and support.

Author contributions statement

K.A., I.B. and D.R. conceived the experiments. K.A., T.M, I.B. and D.R designed the task apparatus. K.A. conducted the experiments. K.A, M.S, T.M and D.R developed the analysis pipeline. K.A. and D.R. analyzed the results. I.B and D.R acquired funding and supervised the project. K.A. and D.R wrote the original draft. All authors reviewed the manuscript.

Discussion

CHAPTER 5

Discussion

In this thesis, I explored the organization of functional projections from the barrel cortex to individual D1/D2 SPNs in the DLS, both in the basal condition and after learning a whisker-guided task.

First, we investigated the organization of functional vibrissal corticostriatal projection to SPNs in the DLS. We observed low input convergence, as cortical neurons innervating a single SPN were either confined to a single cortical column or relatively sparse and scattered across an input field up to 1.6 mm wide. Each SPN exhibited a distinct pattern of innervation from the barrel cortex, though some overlap occurred for neighboring SPNs. We found no significant differences between D1 and D2 SPNs regarding the number of cortical columns innervating them or the strength of cortical inputs. We conclude that CS innervation to a single SPN is sparse and unique.

Second, we tested the hypothesis that the execution of fast and stereotyped actions following learning arises from strengthened CS projections to D1-SPNs and/or weakened connections to D2-SPNs. Contrary to expectations, learning a lateralized whisker-guided foraging task did not alter whisker cortical innervation of D1 or D2 SPNs. Instead, we observed an increase in the excitation of cortical pyramidal neurons. Moreover, in the ipsiversive hemisphere, which was not actively engaged in task execution, cortical excitation remained unchanged;

however, cortical inputs to SPNs were significantly increased. Thus, lateralized sensorimotor learning appears to affect the corticostriatal circuit asymmetrically in both hemispheres, and we hypothesized that the changes observed in CS projections to SPNs in the ipsiversive hemisphere might reflect homeostatic mechanisms to maintain similar levels of excitation to both DLS.

Contents

5.1 Organization of Corticostriatal Inputs to SPNs 137
5.1.1 Topography of Cortical Inputs 137
5.1.2 Layer-Specific Patterns of Innervation to SPNs 138
5.1.3 Cortical Sensory Projections to SPNs 139
5.2 Cortical and Thalamic Contributions to Striatal Sensory Processing 141
5.3 Development of a Lateralized Whisker-Guided Foraging Task . . 142
5.4 Plasticity in the Cortex Following Learning 144
5.5 Corticostriatal Projections After Learning 145
5.5.1 Asymmetry in the CS connectivity 145
5.5.2 Beyond the D1/D2 Dichotomy in Learning 146
5.5.3 Task-Specific Neuronal Ensembles and Inhibitory Reorganization 147
5.5.4 Interplay of Cortical and Thalamic Inputs in Learning . . . 148
5.5.5 Modulation of Striatal Responses: Role of the Dopamine . 149
5.6 Conclusion 151

5.1 Organization of Corticostriatal Inputs to SPNs

In the first study, we mapped the basal organization of functional projections from the barrel cortex to individual SPNs in the DLS. Our aim was to investigate the extent to which single SPNs integrate cortical inputs. We observed sparse input patterns and selectivity in the sensory corticostriatal connections to individual SPNs.

5.1.1 Topography of Cortical Inputs

We found that the CS projection was loosely topographical, with medial SPNs receiving inputs from the medial barrel cortex and lateral SPNs from the lateral cortex, consistent with previous anatomical descriptions (Alloway *et al.* 1999; Wright *et al.* 1999; Leergaard *et al.* 2000). While most SPN pairs did not share overlapping inputs, overlap increased for SPNs located within ~200 µm of each other. This suggests a process where neurons close together in the cortex (< 100 µm) grow their axons into the same striatal subregion (< 400 µm), potentially facilitating the formation of functional clusters in the striatum (Carelli & West 1991; Jaeger *et al.* 1995; Barbera *et al.* 2016; Klaus *et al.* 2017; Badreddine *et al.* 2022), resulting in nearby neurons responding to the same stimulus.
However, neighboring neurons did not share all their inputs, which may explain *in vivo* findings showing that neighboring striatal neurons can exhibit different response latencies or different directional selectivities to stimulation of the same body part (Jaeger *et al.* 1995).
Thus, our results indicate that CS projections are organized such that each striatal region receives inputs from distinct, yet topographically organized, groups of cortical neurons. Although the corticostriatal input field of some cells is relatively broad (with a median of approximately 750 µm), individual SPNs receive inputs from a limited number of cortical columns, resulting in relatively low convergence from the cortex to single SPNs. This selective arrangement likely enables specific striatal regions to integrate focused signals from defined cortical sources, thereby allowing for precise modulation of striatal functions, including motor coordination and sensory processing.

5.1.2 Layer-Specific Patterns of Innervation to SPNs

We found that the upper layer 5 (L5a and upper L5b) was the principal source of inputs to SPNs in the DLS, corroborating prior works (Wise & Jones 1977; Reiner *et al.* 2003; Wright *et al.* 1999; Wall *et al.* 2013). Moreover, SPNs also received inputs from deeper and superficial layers, though to a lesser extent, as previously described (Guo *et al.* 2017; Yamashita *et al.* 2018; Bertero *et al.* 2022). Interestingly, our data showed no global bias in the innervation of D1 versus D2 SPNs in terms of projection strength or in the number of cortical columns involved. Instead, we found layer-specific biases: L2/3 favored D2 SPNs, while L6 preferentially targeted D1 SPNs. These findings differ from previous studies, which reported stronger *in vivo* responses in D1 SPNs to whisker deflections (Reig & Silberberg 2014; Filipović *et al.* 2019) and suggested a bias toward D1 SPNs for S1 cortical inputs in both optogenetic (Kress *et al.* 2013; Parker *et al.* 2016) and anatomical studies (Wall *et al.* 2013). In contrast, our results reveal a more nuanced pattern of corticostriatal innervation, characterized by distinct layer-specific preferences: L2/3 favors D2 SPNs, while L6 predominantly innervates D1 SPNs. This pattern may have important functional implications, shaping how D1 and D2 SPNs integrate and process sensory information. For instance, the preferential L2/3 inputs to D2 SPNs could allow these neurons to process higher-order integrative sensory information, while L6 inputs may provide contextual information and modulatory signals to D1 SPNs, as L6 has been implicated in modulating both cortical and thalamic activities (Harris & Mrsic-Flogel 2013). Further investigation is needed to examine in detail the roles of projections from upper and lower cortical layers and how these projections influence sensory integration dynamics in the direct and indirect pathways of the DLS. In conclusion, this layer-specific pattern highlights the diversity in sensory integration pathways for D1 and D2 SPNs.

Different innervation of D1 and D2 SPNs by PT and IT CS projections has been described both anatomically (Lei *et al.* 2004; Reiner *et al.* 2003; Reiner 2010; Deng *et al.* 2015) and functionally (Kress *et al.* 2013; Ding *et al.* 2008; Takada *et al.* 2013). We found that the majority of neurons in layer 5a and upper layer 5b were regular spiking cells, characteristic of IT pyramidal neurons (Harris & Shepherd 2015; Petersen 2019; Steiner & Tseng 2017). Moreover, we found that if only PT neurons were activated, roughly 10% of the initial inputs to single SPNs

were preserved, with considerable variability. These findings are consistent with greater IT neurons involvement in the innervation of both types of SPNs. IT neurons are known for their bilateral projections to the striatum (Cowan & Wilson 1994; Wilson 1987; Zheng & Wilson 2002), and SPNs in the DLS integrate sensory information from both hemispheres (Reig & Silberberg 2016; de la Torre-Martinez *et al.* 2023). These bilateral CS inputs from IT neurons may contribute to coordinated sensory processing across hemispheres and support bilaterally coordinated movements (Pimentel-Farfan *et al.* 2022).

In our second study that involved older animals ([PND]: 22–43 / 30–45), we found that up to 40% of SPNs received inputs from layer 2/3. This suggests that development and learning are accompanied by an increase in inputs from higher-order sensory integration regions, potentially allowing for more refined motor control and sensory discrimination (Kwon *et al.* 2016; Han & Helmchen 2024; Oryshchuk *et al.* 2024). Moreover, L2/3 neurons exhibit distinctive activity during mouse displacement, with sustained responses to ongoing wall touches, contrasting with the transient responses observed in L5 (Ayaz *et al.* 2019). These increased inputs from L2/3 in older animals may contribute to the increase in speed of displacement notice in older mice (Pitzer *et al.* 2021; Reiber *et al.* 2022), potentially facilitating sensorimotor processing.

5.1.3 Cortical Sensory Projections to SPNs

We observed low convergence of whisker-related CS inputs to individual SPNs in the DLS. Approximately 60% of SPNs in the DLS responded to stimulation from only one or two cortical columns present in the slice. Even when multiple clusters projected to a single SPN, a dominant cluster often emerged, which likely contributed to the sharp receptive fields observed in *in vivo* studies. This findings suggests that individual SPNs receive a selective, non-exhaustive set of cortical inputs, with SPN representations complementing one another to support sensory integration at the population level.

While earlier studies suggested that S1 CS axonal projections were abundant and overlapping (Flaherty & Graybiel 1991; Alloway *et al.* 1999; Wright *et al.* 2000; Wright *et al.* 1999; Hintiryan *et al.* 2016; Hooks *et al.* 2018), our results are more

consistent with earlier *in vivo* studies showing that SPNs respond to selective somatosensory inputs, such as stimulation of individual whiskers (Carelli & West 1991; Cho & West 1997). Although CS projections exhibit loose topography at a large scale, the low convergence we observed at the level of individual SPNs suggests that local input patterns are more selective. This sparse innervation could play an important role in sensorimotor tasks requiring precise tactile detection through whisker input.

Although one could argue that our results may not generalize to CS projections from other sensory cortices, similar organizational features have been observed in other modalities. For instance, in the posterior striatum, a large fraction of neurons exhibit selectivity to sound features (Znamenskiy & Zador 2013; Guo *et al.* 2018; Bordi & LeDoux 1992). Future research should investigate whether the sparse innervation pattern we observed in the DLS generalizes to other cortical regions, such as M1 or S2, which may exhibit distinct organizational properties.

It is worth noting that our slice recordings likely missed some inputs originating from other barrel columns. While barrel columns from the same row (e.g., D1-D5) were preserved, the arc organization was not fully maintained, possibly limiting our ability to capture the complete CS organization. According to Alloway *et al.* (1999), CS projections from barrels within the same row have more overlapping terminals in the DLS compared to projections from different rows. Given that our slice preparation preserved inputs primarily from the same row, our conditions maximized the chance of observing convergence if it existed. However, since we observed low convergence, it suggests that convergence onto single SPNs in the DLS is limited even within row-based inputs, and likely even less frequent for inputs originating from different rows.
Our observation that neighboring SPNs in the DLS share overlapping cortical inputs, combined with the somatotopic organization of CS projections, suggests that this arrangement supports row-based sensory integration within the DLS. During exploration, rodents perform rhythmic forward (protraction) and backward (retraction) movements with their whiskers, resulting in row-based activation patterns. Consequently, the organization of functional CS projections implies that close by SPNs are more likely to be co-activated or activated in close temporal sequence by stimulation of adjacent whiskers in the same row, a

natural pattern in whisking behavior. The specific spatiotemporal patterns of whisker activation may encode key aspects of sensorimotor information essential for guiding rodents in their movements.

Finally, while our study focused on the convergence of sensory inputs from a single modality, higher convergence may be observed if one considers inputs from multiple modalities. As described by Reig & Silberberg (2016) and Charpier *et al.* (2020), in the DMS, motor and multisensory inputs converge onto individual SPNs. Future studies should explore this multi-modal convergence to better understand how various sensory and motor inputs integrate within the DLS.

5.2 Cortical and Thalamic Contributions to Striatal Sensory Processing

We found that CS inputs were sparse at the level of individual SPNs. However, sensory information reaches the striatum not only through CS projections but also via the thalamostriatal pathway. While most projections to the DLS arise from the sensorimotor cortex (Brown *et al.* 1998; Wall *et al.* 2013; Alloway *et al.* 2006), approximately 20% of its glutamatergic inputs come from thalamostriatal projections, mainly from the posterior medial nucleus of the thalamus (POm) nuclei (Smith *et al.* 2012), and direct comparisons of stimulus-evoked activity in the DLS and S1 suggest the involvement of additional brain regions, likely the thalamus, in shaping DLS sensory responses (Mowery *et al.* 2011; Smith *et al.* 2012; Alloway *et al.* 2014).

The POm nucleus is characterized by ascending and descending somesthetic inputs from the trigeminal nuclei and cortical areas (Chiaia *et al.* 1991a; Chiaia *et al.* 1991b; Diamond *et al.* 1992; Williams *et al.* 1994; Veinante *et al.* 2000; Alloway *et al.* 2003; Killackey & Sherman 2003). Thalamocortical projections from the POm to S1 primarily target L5a neuron (subsection 1.1.3), which contains most of the CS neurons projecting to the DLS, as described in our first study (Amroune *et al.* 2024; Wise & Jones 1977; Reiner *et al.* 2003; Wall *et al.* 2013). Moreover the POm also projects to the DLS through axonal collaterals that target sensorimotor cortices (S1, S2, and M1) (Ohno *et al.* 2012; Deschenes *et al.* 1995). Together, stri-

atal inputs from both the POm and L5a suggest that the paralemniscal pathway plays a central role in somatosensory integration in SPNs, as opposed to the classical lemniscal pathway (VPM), which primarily targets the L4 barrels and L5b (subsection 1.1.3). Furthermore, the convergence of cortical and thalamic inputs may allow the dendritic spines of SPNs in the DLS to receive near-coincident excitatory inputs from both thalamostriatal and corticostriatal sources, likely enhancing sensory processing within the DLS.

To further clarify the role of thalamostriatal inputs in sensory processing, future experiments should focus on understanding the precise topography and organization of these projections. Recording from SPNs while simultaneously stimulating both thalamic and corticostriatal inputs could provide insights into how these pathways integrate and refine sensory processing within the DLS.

5.3 Development of a Lateralized Whisker-Guided Foraging Task

We developed a novel lateralized whisker-guided foraging task in freely moving mice to test the hypothesis that faster and more stereotyped actions performed after learning are associated with differential strength in CS inputs to D1 and D2 SPNs. It is well established that unilateral activation of D1 and D2 SPNs have opponent effect of behavior (contraversive/ipsiversive turns respectively) (Tecuapetla *et al.* 2014; Kravitz *et al.* 2010; Bay Kønig *et al.* 2019). Therefore, in our task, mice were required to perform unidirectional 90-degree turns in complete darkness to receive water rewards. By designing this highly lateralized task, we aimed to elucidate the distinct contributions of CS projections to D1 and D2 SPNs in controlling lateralized behaviors.
However, an important aspect of the task design emerged during initial observations. The square shape of the towers led mice to consistently perform an ipsiversive turn followed by a contraversive 90-degree turn after drinking, forming a predictable circling pattern around the tower (Figure 5.1). This movement sequence may have introduced an unintended bias, potentially weakening the lateralized actions we aimed to elicit. To address this, future task iterations could incorporate round objects, which may reduce directional bias and allow for a

more balanced representation of ipsiversive and contraversive movements.

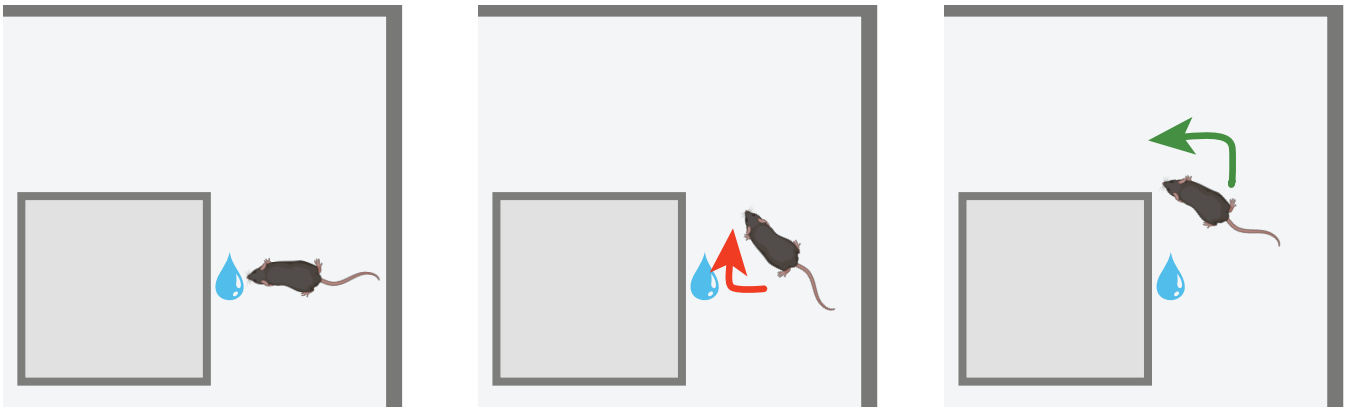

Figure 5.1: Schematic representation of the lateralized movement pattern in the whisker-guided foraging task.
After drinking, the mouse initially makes a CW turn (red arrow) to follow the wall, followed by a CCW 90-degree turn (green arrow) to continue circling around the tower.

To determine the role of whiskers in task execution, we trimmed them and observed the behavioral effects. While whisker trimming altered key movement parameters, such as reducing movement speed and decreasing stereotypy, mice continued to perform the learned task correctly: they still made a higher proportion of CCW turns, and the overall number of CCW movements remained consistent. This outcome suggests that while whiskers are crucial for navigating and fine-tuning of movements, consistent with studies showing that rodents use whiskers to detect obstacles and regulate speed (Warren *et al.* 2021; Chorev *et al.* 2016), sensory deprivation does not erase learned motor behavior.
Mice likely compensated for the lack of whisker inputs by using alternative tactile cues from their bodies or by relying on egocentric memory, or even spatial memory through the hippocampus. To further dissect the contributions of different sensory and memory systems to task performance, targeted inactivation or lesion studies could provide valuable insights into the specific roles of each structure.

5.4 Plasticity in the Cortex Following Learning

Following learning, we observed increased excitation of layer 5 pyramidal neurons in the barrel cortex of the contraversive hemisphere, associated with the side receiving sensory stimulation. Glutamate uncaging under consistent stimulation parameters resulted in a higher number of action potentials in these contraversive neurons, indicating heightened excitation. This suggests that cortical plasticity occurred during learning, likely enhancing sensory processing of whisker-related stimuli. These findings align with previous studies that reported increased barrel cortex activity following sensorimotor learning (Sachidhanandam *et al.* 2013; Yang *et al.* 2016; Mehta *et al.* 2007; Knutsen *et al.* 2006; O'Connor *et al.* 2010; Yamashita & Petersen 2016), although the majority of those recording targeted layer 2/3 neurons. Sensory learning has been associated with structural changes, such as the growth of persistent dendritic spines in response to behavioral training. These changes have been observed in Layer 5 neurons of the auditory cortex (Moczulska *et al.* 2013) and in layer 2/3 of the barrel cortex (Kuhlman *et al.* 2014), where they are linked to the formation of new synapses (Feldman & Brecht 2005). This structural plasticity could includes an increase in AMPA receptors at the synaptic membrane (Zhang *et al.* 2015), which would make neurons more sensitive to ambient glutamate levels. Such changes would explain the observed increase in excitation, reflecting a more finely tuned cortical response to sensory inputs following learning.
Another possible explanation for the heightened excitation in layer 5 pyramidal neurons is a change in intrinsic neuronal properties rather than solely synaptic modifications. To explore this, we also performed depolarizing current step injections, which may help distinguish between synaptic and intrinsic changes. This analysis is still ongoing.

The observed increase in cortical excitation might also be associated with changes in CS activity in the striatum following sensorimotor learning. For example, Xiong *et al.* (2015) described enhanced CS activity *in vivo* after learning an auditory task. One possibility is that increased excitation in corticostriatal neurons could elevate CS projection activity without necessarily altering the number or strength of projections to the DLS. It's important to note that not all cortical pyramidal neurons project to the striatum. To directly assess changes in excitabil-

ity among neurons specifically targeting the DLS, retrograde labeling could be used to identify corticostriatal neurons and determine whether their excitability is modulated by task learning. Furthermore, it would be of great interest to examine whether CS neurons specifically innervating D1 or D2 SPNs exhibit distinct excitability levels.

5.5 Corticostriatal Projections After Learning

In the second study, we observed improvements in behavioral performance and increased cortical excitation following learning. However, contrary to what would be expected based on classical BG models, we did not observe significant changes in CS inputs to D1 or D2 SPNs in the DLS. In this section, I will explore several non-exclusive hypotheses that could account for these results.

5.5.1 Asymmetry in the CS connectivity

One intriguing observation was the asymmetry in CS connectivity between the hemispheres. In the ipsiversive DLS, which was not directly engaged in the task, there was an increase in CS projections, particularly in the number of cortical columns contributing to SPNs. In contrast, the contraversive hemisphere exhibited increased excitation in cortical neurons, but no corresponding rise in CS projections. This asymmetry suggests a potential relationship between cortical excitation and CS connectivity.

We hypothesize that homeostatic plasticity may play a role in these observations. This mechanism helps maintain average firing rates around a homeostatic set point by adjusting synaptic strengths or the number of synapses in response to changes in network activity (Turrigiano 2008; Wen & Turrigiano 2024). In our study, the increased excitation in the contraversive barrel cortex might have triggered such homeostatic mechanisms, which would limit further increases in CS projections to individual SPN. On the other hand, the ipsiversive hemisphere, not directly involved in task performance, might have undergone compensatory plasticity, increasing its CS projections to maintain balance activity across both DLS. This would explain the hemispheric asymmetry in CS projection changes we observed after learning.

However, it is important to note that some CS projections in one hemisphere

extend into the opposite striatum hemisphere as well (subsection 1.1.4), introducing additional complexity to these interpretations. Our slice recordings only capture unilateral CS connectivity, meaning that inter-hemispheric aspect of CS projections is not represented in our data. Consequently, the rearrangements we observed in CS circuits may also be accompanied by changes in bilateral CS projections to the contralateral DLS. This limitation suggests that the observed asymmetry may only partially reflect the full scope of CS connectivity changes following learning. Further studies that include bilateral recordings are needed to provide a more comprehensive understanding of CS organization.

5.5.2 Beyond the D1/D2 Dichotomy in Learning

We did not observe significant changes in CS inputs to D1 and D2 SPNs when analyzed by cell type following learning. However, examining SPNs as a whole population we detected an overall increase in total synaptic inputs to SPNs, regardless of their type. This suggests that, even though there may not be clear distinctions in how D1 and D2 SPNs are specifically modulated by CS inputs post-learning, the striatal circuitry could still undergo adaptations at the population level.

At first glance, this finding might appear to diverge from the traditional Go/No-Go model, which posits that D1 SPNs facilitate action ("Go") while D2 SPNs suppress it ("No-Go") (Mink 1996; Kravitz *et al.* 2010; Kravitz *et al.* 2012, see subsection 2.2.2). These results may instead reflect a more integrated mechanism of learning-induced plasticity within the striatum.

Specifically, this broader modulation implies that D1 and D2 pathways may be co-activated or function in complementary ways during this particular foraging task. Studies have demonstrated that D1 and D2 SPNs are frequently co-activated during movement (Cui *et al.* 2013; Barbera *et al.* 2016; Klaus *et al.* 2017). These findings suggest that striatal output is not simply a balance between opposing forces but involves a coordinated integration of inputs from both pathways, working together to control behavior.

Further investigations are needed to clarify the contribution of D1 and D2 SPNs to motor learning. *In vivo* recordings and manipulation during the whisker-guided foraging task could reveal how each pathway contributes to task execution. Additionally, it is also possible that our experimental design—specifically,

the relatively small sample size and reliance on single spike-evoked cortical stimulation—may have limited our ability to detect finer, pathway-specific modulations.

5.5.3 Task-Specific Neuronal Ensembles and Inhibitory Reorganization

One possible confounding factor for the lack of observed changes in CS innervation to D1 and D2 SPNs in the contraversive DLS is that we recorded from all SPNs, without distinguishing their specific roles in the task. Functional clusters in the DLS have been associated with distinct motor behaviors such as turning, running, and rearing (Barbera *et al.* 2016; Klaus *et al.* 2017). Following learning, striatal circuits can undergo substantial reorganization, with certain neurons becoming highly active while others are more inhibited (Badreddine *et al.* 2022; Sheng *et al.* 2019). The absence of observable changes in CS inputs at the broader population level may suggest that synaptic plasticity is confined to these task-specific neuronal ensembles. Targeted recordings from these ensembles could reveal changes that are not detectable in a general analysis.
To better isolate task-related changes, techniques like c-Fos GFP labeling in mice could be used. This approach would allow us to record specifically from c-Fos-positive SPNs—neurons activated during the task. These targeted methods could help reveal how learning influences synaptic inputs to specific neuronal clusters.

The formation of task-related neuronal ensembles may also involve a reorganization of inhibitory networks targeting SPNs. In addition to SPNs, various types of interneurons in the striatum, such as PV and SST interneurons, also receive glutamatergic inputs from CS projections. CS inputs to these interneurons could undergo plastic changes during motor learning which influence overall striatal activity.
PV interneurons are known to play a crucial role in regulating habitual behaviors. Their activity is often enhanced during the execution of learned, habitual tasks (O'Hare et al., 2017). Disruption of PV interneurons leads to impaired learning by disinhibiting SPNs, suggesting that they are key modulators of striatal circuitry (Owen et al., 2017). Moreover, Sippy *et al.* (2015) described an increase in the early membrane response of D1 SPNs, but not D2 SPNs, following sensorimotor

learning. This suggests that PV interneurons might preferentially modulate D2 SPNs through enhanced feedforward inhibition, thereby leading to difference in the response of both types of SPNs. Investigating whether CS inputs to interneurons change after learning could offer a more nuanced perspective on striatal reorganization.

Lastly, another possibility is that the weight of inhibitory inputs to SPNs changes following learning. Investigating whether these inhibitory inputs are modified after task learning would be essential to fully understand striatal circuit plasticity. Such changes could involve adjustments in the strength or connectivity of PV and SST interneurons to SPNs, or even in SPN-to-SPN connections, as SPNs themselves are GABAergic. Identifying whether plasticity occurs within these inhibitory circuits after learning our foraging task could reveal new insights into the role of inhibition in striatal adaptation.

5.5.4 Interplay of Cortical and Thalamic Inputs in Learning

As we discussed in section 5.2, the thalamus is another crucial glutamatergic input to the DLS. CS and thalamostriatal inputs may work together in a complementary manner to support learning and task execution, as suggested by recent studies (Wolff *et al.* 2022; Yonk *et al.* 2024).
Thalamostriatal synapses can undergo plastic changes (Mendes *et al.* 2020), which could have an important role in motor learning. Wolff *et al.* (2022) revealed that while CS projections from the motor cortex to the DLS are important in the acquisition of complex motor tasks, the thalamus is essential for executing those learned sequences, as silencing thalamostriatal inputs after learning resulted in impaired task performance. Thus, both CS and thalamostriatal inputs might be important at different timepoints during learning.
Supporting this, Yonk *et al.* (2024) investigated the role of POm-striatal projections in a whisker discrimination task. Inhibiting POm-striatal axons during learning led to slower reaction times and increased training, suggesting that these inputs facilitate the activation of striatal circuits in response to task-related sensory cues. Thus, during whisker-based learning, POm-striatal projections are an important actor in sensorimotor learning.

To conclude, it appears that both CS projections and thalamostriatal projections could be key partners in sensorimotor learning. Understanding their respective roles is crucial for a comprehensive view of how sensorimotor behaviors are acquired and refined. To better assess the distinct contributions of each pathway, we could investigate the strength and organization of both CS and thalamostriatal projections at multiple time points throughout task acquisition, rather than only post-learning. This approach could reveal dynamic shifts in CS input strength, particularly in conjunction with thalamostriatal modulation, providing a clearer picture of how these circuits interact throughout learning.

5.5.5 Modulation of Striatal Responses: Role of the Dopamine

Dopamine plays a crucial role in modulating striatal activity and plasticity. It dynamically affects SPN excitability and synaptic plasticity, enhancing D1-SPN activity while inhibiting D2-SPNs (Nelson & Kreitzer 2014). Recent studies have expanded our understanding of DA signaling, showing that phasic DA signals not only represent reward prediction errors but also encode sensory prediction errors, internal states, and motor performance (Stalnaker *et al.* 2019; Gardner *et al.* 2018; Gadagkar *et al.* 2016). This suggests that DA influences how glutamatergic inputs are processed during both exploratory behavior, but also reward-based tasks, such as our whisker-guided foraging task.

Upon release, dopamine binds to D1-like receptors (D1 and D5) or D2-like receptors (D2, D3, D4), initiating different G-protein-coupled receptor (GPCR) signaling cascades. Dopamine enhances D1-SPN activity while inhibiting D2-SPNs by effects on voltage-gated sodium, potassium, and calcium channels, which regulate action potential firing (Nelson & Kreitzer 2014; Tritsch & Sabatini 2012; Gerfen & Surmeier 2011; Planert *et al.* 2013). Consequently, dopamine could differentially modulate the integration of CS inputs by D1 and D2 SPNs *in vivo*, even if the two pathways have similar CS innervation patterns. The extremely low levels of dopamine in most slice experiments could contribute to differences between *in vivo* and *ex vivo* observations.
Dopamine can also directly act at CS inputs, as they also express dopamine D2 receptors in the DLS (Wang & Pickel 2002; Burke *et al.* 2017). Dopamine can thus decrease glutamate release at synapses, weaken synaptic signaling, and

alter neuronal excitability (Burke *et al.* 2017; Higley & Sabatini 2010; Gerfen & Surmeier 2011).
Finally, dopamine has a dynamic influence on the size and activity of striatal ensembles. Maltese *et al.* (2021) demonstrated that dopamine modulates the recruitment of D1- and D2-SPN ensembles during movement, affecting the number of neurons involved in specific behaviors. Thus, while we did not detect differences in the CS innervation of D1 and D2 SPNs in our studies, dopamine may still play a crucial role in the functional recruitment of SPNs during whisker-guided locomotion.

In conclusion, *in vivo* fluctuations of dopamine likely have a profound impact on striatal cell activity. To gain a clearer understanding of how dopamine influences the two striatal pathways, recording dopamine release and D1/D2 SPN activity *in vivo* during task performance could provide valuable insights. Additionally, performing similar electrophysiological experiments as we did (recording from D1/D2 SPNs while uncaging glutamate in the barrel cortex) in the presence or absence of dopamine would help clarify its impact on glutamatergic integration.

5.6 Conclusion

In this thesis, I studied the organization of functional projections from the barrel cortex to individual D1 and D2 SPNs in the DLS, both in the basal state and after learning a whisker-guided task.

We found that cortical innervation within a single sensory modality is sparse, with limited convergence from different cortical columns. Each SPN exhibited a distinct pattern of cortical innervation, suggesting that SPN complements one another to support sensory integration at the population level. We designed a lateralized whisker-guided foraging task to study how CS inputs to each striatal pathways, D1-D2 SPNs, can change to support sensorimotor learning. Learning this task led to an asymmetrical reorganization in CS circuits, with increased excitation of pyramidal neurons in the contraversive barrel cortex, yet without changes in the pattern or strength of CS projections to D1 or D2 SPNs. In contrast, there was no change in the excitation of cortical pyramidal neurons in the non-associated (ipsiversive) hemisphere, though surprisingly, there was an increase in CS connections to the DLS. We propose that these asymmetrical may be driven by homeostatic mechanisms aimed at maintaining balanced excitation levels across both DLS regions.

Overall, our findings provide new insights into how single SPNs in the DLS integrate sensory information and highlight the potential for CS circuits to undergo asymmetric plastic changes during sensorimotor learning.

BIBLIOGRAPHY

1. Alexander, G. E. & Crutcher, M. D. Functional architecture of basal ganglia circuits: neural substrates of parallel processing. *Trends in Neurosciences* **13,** 266–271 (July 1990) (cit. on p. 38).
2. Alloway, K. D., Crist, J., Mutic, J. J. & Roy, S. A. Corticostriatal projections from rat barrel cortex have an anisotropic organization that correlates with vibrissal whisking behavior. *The Journal of Neuroscience: The Official Journal of the Society for Neuroscience* **19,** 10908–10922 (Dec. 15, 1999) (cit. on pp. 46, 47, 69, 137, 139, 140).
3. Alloway, K. D., Hoffer, Z. S. & Hoover, J. E. Quantitative comparisons of corticothalamic topography within the ventrobasal complex and the posterior nucleus of the rodent thalamus. *Brain Research* **968,** 54–68 (Apr. 2003) (cit. on p. 141).
4. Alloway, K. D., Lou, L., Nwabueze-Ogbo, F. & Chakrabarti, S. Topography of cortical projections to the dorsolateral neostriatum in rats: Multiple overlapping sensorimotor pathways. *The Journal of Comparative Neurology* **499,** 33–48 (Nov. 1, 2006) (cit. on p. 141).
5. Alloway, K. D., Mutic, J. J., Hoffer, Z. S. & Hoover, J. E. Overlapping corticostriatal projections from the rodent vibrissal representations in primary and secondary somatosensory cortex. *The Journal of Comparative Neurology* **428,** 51–67 (Dec. 25, 2000) (cit. on p. 46).
6. Alloway, K. D., Smith, J. B. & Watson, G. D. R. Thalamostriatal projections from the medial posterior and parafascicular nuclei have distinct topographic and physiologic properties. *Journal of Neurophysiology* **111,** 36–50 (Jan. 1, 2014) (cit. on p. 141).
7. Amroune, K., Fontolan, L., Robbe, D. & Bureau, I. *Sparse and specific somatosensory functional innervation of dorsolateral striatal neurons* working paper or preprint. May 2024 (cit. on p. 141).

8. Apicella, P. Leading tonically active neurons of the striatum from reward detection to context recognition. *Trends in Neurosciences* **30,** 299–306 (June 2007) (cit. on p. 37).
9. Apicella, P., Ravel, S., Deffains, M. & Legallet, E. The role of striatal tonically active neurons in reward prediction error signaling during instrumental task performance. *The Journal of Neuroscience: The Official Journal of the Society for Neuroscience* **31,** 1507–1515 (Jan. 26, 2011) (cit. on p. 37).
10. Armstrong-James, M. & Fox, K. Spatiotemporal convergence and divergence in the rat S1 "barrel" cortex. *The Journal of Comparative Neurology* **263,** 265–281 (Sept. 8, 1987) (cit. on p. 21).
11. Audette, N. J., Bernhard, S. M., Ray, A., Stewart, L. T. & Barth, A. L. Rapid Plasticity of Higher-Order Thalamocortical Inputs during Sensory Learning. *Neuron* **103,** 277–291.e4 (July 2019) (cit. on p. 27).
12. Ayaz, A., Stäuble, A., Hamada, M., Wulf, M.-A., Saleem, A. B. & Helmchen, F. Layer-specific integration of locomotion and sensory information in mouse barrel cortex. *Nature Communications* **10,** 2585 (June 13, 2019) (cit. on p. 139).
13. Badreddine, N., Zalcman, G., Appaix, F., Becq, G., Tremblay, N., Saudou, F., Achard, S. & Fino, E. Spatiotemporal reorganization of corticostriatal networks encodes motor skill learning. *Cell Reports* **39,** 110623 (Apr. 5, 2022) (cit. on pp. 137, 147).
14. Ballion, B., Mallet, N., Bézard, E., Lanciego, J. L. & Gonon, F. Intratelencephalic corticostriatal neurons equally excite striatonigral and striatopallidal neurons and their discharge activity is selectively reduced in experimental parkinsonism. *European Journal of Neuroscience* **27,** 2313–2321 (May 2008) (cit. on p. 43).
15. Bamford, N. S., Zhang, H., Schmitz, Y., Wu, N.-P., Cepeda, C., Levine, M. S., Schmauss, C., Zakharenko, S. S., Zablow, L. & Sulzer, D. Heterosynaptic dopamine neurotransmission selects sets of corticostriatal terminals. *Neuron* **42,** 653–663 (May 27, 2004) (cit. on p. 35).
16. Barbera, G., Liang, B., Zhang, L., Gerfen, C. R., Culurciello, E., Chen, R., Li, Y. & Lin, D.-T. Spatially Compact Neural Clusters in the Dorsal Striatum Encode Locomotion Relevant Information. *Neuron* **92,** 202–213 (Oct. 5, 2016) (cit. on pp. 57, 62, 68, 137, 146, 147).
17. Barnes, T. D., Kubota, Y., Hu, D., Jin, D. Z. & Graybiel, A. M. Activity of striatal neurons reflects dynamic encoding and recoding of procedural memories. *Nature* **437,** 1158–1161 (Oct. 2005) (cit. on p. 55).

18. Bay Kønig, A., Ciriachi, C., Gether, U. & Rickhag, M. Chemogenetic Targeting of Dorsomedial Direct-pathway Striatal Projection Neurons Selectively Elicits Rotational Behavior in Mice. *Neuroscience* **401,** 106–116 (Mar. 2019) (cit. on p. 142).

19. Bennett, B. D. & Bolam, J. P. Characterization of calretinin-immunoreactive structures in the striatum of the rat. *Brain Research* **609,** 137–148 (Apr. 23, 1993) (cit. on p. 35).

20. Bentivoglio, M., Van Der Kooy, D. & Kuypers, H. G. The organization of the efferent projections of the substantia nigra in the rat. A retrograde fluorescent double labeling study. *Brain Research* **174,** 1–17 (Sept. 1979) (cit. on p. 34).

21. Berendse, H. W. & Groenewegen, H. J. Organization of the thalamostriatal projections in the rat, with special emphasis on the ventral striatum. *The Journal of Comparative Neurology* **299,** 187–228 (Sept. 8, 1990) (cit. on p. 34).

22. Bertero, A., Verrillo, L. & Apicella, A. J. A Novel Layer 4 Corticofugal Cell Type/Projection Involved in Thalamo-Cortico-Striatal Sensory Processing. *The Journal of Neuroscience: The Official Journal of the Society for Neuroscience* **42,** 1383–1405 (Feb. 23, 2022) (cit. on p. 138).

23. Blumenstock, S. & Dudanova, I. Cortical and Striatal Circuits in Huntington's Disease. *Frontiers in Neuroscience* **14,** 82 (Feb. 6, 2020) (cit. on p. 30).

24. Bolam, J., Wainer, B. & Smith, A. Characterization of cholinergic neurons in the rat neostriatum. A combination of choline acetyltransferase immunocytochemistry, Golgi-impregnation and electron microscopy. *Neuroscience* **12,** 711–718 (July 1984) (cit. on p. 37).

25. Bordi, F. & LeDoux, J. Sensory tuning beyond the sensory system: an initial analysis of auditory response properties of neurons in the lateral amygdaloid nucleus and overlying areas of the striatum. *The Journal of Neuroscience* **12,** 2493–2503 (July 1, 1992) (cit. on p. 140).

26. Braitenberg, V. & Schüz, A. *Cortex: Statistics and Geometry of Neuronal Connectivity* (Springer Berlin Heidelberg, Berlin, Heidelberg, 1998) (cit. on p. 48).

27. Brown, L. L., Smith, D. M. & Goldbloom, L. M. Organizing principles of cortical integration in the rat neostriatum: corticostriate map of the body surface is an ordered lattice of curved laminae and radial points. *The Journal of Comparative Neurology* **392,** 468–488 (Mar. 23, 1998) (cit. on pp. 40, 141).

28. Bureau, I., von Saint Paul, F. & Svoboda, K. Interdigitated paralemniscal and lemniscal pathways in the mouse barrel cortex. *PLoS biology* **4,** e382 (Nov. 2006) (cit. on p. 26).

29. Burke, D. A., Rotstein, H. G. & Alvarez, V. A. Striatal Local Circuitry: A New Framework for Lateral Inhibition. *Neuron* **96,** 267–284 (Oct. 2017) (cit. on pp. 149, 150).

30. Calabresi, P., Maj, R., Pisani, A., Mercuri, N. & Bernardi, G. Long-term synaptic depression in the striatum: physiological and pharmacological characterization. *The Journal of Neuroscience* **12,** 4224–4233 (Nov. 1, 1992) (cit. on pp. 63, 64).

31. Calabresi, P., Pisani, A., Mercuri, N. B. & Bernardi, G. Long-term Potentiation in the Striatum is Unmasked by Removing the Voltage-dependent Magnesium Block of NMDA Receptor Channels. *The European Journal of Neuroscience* **4,** 929–935 (1992) (cit. on pp. 63–65).

32. Calabresi, P., Picconi, B., Tozzi, A. & Di Filippo, M. Dopamine-mediated regulation of corticostriatal synaptic plasticity. *Trends in Neurosciences* **30,** 211–219 (May 2007) (cit. on p. 64).

33. Camon, J., Hugues, S., Erlandson, M. A., Robbe, D., Lagoun, S., Marouane, E. & Bureau, I. The Timing of Sensory-Guided Behavioral Response is Represented in the Mouse Primary Somatosensory Cortex. *Cerebral Cortex (New York, N.Y.: 1991)* **29,** 3034–3047 (July 5, 2019) (cit. on p. 53).

34. Carannante, I., Scolamiero, M., Hjorth, J. J. J., Kozlov, A., Bekkouche, B., Guo, L., Kumar, A., Chachólski, W. & Kotaleski, J. H. The impact of Parkinson's disease on striatal network connectivity and cortico-striatal drive: an in-silico study. *Network Neuroscience*, 1–35 (June 17, 2024) (cit. on pp. 34, 37, 44).

35. Carelli, R. M. & West, M. O. Representation of the body by single neurons in the dorsolateral striatum of the awake, unrestrained rat. *The Journal of Comparative Neurology* **309,** 231–249 (July 8, 1991) (cit. on pp. 48, 69, 137, 140).

36. Centonze, D., Gubellini, P., Picconi, B., Calabresi, P., Giacomini, P. & Bernardi, G. Unilateral Dopamine Denervation Blocks Corticostriatal LTP. *Journal of Neurophysiology* **82,** 3575–3579 (Dec. 1, 1999) (cit. on p. 64).

37. Cepeda, C., André, V. M., Yamazaki, I., Wu, N., Kleiman-Weiner, M. & Levine, M. S. Differential electrophysiological properties of dopamine D1 and D2 receptor-containing striatal medium-sized spiny neurons. *The European Journal of Neuroscience* **27,** 671–682 (Feb. 2008) (cit. on p. 33).

38. Charpier, S. & Deniau, J. M. In vivo activity-dependent plasticity at cortico-striatal connections: evidence for physiological long-term potentiation. *Proceedings of the National Academy of Sciences of the United States of America* **94,** 7036–7040 (June 24, 1997) (cit. on pp. 33, 64, 65).

39. Charpier, S., Mahon, S. & Deniau, J. M. In vivo induction of striatal long-term potentiation by low-frequency stimulation of the cerebral cortex. *Neuroscience* **91,** 1209–1222 (1999) (cit. on p. 64).

40. Charpier, S., Pidoux, M. & Mahon, S. Converging sensory and motor cortical inputs onto the same striatal neurons: An in vivo intracellular investigation. *PLOS ONE* **15** (ed Mothet, J.-P.) e0228260 (Feb. 5, 2020) (cit. on pp. 40, 48, 141).

41. Chiaia, N. L., Rhoades, R. W., Bennett-Clarke, C. A., Fish, S. E. & Killackey, H. P. Thalamic processing of vibrissal information in the rat. I. Afferent input to the medial ventral posterior and posterior nuclei. *Journal of Comparative Neurology* **314,** 201–216 (Dec. 8, 1991) (cit. on pp. 27, 141).

42. Chiaia, N. L., Rhoades, R. W., Fish, S. E. & Killackey, H. P. Thalamic processing of vibrissal information in the rat: II. Morphological and functional properties of medial ventral posterior nucleus and posterior nucleus neurons. *Journal of Comparative Neurology* **314,** 217–236 (Dec. 8, 1991) (cit. on p. 141).

43. Cho, J. & West, M. O. Distributions of single neurons related to body parts in the lateral striatum of the rat. *Brain Research* **756,** 241–246 (May 9, 1997) (cit. on p. 140).

44. Choi, E. Y., Yeo, B. T. T. & Buckner, R. L. The organization of the human striatum estimated by intrinsic functional connectivity. *Journal of Neurophysiology* **108,** 2242–2263 (Oct. 2012) (cit. on p. 39).

45. Chorev, E., Preston-Ferrer, P. & Brecht, M. Representation of egomotion in rat's trident and E-row whisker cortices. *Nature Neuroscience* **19,** 1367–1373 (Oct. 2016) (cit. on p. 143).

46. Chudler, E. H., Sugiyama, K. & Dong, W. K. Multisensory convergence and integration in the neostriatum and globus pallidus of the rat. *Brain Research* **674,** 33–45 (Mar. 13, 1995) (cit. on p. 40).

47. Chuhma, N., Mingote, S., Kalmbach, A., Yetnikoff, L. & Rayport, S. Heterogeneity in Dopamine Neuron Synaptic Actions Across the Striatum and Its Relevance for Schizophrenia. *Biological Psychiatry* **81,** 43–51 (Jan. 1, 2017) (cit. on p. 39).

48. Compton, D. Behavior strategy learning in rat: effects of lesions of the dorsal striatum or dorsal hippocampus. *Behavioural Processes* **67,** 335–342 (Nov. 30, 2004) (cit. on p. 54).

49. Cowan, R. L. & Wilson, C. J. Spontaneous firing patterns and axonal projections of single corticostriatal neurons in the rat medial agranular cortex. *Journal of Neurophysiology* **71,** 17–32 (Jan. 1994) (cit. on pp. 27, 41–43, 139).

50. Cruz, K. G., Leow, Y. N., Le, N. M., Adam, E., Huda, R. & Sur, M. Cortical-subcortical interactions in goal-directed behavior. *Physiological Reviews* **103,** 347–389 (Jan. 1, 2023) (cit. on pp. 27, 28).

51. Cui, G., Jun, S. B., Jin, X., Pham, M. D., Vogel, S. S., Lovinger, D. M. & Costa, R. M. Concurrent activation of striatal direct and indirect pathways during action initiation. *Nature* **494,** 238–242 (Feb. 14, 2013) (cit. on pp. 62, 68, 146).

52. Dang, M. T., Yokoi, F., Yin, H. H., Lovinger, D. M., Wang, Y. & Li, Y. Disrupted motor learning and long-term synaptic plasticity in mice lacking *NMDAR1* in the striatum. *Proceedings of the National Academy of Sciences* **103,** 15254–15259 (Oct. 10, 2006) (cit. on p. 65).

53. De Kock, C. P. J., Pie, J., Pieneman, A. W., Mease, R. A., Bast, A., Guest, J. M., Oberlaender, M., Mansvelder, H. D. & Sakmann, B. High-frequency burst spiking in layer 5 thick-tufted pyramids of rat primary somatosensory cortex encodes exploratory touch. *Communications Biology* **4,** 709 (June 10, 2021) (cit. on p. 43).

54. De la Torre-Martinez, R., Ketzef, M. & Silberberg, G. Ongoing movement controls sensory integration in the dorsolateral striatum. *Nature Communications* **14,** 1004 (Feb. 22, 2023) (cit. on pp. 38, 139).

55. Deng, Y., Lanciego, J., Kerkerian-Le-Goff, L., Coulon, P., Salin, P., Kachidian, P., Lei, W., Del Mar, N. & Reiner, A. Differential organization of cortical inputs to striatal projection neurons of the matrix compartment in rats. *Frontiers in Systems Neuroscience* **9,** 51 (2015) (cit. on pp. 43, 44, 100, 138).

56. Deschenes, M., Bourassa, J. & Parent, A. Two different types of thalamic fibers innervate the rat striatum. *Brain Research* **701,** 288–292 (Dec. 1995) (cit. on p. 141).

57. Dhawale, A. K., Wolff, S. B. E., Ko, R. & Ölveczky, B. P. The basal ganglia control the detailed kinematics of learned motor skills. *Nature Neuroscience* **24,** 1256–1269 (Sept. 2021) (cit. on p. 57).

58. Di Filippo, M., Picconi, B., Tantucci, M., Ghiglieri, V., Bagetta, V., Sgobio, C., Tozzi, A., Parnetti, L. & Calabresi, P. Short-term and long-term plasticity at corticostriatal synapses: Implications for learning and memory. *Behavioural Brain Research* **199,** 108–118 (Apr. 2009) (cit. on p. 64).

59. Diamond, M. E., Armstrong-James, M. & Ebner, F. F. Somatic sensory responses in the rostral sector of the posterior group (POm) and in the ventral posterior medial nucleus (VPM) of the rat thalamus. *Journal of Comparative Neurology* **318,** 462–476 (Apr. 22, 1992) (cit. on pp. 27, 141).

60. Diering, G. H. & Huganir, R. L. The AMPA Receptor Code of Synaptic Plasticity. *Neuron* **100,** 314–329 (Oct. 24, 2018) (cit. on p. 63).

61. Difiglia, M. Synaptic organization of cholinergic neurons in the monkey neostriatum. *Journal of Comparative Neurology* **255,** 245–258 (Jan. 8, 1987) (cit. on p. 37).

62. Ding, J., Peterson, J. D. & Surmeier, D. J. Corticostriatal and thalamostriatal synapses have distinctive properties. *The Journal of Neuroscience: The Official Journal of the Society for Neuroscience* **28,** 6483–6492 (June 18, 2008) (cit. on pp. 43, 100, 138).

63. Donoghue, J. P. & Kitai, S. T. A collateral pathway to the neostriatum from corticofugal neurons of the rat sensory-motor cortex: an intracellular HRP study. *The Journal of Comparative Neurology* **201,** 1–13 (Sept. 1, 1981) (cit. on p. 43).

64. Eshel, N., Bukwich, M., Rao, V., Hemmelder, V., Tian, J. & Uchida, N. Arithmetic and local circuitry underlying dopamine prediction errors. *Nature* **525,** 243–246 (Sept. 10, 2015) (cit. on p. 50).

65. Esmaeili, V., Tamura, K., Foustoukos, G., Oryshchuk, A., Crochet, S. & Petersen, C. C. Cortical circuits for transforming whisker sensation into goal-directed licking. *Current Opinion in Neurobiology* **65,** 38–48 (Dec. 2020) (cit. on p. 53).

66. Featherstone, R. & McDonald, R. Lesions of the dorsolateral or dorsomedial striatum impair performance of a previously acquired simple discrimination task. *Neurobiology of Learning and Memory* **84,** 159–167 (Nov. 2005) (cit. on p. 54).

67. Feldman, D. E. & Brecht, M. Map Plasticity in Somatosensory Cortex. *Science* **310,** 810–815 (Nov. 4, 2005) (cit. on p. 144).

68. Ferrier, D. *The functions of the brain* (Smith, Elder, 1876) (cit. on p. 29).

69. Filipović, M., Ketzef, M., Reig, R., Aertsen, A., Silberberg, G. & Kumar, A. Direct pathway neurons in mouse dorsolateral striatum in vivo receive stronger synaptic input than indirect pathway neurons. *Journal of Neurophysiology* **122,** 2294–2303 (Dec. 1, 2019) (cit. on pp. 44, 48, 69, 138).

70. Fino, E., Glowinski, J. & Venance, L. Bidirectional Activity-Dependent Plasticity at Corticostriatal Synapses. *The Journal of Neuroscience* **25,** 11279–11287 (Dec. 7, 2005) (cit. on p. 64).

71. Fino, E., Vandecasteele, M., Perez, S., Saudou, F. & Venance, L. Region-specific and state-dependent action of striatal GABAergic interneurons. *Nature Communications* **9,** 3339 (Aug. 21, 2018) (cit. on p. 36).

72. Flaherty, A. W. & Graybiel, A. M. Corticostriatal transformations in the primate somatosensory system. Projections from physiologically mapped body-part representations. *Journal of Neurophysiology* **66,** 1249–1263 (Oct. 1991) (cit. on pp. 40, 139).

73. Flaherty, A. W. & Graybiel, A. M. Input-output organization of the sensorimotor striatum in the squirrel monkey. *The Journal of Neuroscience: The Official Journal of the Society for Neuroscience* **14,** 599–610 (Feb. 1994) (cit. on p. 40).

74. Flaherty, A. W. & Graybiel, A. M. Motor and somatosensory corticostriatal projection magnifications in the squirrel monkey. *Journal of Neurophysiology* **74,** 2638–2648 (Dec. 1995) (cit. on p. 40).

75. Foster, N. N., Barry, J., Korobkova, L., Garcia, L., Gao, L., Becerra, M., Sherafat, Y., Peng, B., Li, X., Choi, J.-H., Gou, L., Zingg, B., Azam, S., Lo, D., Khanjani, N., Zhang, B., Stanis, J., Bowman, I., Cotter, K., Cao, C., Yamashita, S., Tugangui, A., Li, A., Jiang, T., Jia, X., Feng, Z., Aquino, S., Mun, H.-S., Zhu, M., Santarelli, A., Benavidez, N. L., Song, M., Dan, G., Fayzullina, M., Ustrell, S., Boesen, T., Johnson, D. L., Xu, H., Bienkowski, M. S., Yang, X. W., Gong, H., Levine, M. S., Wickersham, I., Luo, Q., Hahn, J. D., Lim, B. K., Zhang, L. I., Cepeda, C., Hintiryan, H. & Dong, H.-W. The mouse cortico–basal ganglia–thalamic network. *Nature* **598,** 188–194 (Oct. 7, 2021) (cit. on p. 40).

76. Fox, K. *Barrel cortex* OCLC: 227160818 (Cambridge University Press, Cambridge, 2008) (cit. on p. 27).

77. Freeze, B. S., Kravitz, A. V., Hammack, N., Berke, J. D. & Kreitzer, A. C. Control of basal ganglia output by direct and indirect pathway projection neurons. *The Journal of Neuroscience: The Official Journal of the Society for Neuroscience* **33,** 18531–18539 (Nov. 20, 2013) (cit. on p. 60).

78. Gadagkar, V., Puzerey, P. A., Chen, R., Baird-Daniel, E., Farhang, A. R. & Goldberg, J. H. Dopamine neurons encode performance error in singing birds. *Science* **354,** 1278–1282 (Dec. 9, 2016) (cit. on p. 149).

79. Gambino, F., Pagès, S., Kehayas, V., Baptista, D., Tatti, R., Carleton, A. & Holtmaat, A. Sensory-evoked LTP driven by dendritic plateau potentials in vivo. *Nature* **515,** 116–119 (Nov. 2014) (cit. on p. 27).

80. Gardner, M. P. H., Schoenbaum, G. & Gershman, S. J. Rethinking dopamine as generalized prediction error. *Proceedings of the Royal Society B: Biological Sciences* **285,** 20181645 (Nov. 21, 2018) (cit. on p. 149).

81. Geinisman, Y. Perforated axospinous synapses with multiple, completely partitioned transmission zones: Probable structural intermediates in synaptic plasticity. *Hippocampus* **3,** 417–433 (Oct. 1993) (cit. on p. 44).

82. Gerfen, C. R., Paletzki, R. & Heintz, N. GENSAT BAC Cre-Recombinase Driver Lines to Study the Functional Organization of Cerebral Cortical and Basal Ganglia Circuits. *Neuron* **80,** 1368–1383 (Dec. 2013) (cit. on p. 43).

83. Gerfen, C. R. & Surmeier, D. J. Modulation of striatal projection systems by dopamine. *Annual Review of Neuroscience* **34,** 441–466 (2011) (cit. on pp. 30, 34, 35, 149, 150).

84. Gertler, T. S., Chan, C. S. & Surmeier, D. J. Dichotomous anatomical properties of adult striatal medium spiny neurons. *The Journal of Neuroscience: The Official Journal of the Society for Neuroscience* **28,** 10814–10824 (Oct. 22, 2008) (cit. on p. 33).

85. Gittis, A. H., Nelson, A. B., Thwin, M. T., Palop, J. J. & Kreitzer, A. C. Distinct roles of GABAergic interneurons in the regulation of striatal output pathways. *The Journal of Neuroscience: The Official Journal of the Society for Neuroscience* **30,** 2223–2234 (Feb. 10, 2010) (cit. on p. 36).

86. Gómez-Ocádiz, R. & Silberberg, G. Corticostriatal pathways for bilateral sensorimotor functions. *Current Opinion in Neurobiology* **83,** 102781 (Dec. 2023) (cit. on p. 69).

87. Gong, S., Doughty, M., Harbaugh, C. R., Cummins, A., Hatten, M. E., Heintz, N. & Gerfen, C. R. Targeting Cre recombinase to specific neuron populations with bacterial artificial chromosome constructs. *The Journal of Neuroscience: The Official Journal of the Society for Neuroscience* **27,** 9817–9823 (Sept. 12, 2007) (cit. on p. 43).

88. Guo, C., Peng, J., Zhang, Y., Li, A., Li, Y., Yuan, J., Xu, X., Ren, M., Gong, H. & Chen, S. Single-axon level morphological analysis of corticofugal projection neurons in mouse barrel field. *Scientific Reports* **7,** 2846 (June 6, 2017) (cit. on p. 138).

89. Guo, L., Walker, W. I., Ponvert, N. D., Penix, P. L. & Jaramillo, S. Stable representation of sounds in the posterior striatum during flexible auditory decisions. *Nature Communications* **9,** 1534 (Apr. 18, 2018) (cit. on p. 140).

90. Guo, Z. V., Li, N., Huber, D., Ophir, E., Gutnisky, D., Ting, J. T., Feng, G. & Svoboda, K. Flow of cortical activity underlying a tactile decision in mice. *Neuron* **81,** 179–194 (Jan. 8, 2014) (cit. on p. 52).

91. Han, S. & Helmchen, F. Behavior-relevant top-down cross-modal predictions in mouse neocortex. *Nature Neuroscience* **27,** 298–308 (Feb. 2024) (cit. on p. 139).

92. Harris, K. D. & Shepherd, G. M. G. The neocortical circuit: themes and variations. *Nature Neuroscience* **18,** 170–181 (Feb. 2015) (cit. on pp. 24, 27, 100, 138).

93. Harris, K. D. & Mrsic-Flogel, T. D. Cortical connectivity and sensory coding. *Nature* **503,** 51–58 (Nov. 7, 2013) (cit. on p. 138).

94. Higley, M. J. & Sabatini, B. L. Competitive regulation of synaptic Ca2+ influx by D2 dopamine and A2A adenosine receptors. *Nature Neuroscience* **13,** 958–966 (Aug. 2010) (cit. on p. 150).

95. Hintiryan, H., Foster, N. N., Bowman, I., Bay, M., Song, M. Y., Gou, L., Yamashita, S., Bienkowski, M. S., Zingg, B., Zhu, M., Yang, X. W., Shih, J. C., Toga, A. W. & Dong, H.-W. The mouse cortico-striatal projectome. *Nature Neuroscience* **19,** 1100–1114 (Aug. 2016) (cit. on pp. 39, 40, 46, 69, 139).

96. Hirsh, R. The hippocampus and contextual retrieval of information from memory: A theory. *Behavioral Biology* **12,** 421–444 (Dec. 1974) (cit. on p. 54).

97. Hoffer, Z. S. & Alloway, K. D. Organization of corticostriatal projections from the vibrissal representations in the primary motor and somatosensory cortical areas of rodents. *Journal of Comparative Neurology* **439,** 87–103 (Oct. 8, 2001) (cit. on p. 40).

98. Hong, Y. K., Lacefield, C. O., Rodgers, C. C. & Bruno, R. M. Sensation, movement and learning in the absence of barrel cortex. *Nature* **561,** 542–546 (Sept. 2018) (cit. on p. 52).

99. Hooks, B. M., Papale, A. E., Paletzki, R. F., Feroze, M. W., Eastwood, B. S., Couey, J. J., Winnubst, J., Chandrashekar, J. & Gerfen, C. R. Topographic precision in sensory and motor corticostriatal projections varies across cell type and cortical area. *Nature Communications* **9,** 3549 (Sept. 3, 2018) (cit. on pp. 40, 139).

100. Hoover, J. E., Hoffer, Z. S. & Alloway, K. D. Projections From Primary Somatosensory Cortex to the Neostriatum: The Role of Somatotopic Continuity in Corticostriatal Convergence. *Journal of Neurophysiology* **89,** 1576–1587 (Mar. 1, 2003) (cit. on p. 40).

101. Houweling, A. R. & Brecht, M. Behavioural report of single neuron stimulation in somatosensory cortex. *Nature* **451,** 65–68 (Jan. 3, 2008) (cit. on p. 52).

102. Hunnicutt, B. J., Jongbloets, B. C., Birdsong, W. T., Gertz, K. J., Zhong, H. & Mao, T. A comprehensive excitatory input map of the striatum reveals novel functional organization. *eLife* **5,** e19103 (Nov. 28, 2016) (cit. on p. 39).

103. Hwang, F.-J., Roth, R. H., Wu, Y.-W., Sun, Y., Kwon, D. K., Liu, Y. & Ding, J. B. Motor learning selectively strengthens cortical and striatal synapses of motor engram neurons. *Neuron* **110,** 2790–2801.e5 (Sept. 7, 2022) (cit. on pp. 65, 66).

104. Jaeger, D., Gilman, S. & Aldridge, J. W. Neuronal activity in the striatum and pallidum of primates related to the execution of externally cued reaching movements. *Brain Research* **694,** 111–127 (Oct. 2, 1995) (cit. on p. 137).

105. Jin, X. & Costa, R. M. Start/stop signals emerge in nigrostriatal circuits during sequence learning. *Nature* **466,** 457–462 (July 2010) (cit. on pp. 55, 56, 65).

106. Jin, X., Tecuapetla, F. & Costa, R. M. Basal ganglia subcircuits distinctively encode the parsing and concatenation of action sequences. *Nature Neuroscience* **17,** 423–430 (Mar. 2014) (cit. on p. 62).

107. Johansson, Y. & Silberberg, G. The Functional Organization of Cortical and Thalamic Inputs onto Five Types of Striatal Neurons Is Determined by Source and Target Cell Identities. *Cell Reports* **30,** 1178–1194.e3 (Jan. 28, 2020) (cit. on pp. 44, 45, 48, 69).

108. *Principles of neural science* (eds Kandel, E. R., Koester, J., Mack, S. & Siegelbaum, S.) Sixth edition (McGraw Hill, New York, 2021). 1646 pp. (cit. on p. 22).

109. Kawaguchi, Y., Wilson, C. & Emson, P. Projection subtypes of rat neostriatal matrix cells revealed by intracellular injection of biocytin. *The Journal of Neuroscience* **10,** 3421–3438 (Oct. 1, 1990) (cit. on p. 33).

110. Kawaguchi, Y. Physiological, morphological, and histochemical characterization of three classes of interneurons in rat neostriatum. *The Journal of Neuroscience: The Official Journal of the Society for Neuroscience* **13,** 4908–4923 (Nov. 1993) (cit. on p. 35).

111. Kawaguchi, Y., Wilson, C. J., Augood, S. J. & Emson, P. C. Striatal interneurones: chemical, physiological and morphological characterization. *Trends in Neurosciences* **18,** 527–535 (Dec. 1995) (cit. on p. 35).

112. Kerr, J. & Wickens, J. R. Dopamine D-1/D-5 Receptor Activation Is Required for Long-Term Potentiation in the Rat Neostriatum In Vitro. *Journal of Neurophysiology* **85,** 117–124 (Jan. 1, 2001) (cit. on p. 64).

113. Killackey, H. P. & Sherman, S. M. Corticothalamic Projections from the Rat Primary Somatosensory Cortex. *The Journal of Neuroscience* **23,** 7381–7384 (Aug. 13, 2003) (cit. on p. 141).

114. Kim, E. J., Juavinett, A. L., Kyubwa, E. M., Jacobs, M. W. & Callaway, E. M. Three Types of Cortical Layer 5 Neurons That Differ in Brain-wide Connectivity and Function. *Neuron* **88,** 1253–1267 (Dec. 16, 2015) (cit. on p. 43).

115. Kincaid, A. E. & Wilson, C. J. Corticostriatal innervation of the patch and matrix in the rat neostriatum. *The Journal of Comparative Neurology* **374,** 578–592 (Oct. 28, 1996) (cit. on p. 43).

116. Kincaid, A. E., Zheng, T. & Wilson, C. J. Connectivity and Convergence of Single Corticostriatal Axons. *The Journal of Neuroscience* **18,** 4722 (June 15, 1998) (cit. on pp. 46, 47, 69).

117. Klaus, A., Martins, G. J., Paixao, V. B., Zhou, P., Paninski, L. & Costa, R. M. The Spatiotemporal Organization of the Striatum Encodes Action Space. *Neuron* **95,** 1171–1180.e7 (Aug. 30, 2017) (cit. on pp. 137, 146, 147).

118. Knutsen, P. M., Pietr, M. & Ahissar, E. Haptic object localization in the vibrissal system: behavior and performance. *The Journal of Neuroscience: The Official Journal of the Society for Neuroscience* **26,** 8451–8464 (Aug. 16, 2006) (cit. on pp. 52, 144).

119. Koralek, A. C., Costa, R. M. & Carmena, J. M. Temporally Precise Cell-Specific Coherence Develops in Corticostriatal Networks during Learning. *Neuron* **79,** 865–872 (Sept. 2013) (cit. on p. 64).

120. Koralek, A. C., Jin, X., Long, J. D., Costa, R. M. & Carmena, J. M. Corticostriatal plasticity is necessary for learning intentional neuroprosthetic skills. *Nature* **483,** 331–335 (Mar. 4, 2012) (cit. on pp. 64, 65).

121. Kravitz, A. V., Tye, L. D. & Kreitzer, A. C. Distinct roles for direct and indirect pathway striatal neurons in reinforcement. *Nature Neuroscience* **15,** 816–818 (June 2012) (cit. on p. 146).

122. Kravitz, A. V., Freeze, B. S., Parker, P. R. L., Kay, K., Thwin, M. T., Deisseroth, K. & Kreitzer, A. C. Regulation of parkinsonian motor behaviours by optogenetic control of basal ganglia circuitry. *Nature* **466,** 622–626 (July 29, 2010) (cit. on pp. 59, 60, 68, 70, 142, 146).

123. Kreitzer, A. C. & Malenka, R. C. Endocannabinoid-mediated rescue of striatal LTD and motor deficits in Parkinson's disease models. *Nature* **445,** 643–647 (Feb. 2007) (cit. on p. 43).

124. Kress, G. J., Yamawaki, N., Wokosin, D. L., Wickersham, I. R., Shepherd, G. M. G. & Surmeier, D. J. Convergent cortical innervation of striatal projection neurons. *Nature Neuroscience* **16,** 665–667 (June 2013) (cit. on pp. 44, 100, 138).

125. Kuhlman, S. J., O'Connor, D. H., Fox, K. & Svoboda, K. Structural Plasticity within the Barrel Cortex during Initial Phases of Whisker-Dependent Learning. *The Journal of Neuroscience* **34,** 6078–6083 (Apr. 23, 2014) (cit. on p. 144).

126. Kwon, S. E., Yang, H., Minamisawa, G. & O'Connor, D. H. Sensory and decision-related activity propagate in a cortical feedback loop during touch perception. *Nature Neuroscience* **19,** 1243–1249 (Sept. 2016) (cit. on pp. 52, 139).

127. Landry, P., Wilson, C. J. & Kitai, S. T. Morphological and electrophysiological characteristics of pyramidal tract neurons in the rat. *Experimental Brain Research* **57,** 177–190 (1984) (cit. on p. 43).

128. Le Merre, P., Esmaeili, V., Charrière, E., Galan, K., Salin, P.-A., Petersen, C. C. H. & Crochet, S. Reward-Based Learning Drives Rapid Sensory Signals in Medial Prefrontal Cortex and Dorsal Hippocampus Necessary for Goal-Directed Behavior. *Neuron* **97,** 83–91.e5 (Jan. 3, 2018) (cit. on p. 52).

129. Lee, C. R., Yonk, A. J., Wiskerke, J., Paradiso, K. G., Tepper, J. M. & Margolis, D. J. Opposing Influence of Sensory and Motor Cortical Input on Striatal Circuitry and Choice Behavior. *Current Biology* **29,** 1313–1323.e5 (Apr. 2019) (cit. on p. 44).

130. Lee, J., Wang, W. & Sabatini, B. L. Anatomically segregated basal ganglia pathways allow parallel behavioral modulation. *Nature Neuroscience* **23,** 1388–1398 (Nov. 2020) (cit. on p. 38).

131. Leergaard, T. B., Alloway, K. D., Mutic, J. J. & Bjaalie, J. G. Three-dimensional topography of corticopontine projections from rat barrel cortex: correlations with corticostriatal organization. *The Journal of Neuroscience: The Official Journal of the Society for Neuroscience* **20,** 8474–8484 (Nov. 15, 2000) (cit. on pp. 47, 137).

132. Lei, W., Jiao, Y., Del Mar, N. & Reiner, A. Evidence for differential cortical input to direct pathway versus indirect pathway striatal projection neurons in rats. *The Journal of Neuroscience: The Official Journal of the Society for Neuroscience* **24,** 8289–8299 (Sept. 22, 2004) (cit. on pp. 43, 100, 138).

133. Lemke, S. M., Ramanathan, D. S., Guo, L., Won, S. J. & Ganguly, K. Emergent modular neural control drives coordinated motor actions. *Nature Neuroscience* **22,** 1122–1131 (July 2019) (cit. on p. 64).

134. Lerner, T. N. & Kreitzer, A. C. Neuromodulatory control of striatal plasticity and behavior. *Current Opinion in Neurobiology* **21,** 322–327 (Apr. 2011) (cit. on p. 64).

135. Lovinger, D. M., Tyler, E. C. & Merritt, A. Short- and long-term synaptic depression in rat neostriatum. *Journal of Neurophysiology* **70,** 1937–1949 (Nov. 1993) (cit. on p. 64).

136. Lübke, J. & Feldmeyer, D. Excitatory signal flow and connectivity in a cortical column: focus on barrel cortex. *Brain Structure and Function* **212,** 3–17 (July 3, 2007) (cit. on p. 26).

137. Mahon, S., Delord, B., Deniau, J. M. & Charpier, S. Intrinsic properties of rat striatal output neurones and time-dependent facilitation of cortical inputs in vivo. *The Journal of Physiology* **527 Pt 2,** 345–354 (Pt 2 Sept. 1, 2000) (cit. on p. 33).

138. Mallet, N., Le Moine, C., Charpier, S. & Gonon, F. Feedforward inhibition of projection neurons by fast-spiking GABA interneurons in the rat striatum in vivo. *The Journal of Neuroscience: The Official Journal of the Society for Neuroscience* **25,** 3857–3869 (Apr. 13, 2005) (cit. on p. 48).

139. Maltese, M., March, J. R., Bashaw, A. G. & Tritsch, N. X. Dopamine differentially modulates the size of projection neuron ensembles in the intact and dopamine-depleted striatum. *eLife* **10,** e68041 (May 13, 2021) (cit. on p. 150).

140. Manns, I. D., Sakmann, B. & Brecht, M. Sub- and suprathreshold receptive field properties of pyramidal neurones in layers 5A and 5B of rat somatosensory barrel cortex. *The Journal of Physiology* **556,** 601–622 (Apr. 2004) (cit. on p. 26).

141. Markowitz, J. E., Gillis, W. F., Beron, C. C., Neufeld, S. Q., Robertson, K., Bhagat, N. D., Peterson, R. E., Peterson, E., Hyun, M., Linderman, S. W., Sabatini, B. L. & Datta, S. R. The Striatum Organizes 3D Behavior via Moment-to-Moment Action Selection. *Cell* **174,** 44–58.e17 (June 2018) (cit. on p. 57).

142. Martiros, N., Burgess, A. A. & Graybiel, A. M. Inversely Active Striatal Projection Neurons and Interneurons Selectively Delimit Useful Behavioral Sequences. *Current biology: CB* **28,** 560–573.e5 (Feb. 19, 2018) (cit. on p. 55).

143. Mayrhofer, J. M., El-Boustani, S., Foustoukos, G., Auffret, M., Tamura, K. & Petersen, C. C. H. Distinct Contributions of Whisker Sensory Cortex and Tongue-Jaw Motor Cortex in a Goal-Directed Sensorimotor Transformation. *Neuron* **103,** 1034–1043.e5 (Sept. 25, 2019) (cit. on pp. 52, 53).

144. McGeorge, A. J. & Faull, R. L. The organization of the projection from the cerebral cortex to the striatum in the rat. *Neuroscience* **29,** 503–537 (1989) (cit. on p. 34).

145. Mehta, S. B., Whitmer, D., Figueroa, R., Williams, B. A. & Kleinfeld, D. Active spatial perception in the vibrissa scanning sensorimotor system. *PLoS biology* **5,** e15 (Feb. 2007) (cit. on pp. 52, 144).

146. Mendes, A., Vignoud, G., Perez, S., Perrin, E., Touboul, J. & Venance, L. Concurrent Thalamostriatal and Corticostriatal Spike-Timing-Dependent Plasticity and Heterosynaptic Interactions Shape Striatal Plasticity Map. *Cerebral Cortex* **30,** 4381–4401 (June 30, 2020) (cit. on p. 148).

147. Mercier, B. E., Legg, C. R. & Glickstein, M. Basal ganglia and cerebellum receive different somatosensory information in rats. *Proceedings of the National Academy of Sciences of the United States of America* **87,** 4388–4392 (June 1990) (cit. on pp. 24, 46).

148. Mermelstein, P. G., Song, W. J., Tkatch, T., Yan, Z. & Surmeier, D. J. Inwardly rectifying potassium (IRK) currents are correlated with IRK subunit expression in rat nucleus accumbens medium spiny neurons. *The Journal of Neuroscience: The Official Journal of the Society for Neuroscience* **18,** 6650–6661 (Sept. 1, 1998) (cit. on p. 33).

149. Miller, R. *Meaning and purpose in the intact brain: a philosophical, psychological, and biological account of conscious processes* 239 pp. (Clarendon Press, Oxford, 1981) (cit. on p. 63).

150. Mink, J. W. The basal ganglia: focused selection and inhibition of competing motor programs. *Progress in Neurobiology* **50,** 381–425 (Nov. 1996) (cit. on pp. 29, 59, 70, 146).

151. Mirenowicz, J. & Schultz, W. Preferential activation of midbrain dopamine neurons by appetitive rather than aversive stimuli. *Nature* **379,** 449–451 (Feb. 1996) (cit. on p. 63).

152. Mishkin, M., Malamut, B., Bachevalier, J., Lynch, G., McGaugh, J. & Weinberger, N. Neurobiology of human learning and memory (1984) (cit. on p. 54).

153. Mishkin, M. & Petri, H. L. Memories and habits: Some implications for the analysis of learning and retention. *Neuropsychology of memory,* 287–296 (1984) (cit. on p. 54).

154. Moczulska, K. E., Tinter-Thiede, J., Peter, M., Ushakova, L., Wernle, T., Bathellier, B. & Rumpel, S. Dynamics of dendritic spines in the mouse auditory cortex during memory formation and memory recall. *Proceedings of the National Academy of Sciences* **110,** 18315–18320 (Nov. 5, 2013) (cit. on p. 144).

155. Morita, K., Morishima, M., Sakai, K. & Kawaguchi, Y. Reinforcement learning: computing the temporal difference of values via distinct corticostriatal pathways. *Trends in Neurosciences* **35,** 457–467 (Aug. 2012) (cit. on p. 44).

156. Mountcastle, V. B. Modality and topographic properties of single neurons of cat's somatic sensory cortex. *Journal of Neurophysiology* **20,** 408–434 (July 1957) (cit. on p. 21).

157. Mowery, T. M., Harrold, J. B. & Alloway, K. D. Repeated whisker stimulation evokes invariant neuronal responses in the dorsolateral striatum of anesthetized rats: a potential correlate of sensorimotor habits. *Journal of Neurophysiology* **105,** 2225–2238 (May 2011) (cit. on p. 141).

158. Nagy, A., Paróczy, Z., Norita, M. & Benedek, G. Multisensory responses and receptive field properties of neurons in the substantia nigra and in the caudate nucleus. *The European Journal of Neuroscience* **22,** 419–424 (July 2005) (cit. on p. 40).

159. Nakamura, T., Nagata, M., Yagi, T., Graybiel, A. M., Yamamori, T. & Kitsukawa, T. Learning new sequential stepping patterns requires striatal plasticity during the earliest phase of acquisition. *European Journal of Neuroscience* **45** (ed Smith, Y.) 901–911 (Apr. 2017) (cit. on p. 59).

160. Nelson, A. B. & Kreitzer, A. C. Reassessing models of basal ganglia function and dysfunction. *Annual Review of Neuroscience* **37,** 117–135 (2014) (cit. on p. 149).

161. Nisenbaum, E. S. & Wilson, C. J. Potassium currents responsible for inward and outward rectification in rat neostriatal spiny projection neurons. *The Journal of Neuroscience: The Official Journal of the Society for Neuroscience* **15,** 4449–4463 (June 1995) (cit. on p. 33).

162. O'Connor, D. H., Clack, N. G., Huber, D., Komiyama, T., Myers, E. W. & Svoboda, K. Vibrissa-based object localization in head-fixed mice. *The Journal of Neuroscience: The Official Journal of the Society for Neuroscience* **30,** 1947–1967 (Feb. 3, 2010) (cit. on pp. 52, 144).

163. Oertel, W. H. & Mugnaini, E. Immunocytochemical studies of GABAergic neurons in rat basal ganglia and their relations to other neuronal systems. *Neuroscience Letters* **47,** 233–238 (June 29, 1984) (cit. on p. 31).

164. Ohno, S., Kuramoto, E., Furuta, T., Hioki, H., Tanaka, Y. R., Fujiyama, F., Sonomura, T., Uemura, M., Sugiyama, K. & Kaneko, T. A Morphological Analysis of Thalamocortical Axon Fibers of Rat Posterior Thalamic Nuclei: A Single Neuron Tracing Study with Viral Vectors. *Cerebral Cortex* **22,** 2840–2857 (Dec. 2012) (cit. on p. 141).

165. Oorschot, D. E. Total number of neurons in the neostriatal, pallidal, subthalamic, and substantia nigral nuclei of the rat basal ganglia: a stereological study using the cavalieri and optical disector methods. *The Journal of Comparative Neurology* **366,** 580–599 (Mar. 18, 1996) (cit. on pp. 45, 47).

166. Oryshchuk, A., Sourmpis, C., Weverbergh, J., Asri, R., Esmaeili, V., Modirshanechi, A., Gerstner, W., Petersen, C. C. H. & Crochet, S. Distributed and specific encoding of sensory, motor, and decision information in the mouse neocortex during goal-directed behavior. *Cell Reports* **43,** 113618 (Jan. 23, 2024) (cit. on p. 139).

167. Osaki, H., Kanaya, M., Ueta, Y. & Miyata, M. Distinct nociception processing in the dysgranular and barrel regions of the mouse somatosensory cortex. *Nature Communications* **13,** 3622 (June 29, 2022) (cit. on p. 27).

168. Packard, M. G. Glutamate infused posttraining into the hippocampus or caudate-putamen differentially strengthens place and response learning. *Proceedings of the National Academy of Sciences* **96,** 12881–12886 (Oct. 26, 1999) (cit. on pp. 54, 59).

169. Packard, M. G. Exhumed from thought: Basal ganglia and response learning in the plus-maze. *Behavioural Brain Research* **199,** 24–31 (Apr. 2009) (cit. on p. 55).

170. Packard, M. G. & McGaugh, J. L. Double dissociation of fornix and caudate nucleus lesions on acquisition of two water maze tasks: Further evidence for multiple memory systems. *Behavioral Neuroscience* **106,** 439–446 (1992) (cit. on p. 54).

171. Packard, M. G. & McGaugh, J. L. Inactivation of Hippocampus or Caudate Nucleus with Lidocaine Differentially Affects Expression of Place and Response Learning. *Neurobiology of Learning and Memory* **65,** 65–72 (Jan. 1996) (cit. on pp. 54, 55).

172. Palencia, C. A. & Ragozzino, M. E. The contribution of NMDA receptors in the dorsolateral striatum to egocentric response learning. *Behavioral Neuroscience* **119,** 953–960 (2005) (cit. on p. 59).

173. Parent, A. Extrinsic connections of the basal ganglia. *Trends in Neurosciences* **13,** 254–258 (July 1990) (cit. on p. 38).

174. Parent, A. & Hazrati, L. N. Functional anatomy of the basal ganglia. I. The cortico-basal ganglia-thalamo-cortical loop. *Brain Research. Brain Research Reviews* **20,** 91–127 (Jan. 1995) (cit. on p. 38).

175. Parker, P. R. L., Lalive, A. L. & Kreitzer, A. C. Pathway-Specific Remodeling of Thalamostriatal Synapses in Parkinsonian Mice. *Neuron* **89,** 734–740 (Feb. 17, 2016) (cit. on p. 138).

176. Pawlak, V. & Kerr, J. N. D. Dopamine receptor activation is required for corticostriatal spike-timing-dependent plasticity. *The Journal of Neuroscience: The Official Journal of the Society for Neuroscience* **28,** 2435–2446 (Mar. 5, 2008) (cit. on p. 64).

177. Peters, A. Thalamic input to the cerebral cortex. *Trends in Neurosciences* **2,** 183–185 (Jan. 1979) (cit. on p. 48).

178. Peters, Fabre, J. M. J., Steinmetz, N. A., Harris, K. D. & Carandini, M. Striatal activity topographically reflects cortical activity. *Nature* **591,** 420–425 (Mar. 18, 2021) (cit. on p. 39).

179. Petersen, C. C. H. Sensorimotor processing in the rodent barrel cortex. *Nature Reviews. Neuroscience* **20,** 533–546 (Sept. 2019) (cit. on pp. 22, 24, 26, 27, 47, 100, 138).

180. Petersen, C. C. H. & Sakmann, B. The Excitatory Neuronal Network of Rat Layer 4 Barrel Cortex. *The Journal of Neuroscience* **20,** 7579–7586 (Oct. 15, 2000) (cit. on p. 26).

181. Petty, G. H., Kinnischtzke, A. K., Hong, Y. K. & Bruno, R. M. Effects of arousal and movement on secondary somatosensory and visual thalamus. *eLife* **10,** e67611 (Nov. 29, 2021) (cit. on p. 27).

182. Pidoux, M., Mahon, S., Deniau, J.-M. & Charpier, S. Integration and propagation of somatosensory responses in the corticostriatal pathway: an intracellular study in vivo. *The Journal of Physiology* **589,** 263–281 (Pt 2 Jan. 15, 2011) (cit. on pp. 48, 69).

183. Pimentel-Farfan, A. K., Báez-Cordero, A. S., Peña-Rangel, T. M. & Rueda-Orozco, P. E. Cortico-striatal circuits for bilaterally coordinated movements. *Science Advances* **8,** eabk2241 (Mar. 4, 2022) (cit. on p. 139).

184. Pinto, D. J. Cortical Damping: Analysis of Thalamocortical Response Transformations in Rodent Barrel Cortex. *Cerebral Cortex* **13,** 33–44 (Jan. 1, 2003) (cit. on p. 26).

185. Pitzer, C., Kurpiers, B. & Eltokhi, A. Gait performance of adolescent mice assessed by the CatWalk XT depends on age, strain and sex and correlates with speed and body weight. *Scientific Reports* **11,** 21372 (Nov. 1, 2021) (cit. on p. 139).

186. Planert, H., Berger, T. K. & Silberberg, G. Membrane properties of striatal direct and indirect pathway neurons in mouse and rat slices and their modulation by dopamine. *PloS One* **8,** e57054 (2013) (cit. on pp. 33, 34, 149).

187. *Neuroscience* (eds Purves, D., Augustine, G. J. & Fitzpatrick, D.) Sixth edition (Oxford University Press, Sinauer Associates is an imprint of Oxford Universitiy Press, New York Oxford, 2018). 790 pp. (cit. on pp. 32, 36).

188. Recanzone, G. H., Merzenich, M. M., Jenkins, W. M., Grajski, K. A. & Dinse, H. R. Topographic reorganization of the hand representation in cortical area 3b owl monkeys trained in a frequency-discrimination task. *Journal of Neurophysiology* **67,** 1031–1056 (May 1992) (cit. on p. 52).

189. Reiber, M., Koska, I., Pace, C., Schönhoff, K., Von Schumann, L., Palme, R. & Potschka, H. Development of behavioral patterns in young C57BL/6J mice: a home cage-based study. *Scientific Reports* **12,** 2550 (Feb. 15, 2022) (cit. on p. 139).

190. Reig, R. & Silberberg, G. Multisensory integration in the mouse striatum. *Neuron* **83,** 1200–1212 (Sept. 3, 2014) (cit. on pp. 38, 40, 41, 48, 138).

191. Reig, R. & Silberberg, G. Distinct Corticostriatal and Intracortical Pathways Mediate Bilateral Sensory Responses in the Striatum. *Cerebral Cortex* **26,** 4405–4415 (Dec. 2016) (cit. on pp. 139, 141).

192. Reiner, A. Corticostriatal projection neurons – dichotomous types and dichotomous functions. *Frontiers in Neuroanatomy* **4** (2010) (cit. on pp. 43, 100, 138).

193. Reiner, A., Jiao, Y., Del Mar, N., Laverghetta, A. V. & Lei, W. L. Differential morphology of pyramidal tract-type and intratelencephalically projecting-type corticostriatal neurons and their intrastriatal terminals in rats. *The Journal of Comparative Neurology* **457,** 420–440 (Mar. 17, 2003) (cit. on pp. 43, 69, 100, 138, 141).

194. Reynolds, J. & Wickens, J. Substantia nigra dopamine regulates synaptic plasticity and membrane potential fluctuations in the rat neostriatum, in vivo. *Neuroscience* **99,** 199–203 (Sept. 2000) (cit. on p. 64).

195. Reynolds, J. N. & Wickens, J. R. Dopamine-dependent plasticity of corticostriatal synapses. *Neural Networks* **15,** 507–521 (June 2002) (cit. on p. 63).

196. Robbe, D. To move or to sense? Incorporating somatosensory representation into striatal functions. *Current Opinion in Neurobiology* **52,** 123–130 (Oct. 2018) (cit. on p. 39).

197. Rock, C., Zurita, H., Wilson, C. & Apicella, A. J. An inhibitory corticostriatal pathway. *eLife* **5,** e15890 (May 9, 2016) (cit. on p. 38).

198. Rosen, G. D. & Williams, R. W. Complex trait analysis of the mouse striatum: independent QTLs modulate volume and neuron number. *BMC neuroscience* **2,** 5 (2001) (cit. on p. 29).

199. Roth, R. H., Zhang, Y. & Huganir, R. L. Dynamic imaging of AMPA receptor trafficking in vitro and in vivo. *Current Opinion in Neurobiology* **45,** 51–58 (Aug. 2017) (cit. on p. 63).

200. Rueda-Orozco, P. E. & Robbe, D. The striatum multiplexes contextual and kinematic information to constrain motor habits execution. *Nature Neuroscience* **18,** 453–460 (Mar. 2015) (cit. on pp. 57, 70).

201. Sachidhanandam, S., Sreenivasan, V., Kyriakatos, A., Kremer, Y. & Petersen, C. C. H. Membrane potential correlates of sensory perception in mouse barrel cortex. *Nature Neuroscience* **16,** 1671–1677 (Nov. 2013) (cit. on pp. 52, 53, 144).

202. Sales-Carbonell, C., Taouali, W., Khalki, L., Pasquet, M. O., Petit, L. F., Moreau, T., Rueda-Orozco, P. E. & Robbe, D. No Discrete Start/Stop Signals in the Dorsal Striatum of Mice Performing a Learned Action. *Current Biology* **28,** 3044–3055.e5 (Oct. 2018) (cit. on p. 57).

203. Santos, F. J., Oliveira, R. F., Jin, X. & Costa, R. M. Corticostriatal dynamics encode the refinement of specific behavioral variability during skill learning. *eLife* **4,** e09423 (Sept. 29, 2015) (cit. on pp. 64, 65).

204. Schröder, K. F., Hopf, A., Lange, H. & Thörner, G. [Morphometrical-statistical structure analysis of human striatum, pallidum and subthalamic nucleus]. *Journal Fur Hirnforschung* **16,** 333–350 (1975) (cit. on p. 29).

205. Schubert, D., Staiger, J. F., Cho, N., Kötter, R., Zilles, K. & Luhmann, H. J. Layer-specific intracolumnar and transcolumnar functional connectivity of layer V pyramidal cells in rat barrel cortex. *The Journal of Neuroscience: The Official Journal of the Society for Neuroscience* **21,** 3580–3592 (May 15, 2001) (cit. on p. 24).

206. Schultz, W., Apicella, P. & Ljungberg, T. Responses of monkey dopamine neurons to reward and conditioned stimuli during successive steps of learning a delayed response task. *The Journal of Neuroscience* **13,** 900–913 (Mar. 1, 1993) (cit. on p. 50).

207. Schulz, J. M. & Reynolds, J. N. J. Pause and rebound: sensory control of cholinergic signaling in the striatum. *Trends in Neurosciences* **36,** 41–50 (Jan. 2013) (cit. on pp. 37, 63).

208. Selemon, L. D. & Goldman-Rakic, P. S. Longitudinal topography and interdigitation of corticostriatal projections in the rhesus monkey. *The Journal of Neuroscience: The Official Journal of the Society for Neuroscience* **5,** 776–794 (Mar. 1985) (cit. on p. 38).

209. Shen, W., Flajolet, M., Greengard, P. & Surmeier, D. J. Dichotomous Dopaminergic Control of Striatal Synaptic Plasticity. *Science* **321,** 848–851 (Aug. 8, 2008) (cit. on p. 64).

210. Sheng, M.-j., Lu, D., Shen, Z.-m. & Poo, M.-m. Emergence of stable striatal D1R and D2R neuronal ensembles with distinct firing sequence during motor learning. *Proceedings of the National Academy of Sciences* **116,** 11038–11047 (May 28, 2019) (cit. on p. 147).

211. Shepherd, G. M. G. Corticostriatal connectivity and its role in disease. *Nature Reviews. Neuroscience* **14,** 278–291 (Apr. 2013) (cit. on p. 41).

212. Shepherd, G. M. G. & Svoboda, K. Laminar and columnar organization of ascending excitatory projections to layer 2/3 pyramidal neurons in rat barrel cortex. *The Journal of Neuroscience: The Official Journal of the Society for Neuroscience* **25,** 5670–5679 (June 15, 2005) (cit. on pp. 26, 69).

213. Silver, R. A., Lübke, J., Sakmann, B. & Feldmeyer, D. High-Probability Uniquantal Transmission at Excitatory Synapses in Barrel Cortex. *Science* **302,** 1981–1984 (Dec. 12, 2003) (cit. on p. 26).

214. Simons, D. J. Response properties of vibrissa units in rat SI somatosensory neocortex. *Journal of Neurophysiology* **41,** 798–820 (May 1978) (cit. on p. 21).

215. Sippy, T., Chaimowitz, C., Crochet, S. & Petersen, C. C. H. Cell Type-Specific Membrane Potential Changes in Dorsolateral Striatum Accompanying Reward-Based Sensorimotor Learning. *Function* **2,** zqab049 (Oct. 14, 2021) (cit. on pp. 60–62, 68).

216. Sippy, T., Lapray, D., Crochet, S. & Petersen, C. C. H. Cell-Type-Specific Sensorimotor Processing in Striatal Projection Neurons during Goal-Directed Behavior. *Neuron* **88,** 298–305 (Oct. 21, 2015) (cit. on pp. 48, 60, 61, 68, 147).

217. Smith, J. B., Mowery, T. M. & Alloway, K. D. Thalamic POm projections to the dorsolateral striatum of rats: potential pathway for mediating stimulus–response associations for sensorimotor habits. *Journal of Neurophysiology* **108,** 160–174 (July 1, 2012) (cit. on p. 141).

218. Stalnaker, T. A., Howard, J. D., Takahashi, Y. K., Gershman, S. J., Kahnt, T. & Schoenbaum, G. Dopamine neuron ensembles signal the content of sensory prediction errors. *eLife* **8,** e49315 (Nov. 1, 2019) (cit. on p. 149).

219. *Handbook of basal ganglia structure and function* (eds Steiner, H. & Tseng, K. Y.) Second edition. OCLC: 958864669 (Elsevier/Academic Press, London, 2017) (cit. on pp. 25, 42, 45, 138).

220. Stuart, G. J. & Spruston, N. Dendritic integration: 60 years of progress. *Nature Neuroscience* **18,** 1713–1721 (Dec. 2015) (cit. on p. 65).

221. Sulzer, D. & Pothos, E. N. Regulation of quantal size by presynaptic mechanisms. *Reviews in the Neurosciences* **11,** 159–212 (2000) (cit. on p. 44).

222. Surmeier, D. J., Plotkin, J. & Shen, W. Dopamine and synaptic plasticity in dorsal striatal circuits controlling action selection. *Current Opinion in Neurobiology* **19,** 621–628 (Dec. 2009) (cit. on p. 64).

223. Takada, M., Tokuno, H., Nambu, A. & Inase, M. Corticostriatal projections from the somatic motor areas of the frontal cortex in the macaque monkey: segregation versus overlap of input zones from the primary motor cortex, the supplementary motor area, and the premotor cortex. *Experimental Brain Research* **120,** 114–128 (May 1998) (cit. on p. 40).

224. Takada, M., Inoue, K.-I., Koketsu, D., Kato, S., Kobayashi, K. & Nambu, A. Elucidating information processing in primate basal ganglia circuitry: a novel technique for pathway-selective ablation mediated by immunotoxin. *Frontiers in Neural Circuits* **7** (2013) (cit. on pp. 39, 44, 100, 138).

225. Tanke, N., Borst, J. G. G. & Houweling, A. R. Single-Cell Stimulation in Barrel Cortex Influences Psychophysical Detection Performance. *The Journal of Neuroscience: The Official Journal of the Society for Neuroscience* **38,** 2057–2068 (Feb. 21, 2018) (cit. on p. 52).

226. Tecuapetla, F., Jin, X., Lima, S. Q. & Costa, R. M. Complementary Contributions of Striatal Projection Pathways to Action Initiation and Execution. *Cell* **166,** 703–715 (July 2016) (cit. on p. 56).

227. Tecuapetla, F., Matias, S., Dugue, G. P., Mainen, Z. F. & Costa, R. M. Balanced activity in basal ganglia projection pathways is critical for contraversive movements. *Nature Communications* **5,** 4315 (July 8, 2014) (cit. on pp. 62, 68, 70, 142).

228. Tepper, J. M. & Bolam, J. P. Functional diversity and specificity of neostriatal interneurons. *Current Opinion in Neurobiology* **14,** 685–692 (Dec. 2004) (cit. on p. 37).

229. Tepper, J. M., Tecuapetla, F., Koós, T. & Ibáñez-Sandoval, O. Heterogeneity and Diversity of Striatal GABAergic Interneurons. *Frontiers in Neuroanatomy* **4** (2010) (cit. on pp. 35, 37).

230. Thomson, A. M. & Bannister, A. P. Postsynaptic pyramidal target selection by descending layer III pyramidal axons: dual intracellular recordings and biocytin filling in slices of rat neocortex. *Neuroscience* **84,** 669–683 (June 1998) (cit. on p. 26).

231. Tritsch, N. X. & Sabatini, B. L. Dopaminergic modulation of synaptic transmission in cortex and striatum. *Neuron* **76,** 33–50 (Oct. 4, 2012) (cit. on pp. 35, 37, 149).

232. Turrigiano, G. G. The Self-Tuning Neuron: Synaptic Scaling of Excitatory Synapses. *Cell* **135,** 422–435 (Oct. 2008) (cit. on p. 145).

233. Veinante, P., Jacquin, M. F. & Deschenes, M. Thalamic projections from the whisker-sensitive regions of the spinal trigeminal complex in the rat. *The Journal of Comparative Neurology* **420,** 233–243 (May 1, 2000) (cit. on p. 141).

234. Voorn, P., Vanderschuren, L. J. M. J., Groenewegen, H. J., Robbins, T. W. & Pennartz, C. M. A. Putting a spin on the dorsal-ventral divide of the striatum. *Trends in Neurosciences* **27,** 468–474 (Aug. 2004) (cit. on p. 29).

235. Waelti, P., Dickinson, A. & Schultz, W. Dopamine responses comply with basic assumptions of formal learning theory. *Nature* **412,** 43–48 (July 2001) (cit. on p. 50).

236. Wall, N. R., De La Parra, M., Callaway, E. M. & Kreitzer, A. C. Differential innervation of direct- and indirect-pathway striatal projection neurons. *Neuron* **79,** 347–360 (July 24, 2013) (cit. on pp. 40, 44–46, 48, 69, 138, 141).

237. Wang, H. & Pickel, V. M. Dopamine D2 receptors are present in prefrontal cortical afferents and their targets in patches of the rat caudate-putamen nucleus. *Journal of Comparative Neurology* **442,** 392–404 (Jan. 21, 2002) (cit. on p. 149).

238. Warren, R. A., Zhang, Q., Hoffman, J. R., Li, E. Y., Hong, Y. K., Bruno, R. M. & Sawtell, N. B. A rapid whisker-based decision underlying skilled locomotion in mice. *eLife* **10,** e63596 (Jan. 11, 2021) (cit. on p. 143).

239. Wen, W. & Turrigiano, G. G. Keeping Your Brain in Balance: Homeostatic Regulation of Network Function. *Annual Review of Neuroscience* **47,** 41–61 (Aug. 8, 2024) (cit. on p. 145).

240. Williams, M. N., Zahm, D. S. & Jacquin, M. F. Differential Foci and Synaptic Organization of the Principal and Spinal Trigeminal Projections to the Thalamus in the Rat. *European Journal of Neuroscience* **6,** 429–453 (Mar. 1994) (cit. on p. 141).

241. Wilson, C. J. Morphology and synaptic connections of crossed corticostriatal neurons in the rat. *The Journal of Comparative Neurology* **263,** 567–580 (Sept. 22, 1987) (cit. on pp. 41, 42, 139).

242. Wilson, C. J. The generation of natural firing patterns in neostriatal neurons. *Progress in Brain Research* **99,** 277–297 (1993) (cit. on p. 33).

243. Wilson, C. J. & Groves, P. M. Fine structure and synaptic connections of the common spiny neuron of the rat neostriatum: a study employing intracellular inject of horseradish peroxidase. *The Journal of Comparative Neurology* **194,** 599–615 (Dec. 1, 1980) (cit. on p. 33).

244. Wilson, C. J. & Groves, P. M. Spontaneous firing patterns of identified spiny neurons in the rat neostriatum. *Brain Research* **220,** 67–80 (Sept. 7, 1981) (cit. on p. 33).

245. Wilson, S. A. K. PROGRESSIVE LENTICULAR DEGENERATION: A FAMILIAL NERVOUS DISEASE ASSOCIATED WITH CIRRHOSIS OF THE LIVER. *Brain* **34,** 295–507 (1912) (cit. on p. 29).

246. Wilson, S. A. K. An Experimental Research into the Anatomy and Physiology of the Corpus Striatum. *Brain* **36,** 427–492 (1914) (cit. on p. 29).

247. Wise, S. P. & Jones, E. G. Cells of origin and terminal distribution of descending projections of the rat somatic sensory cortex. *The Journal of Comparative Neurology* **175,** 129–157 (Sept. 15, 1977) (cit. on pp. 42, 138, 141).

248. Wolff, S. B. E., Ko, R. & Ölveczky, B. P. Distinct roles for motor cortical and thalamic inputs to striatum during motor skill learning and execution. *Science Advances* **8,** eabk0231 (Feb. 25, 2022) (cit. on p. 148).

249. Woolsey, T. A. & Van der Loos, H. The structural organization of layer IV in the somatosensory region (SI) of mouse cerebral cortex. The description of a cortical field composed of discrete cytoarchitectonic units. *Brain Research* **17,** 205–242 (Jan. 20, 1970) (cit. on p. 21).

250. Wright, Norrie, Ingham, Hutton, E. A. & Arbuthnott, G. W. Double anterograde tracing of outputs from adjacent "barrel columns" of rat somatosensory cortex. Neostriatal projection patterns and terminal ultrastructure. *Neuroscience* **88,** 119–133 (Jan. 1999) (cit. on pp. 41, 46, 47, 137–139).

251. Wright, Norrie, L. & Arbuthnott, G. W. Corticofugal axons from adjacent 'barrel' columns of rat somatosensory cortex: cortical and thalamic terminal patterns. *Journal of Anatomy* **196 (Pt 3),** 379–390 (Pt 3 Apr. 2000) (cit. on pp. 27, 46, 47, 139).

252. Wright, Ramanathan, S. & Arbuthnott, G. W. Identification of the source of the bilateral projection system from cortex to somatosensory neostriatum and an exploration of its physiological actions. *Neuroscience* **103,** 87–96 (2001) (cit. on p. 41).

253. Xiong, Q., Znamenskiy, P. & Zador, A. M. Selective corticostriatal plasticity during acquisition of an auditory discrimination task. *Nature* **521,** 348–351 (May 2015) (cit. on pp. 66–68, 144).

254. Yamashita, T. & Petersen, C. C. Target-specific membrane potential dynamics of neocortical projection neurons during goal-directed behavior. *eLife* **5,** e15798 (June 21, 2016) (cit. on pp. 52, 144).

255. Yamashita, T., Vavladeli, A., Pala, A., Galan, K., Crochet, S., Petersen, S. S. A. & Petersen, C. C. H. Diverse Long-Range Axonal Projections of Excitatory Layer 2/3 Neurons in Mouse Barrel Cortex. *Frontiers in Neuroanatomy* **12,** 33 (2018) (cit. on p. 138).

256. Yang, H., Kwon, S. E., Severson, K. S. & O'Connor, D. H. Origins of choice-related activity in mouse somatosensory cortex. *Nature Neuroscience* **19,** 127–134 (Jan. 2016) (cit. on pp. 52, 144).

257. Yin, D., Valles, F. E., Fiandaca, M. S., Forsayeth, J., Larson, P., Starr, P. & Bankiewicz, K. S. Striatal volume differences between non-human and human primates. *Journal of Neuroscience Methods* **176,** 200–205 (Jan. 30, 2009) (cit. on p. 29).

258. Yin, H. H., Mulcare, S. P., Hilário, M. R. F., Clouse, E., Holloway, T., Davis, M. I., Hansson, A. C., Lovinger, D. M. & Costa, R. M. Dynamic reorganization of striatal circuits during the acquisition and consolidation of a skill. *Nature Neuroscience* **12,** 333–341 (Mar. 2009) (cit. on p. 64).

259. Yonk, A. J., Linares-García, I., Pasternak, L., Juliani, S. E., Gradwell, M. A., George, A. J. & Margolis, D. J. *Role of Posterior Medial Thalamus in the Modulation of Striatal Circuitry and Choice Behavior* July 8, 2024 (cit. on p. 148).

260. Yttri, E. A. & Dudman, J. T. Opponent and bidirectional control of movement velocity in the basal ganglia. *Nature* **533,** 402–406 (May 19, 2016) (cit. on pp. 59, 60, 70).

261. Yu, X. & Zuo, Y. Spine plasticity in the motor cortex. *Current Opinion in Neurobiology* **21,** 169–174 (Feb. 2011) (cit. on p. 63).

262. Zareian, B., Lam, A. & Zagha, E. Dorsolateral Striatum is a Bottleneck for Responding to Task-Relevant Stimuli in a Learned Whisker Detection Task in Mice. *The Journal of Neuroscience: The Official Journal of the Society for Neuroscience* **43,** 2126–2139 (Mar. 22, 2023) (cit. on pp. 57, 58, 70).

263. Zhang, W. & Bruno, R. M. High-order thalamic inputs to primary somatosensory cortex are stronger and longer lasting than cortical inputs. *eLife* **8,** e44158 (Feb. 11, 2019) (cit. on p. 27).

264. Zhang, Y., Cudmore, R. H., Lin, D.-T., Linden, D. J. & Huganir, R. L. Visualization of NMDA receptor–dependent AMPA receptor synaptic plasticity in vivo. *Nature Neuroscience* **18,** 402–407 (Mar. 2015) (cit. on p. 144).

265. Zheng, T. & Wilson, C. J. Corticostriatal combinatorics: the implications of corticostriatal axonal arborizations. *Journal of Neurophysiology* **87,** 1007–1017 (Feb. 2002) (cit. on pp. 42, 46, 139).

266. Znamenskiy, P. & Zador, A. M. Corticostriatal neurons in auditory cortex drive decisions during auditory discrimination. *Nature* **497,** 482–485 (May 23, 2013) (cit. on pp. 65, 67, 68, 140).